

# **Lava Falls Rapid in Grand Canyon: Effects of Late Holocene Debris Flows on the Colorado River**

**Professional Paper 1591**

# Availability of Publications of the U.S. Geological Survey

Order U.S. Geological Survey (USGS) publications from the offices listed below. Detailed ordering instructions, along with prices of the last offerings, are given in the current-year issues of the catalog "New Publications of the U.S. Geological Survey."

## Books, Maps, and Other Publications

### *By Mail*

Books, maps, and other publications are available by mail from—

USGS Information Services  
Box 25286, Federal Center  
Denver, CO 80225

Publications include Professional Papers, Bulletins, Water-Supply Papers, Techniques of Water-Resources Investigations, Circulars, Fact Sheets, publications of general interest, single copies of permanent USGS catalogs, and topographic and thematic maps.

### *Over the Counter*

Books, maps, and other publications of the U.S. Geological Survey are available over the counter at the following USGS Earth Science Information Centers (ESIC's), all of which are authorized agents of the Superintendent of Documents:

- Anchorage, Alaska—Rm. 101, 4230 University Dr.
- Denver, Colorado—Bldg. 810, Federal Center
- Menlo Park, California—Rm. 3128, Bldg. 3, 345 Middlefield Rd.
- Reston, Virginia—Rm. 1C402, USGS National Center, 12201 Sunrise Valley Dr.
- Salt Lake City, Utah—2222 West, 2300 South (books and maps available for inspection only)
- Spokane, Washington—Rm. 135, U.S. Post Office Building, 904 West Riverside Ave.
- Washington, D.C.—Rm. 2650, Main Interior Bldg., 18th and C Sts., NW.

Maps only may be purchased over the counter at the following USGS office:

- Rolla, Missouri—1400 Independence Rd.

### *Electronically*

Some USGS publications, including the catalog "New Publications of the U.S. Geological Survey" are also available electronically on the USGS's World Wide Web home page at <http://www.usgs.gov>

## Preliminary Determination of Epicenters

Subscriptions to the periodical "Preliminary Determination of Epicenters" can be obtained only from the Superintendent of

Documents. Check or money order must be payable to the Superintendent of Documents. Order by mail from—

Superintendent of Documents  
Government Printing Office  
Washington, DC 20402

## Information Periodicals

Many Information Periodicals products are available through the systems or formats listed below:

### *Printed Products*

Printed copies of the Minerals Yearbook and the Mineral Commodity Summaries can be ordered from the Superintendent of Documents, Government Printing Office (address above). Printed copies of Metal Industry Indicators and Mineral Industry Surveys can be ordered from the Center for Disease Control and Prevention, National Institute for Occupational Safety and Health, Pittsburgh Research Center, P.O. Box 18070, Pittsburgh, PA 15236-0070.

### *Mines FaxBack: Return fax service*

1. Use the touch-tone handset attached to your fax machine's telephone jack. (ISDN [digital] telephones cannot be used with fax machines.)
2. Dial (703) 648-4999.
3. Listen to the menu options and punch in the number of your selection, using the touch-tone telephone.
4. After completing your selection, press the start button on your fax machine.

### *CD-ROM*

A disc containing chapters of the Minerals Yearbook (1993-95), the Mineral Commodity Summaries (1995-97), a statistical compendium (1970-90), and other publications is updated three times a year and sold by the Superintendent of Documents, Government Printing Office (address above).

### *World Wide Web*

Minerals information is available electronically at <http://minerals.er.usgs.gov/minerals/>

## Subscription to the catalog "New Publications of the U.S. Geological Survey"

Those wishing to be placed on a free subscription list for the catalog "New Publications of the U.S. Geological Survey" should write to—

U.S. Geological Survey  
903 National Center  
Reston, VA 20192

# Lava Falls Rapid in Grand Canyon: Effects of Late Holocene Debris Flows on the Colorado River

*By* ROBERT H. WEBB, THEODORE S. MELIS, PETER G. GRIFFITHS, JOHN G. ELLIOTT, THURE E. CERLING, ROBERT J. POREDA, THOMAS W. WISE, *and* JAMES E. PIZZUTO

---

U.S. GEOLOGICAL SURVEY PROFESSIONAL PAPER 1591

# U.S. DEPARTMENT OF THE INTERIOR

BRUCE BABBITT, Secretary

## U.S. GEOLOGICAL SURVEY

Charles G. Groat, Director

Any use of trade, product, or firm names in this report is for identification purposes only and does not constitute endorsement by the U.S. Government.

Reston, Virginia 1999

---

### Library of Congress Cataloging in Publications Data

Lava Falls Rapid in Grand Canyon : effects of late Holocene Debris  
flows on the Colorado River / by Robert H. Webb ... [et al.].  
p. cm. — (U.S. Geological Survey professional paper : 1591)  
Includes bibliographical references.  
ISBN 0-607-88966-7  
Supt. of Docs. no.: I 19.16: 1591  
1. Debris avalanches--Arizona--Grand Canyon. 2. Geology,  
Stratigraphic--Holocene. 3. Rapids--Arizona--Grand Canyon.  
4. Lava Falls Rapid (Ariz.) I. Webb, Robert H. II. Series.  
QE599.U5L38 1999  
551.48'3'097132--dc21

99-2717  
CIP

---

For sale by U.S. Geological Survey, Information Services,  
Box 25286, Federal Center,  
Denver, CO 80225



# CONTENTS

Abstract .....	1
Introduction .....	2
Purpose and Scope.....	3
Acknowledgments .....	3
The Debris-flow Process .....	4
Characteristics of Debris Flows in Grand Canyon .....	6
Age Dating of Debris Flows.....	7
Effects of Debris Flows on the Colorado River .....	8
Methods .....	11
The Prospect Valley Drainage Basin.....	11
Mapping of Debris-flow Surfaces .....	11
Age Dating of Debris Flows.....	12
Repeat Photography.....	12
<sup>3</sup> He .....	12
<sup>14</sup> C .....	13
<sup>137</sup> Cs .....	13
Pedogenic Calcium Carbonate.....	13
Desert Plant Assemblages.....	14
Clonal Rings of Creosote Bush.....	15
Climatic and Hydrologic Data.....	15
Characterization of Debris Flows and Debris Fans .....	18
Discharge Estimates and Water Content .....	19
Debris-fan Area and Volume.....	19
Debris-fan Frequency .....	20
Constrictions of the Colorado River .....	20
River Velocities and Reworking.....	20
Surficial Geology of the Prospect Canyon Debris Fan .....	21
General Characteristics of Debris Fans .....	21
Upper Debris-flow Surfaces .....	22
tua .....	22
tub .....	24
tuc .....	25
Inset Debris-flow Surfaces .....	25
tia .....	25
tib .....	26
tic .....	26
tid .....	26
tie .....	26
tif.....	26
tig .....	27
tih .....	27
tii.....	28
tij.....	28
Colluvium and Steep Slopes.....	28
tc .....	28
Reworked Debris-flow Deposits .....	28
rwr.....	28
rwc .....	29
rwfd.....	29
Historical Change in Lava Falls Rapid .....	30
Navigation of Lava Falls Rapid in 1994.....	30

## CONTENTS—continued

The Wide, Stable Rapid (1872-1939).....	32
The Period of Frequent Debris Flows (1939-1966) .....	39
Quiescence (1966-1995).....	49
The 1995 Debris Flow .....	49
Initiation of Debris Flows in Prospect Canyon.....	60
Hydroclimatology.....	60
The Firehose Effect .....	61
Magnitude and Frequency of Debris Flows .....	68
Discharge Estimates .....	68
Debris-fan Volumes.....	68
Constrictions of the Colorado River.....	71
Debris-fan Frequency .....	71
Reworking of Debris Fans by the Colorado River.....	73
Reworking of Historical Debris Fans .....	73
Reworking of the 1995 Debris Fan .....	75
Discussion and Conclusions.....	77
Age Dating and Frequency of Debris Flows .....	77
Conceptual Model of Debris-fan Reworking .....	80
Rapids and Management of Glen Canyon Dam .....	81
References Cited .....	83

## PLATES

[Plate is in pocket]

1. Surficial geology of the Prospect Canyon debris fan.

## FIGURES

1. Maps showing study area and streamflow gaging station locations.	
(A) Grand Canyon National Park .....	4
(B) Prospect Valley drainage basin .....	5
2. Map showing Lava Falls and Lower Lava Rapids .....	9
3. Map showing geology of Prospect Canyon .....	10
4. Graphs showing particle-size distributions for debris flows in Prospect Canyon .....	18
5. Graph showing source materials transported by debris flows in Prospect Canyon .....	18
6. Cross section showing the relative elevations and positions of debris-flow surfaces.....	19
7. Photograph of the Prospect Canyon debris fan.....	22
8. Photograph showing the stratigraphy of surface tua on the Prospect Canyon debris fan .....	25
9. Stratigraphy of the 1939 debris-flow deposit (surface tig) .....	29
10. Stratigraphy of the 1955 debris-flow deposits (surface tih).....	30
11. Maps of Lava Falls Rapid in 1994 and 1872-1939 .....	31
12. Replicate photographs of Prospect Canyon and Lava Falls Rapid from Toroweap Overlook .....	34
13. Replicate photographs of Lava Falls Rapid from the high surface on the left side .....	37
14. Upstream photograph of Lava Falls Rapid from the left side.....	38
15. Replicate photographs of the head of Lava Falls Rapid from the right side.....	40
16. Replicate photographs of the right side of Lava Falls Rapid .....	42
17. Photograph of Lava Falls Rapid from the left side .....	44
18. Replicate photographs of Lava Falls Rapid from the left side.....	45
19. Replicate photographs of Lava Falls Rapid from the left side.....	46
20. Replicate photographs of Lava Falls Rapid from the left side.....	48
21. Oblique aerial photographs of Lava Falls Rapid and Prospect Canyon.....	50

## FIGURES—continued

22. Replicate photographs of Prospect Canyon debris fan and the tailwaves of Lava Falls Rapid .....	53
23. Replicate photographs of Lava Falls Rapid from the right side.....	54
24. Oblique aerial photograph of Lava Falls Rapid and Prospect Canyon .....	56
25. Replicate photographs from the left side across the top of Lava Falls Rapid.....	57
26. Replicate photographs of Lava Falls Rapid from the high surface on the left side .....	58
27. Photograph of the firehose effect in Prospect Canyon on March 6, 1995 .....	59
28. Replicate vertical aerial photographs of Lava Falls Rapid .....	62
29. Graphs showing the water-surface profile of the right side of Lava Falls Rapid .....	64
30. Graphs showing standardized seasonal precipitation for western Grand Canyon .....	65
31. Graphs showing monthly precipitation near the Prospect Valley drainage basin associated with Prospect Canyon debris flows and floods .....	66
32. Graphs showing hourly precipitation at Tuweep Ranger Station and Grand Canyon during three historical debris flows and one flood in Prospect Canyon .....	67
33. Map showing the spatial extent of five debris fans deposited by Holocene debris flows from Prospect Canyon.....	69
34. Graph showing the volume of sediments deposited on debris fans by historical debris flows in Grand Canyon and by Holocene debris flows from Prospect Canyon.....	71
35. Graphs showing the constrictions of debris fans at Prospect Canyon and in Grand Canyon .....	71
36. Graph showing annual series of instantaneous peak discharges for the Colorado River near Grand Canyon, Arizona.....	73
37. Hydrographs of the Colorado River showing the timing of tributary floods and debris flows and reworking by river discharges .....	74
38. Hydrographs of the Colorado River from December 1966 to 1974 showing the timing of the 1966 debris flow and releases from Glen Canyon Dam.....	74
39. Graphs showing the effects of river reworking on sediment particle size and lithology on the Prospect Canyon debris fan.....	75
40. Hydrographs showing the relation between stage, discharge, and reworking at Lava Falls Rapid during the 1996 controlled flood .....	76
41. Map showing depositional sites of eight radio-tagged cobbles and boulders downstream from Lava Falls Rapid.....	78
42. Diagram of a conceptual model of aggradation and river reworking of a typical debris fan in Grand Canyon.....	82

## TABLES

1. Analytical data for cosmogenic $^3\text{He}$ analyses of basalt boulders from the Prospect Canyon debris fan .....	14
2. Radiocarbon dates of organic material collected from debris-flow deposits at the mouth of Prospect Canyon.....	15
3. $^{137}\text{Cs}$ activities of sediment from historical debris-flow deposits on the Prospect Canyon debris fan .....	16
4. Characteristics of climate stations in the vicinity of Prospect Canyon .....	17
5. Rankings of the area and volume of debris fans of probable Holocene age on the Colorado River in Grand Canyon National Park.....	23
6. Mineralogy of the clay-size fraction of Prospect Canyon debris flows compared with other Grand Canyon debris flows .....	24
7. Dates and photographic evidence for debris flows and other floods in Prospect Canyon .....	43
8. Peak discharge estimates from superelevation evidence for the debris flows of 1939, 1955, and 1963 in Prospect Canyon at cross section A - A' .....	68
9. Characteristics of late Holocene debris fans deposited at the mouth of Prospect Canyon .....	70

## TABLES—continued

10. Constrictions of historic aggraded and reworked debris fans at the mouth of Prospect Canyon.....	72
11. Characteristics of radio-tagged particles at Lava Falls Rapid transported during the 1996 controlled flood in Grand Canyon.....	77

## CONVERSION FACTORS

For readers who prefer to use inch-pound units, conversion factors for the terms in this report are listed below:

Multiply	By	To obtain
millimeter (mm)	0.03937	inch (in.)
meter (m)	3.281	foot (ft)
square meter (m <sup>2</sup> )	10.76	square foot (ft <sup>2</sup> )
cubic meter (m <sup>3</sup> )	35.31	cubic foot (ft <sup>3</sup> )
kilometer (km)	0.6214	mile (mi)
square kilometer (km <sup>2</sup> )	0.3861	square mile (mi <sup>2</sup> )
cubic meter per second (m <sup>3</sup> /s)	35.31	cubic foot per second (ft <sup>3</sup> /s)
gram (g)	0.03527	ounce avoirdupois (oz. avdp)
kilogram (kg)	2.205	pound avoirdupois (lb avdp)
megagram (M)	1.102	tons, short (2,000 pounds)

Sea level: In this report, "sea level" refers to the National Geodetic Vertical Datum of 1929 (NGVD of 1929)—a geodetic datum derived from a general adjustment of the first-order level nets of the United States and Canada, formerly called Sea Level Datum of 1929.

# Lava Falls Rapid In Grand Canyon: Effects of Late Holocene Debris Flows on the Colorado River

By Robert H. Webb, Theodore S. Melis, Peter G. Griffiths, John G. Elliott, Thure E. Cerling, Robert J. Poreda, Thomas W. Wise, *and* James E. Pizzuto

## ABSTRACT

Lava Falls Rapid is the most formidable reach of whitewater on the Colorado River in Grand Canyon and is one of the most famous rapids in the world. Once thought to be controlled by the remnants of lava dams of Pleistocene age, Lava Falls Rapid actually was created and is maintained by frequent debris flows from Prospect Canyon. Debris flows in Prospect Canyon are initiated by streamflow pouring over a 325-m waterfall onto unconsolidated colluvium, a process called the firehose effect. Floods in Prospect Valley above the waterfall are generated during regional winter storms, localized summer thunderstorms, and occasional tropical cyclones. Winter precipitation has increased in the Grand Canyon region since the early 1960's, and the two most recent debris flows have occurred during winter storms. Summer rainfall has declined in the same period, decreasing the potential for debris flows in the summer months.

We used a number of techniques—cosmogenic  $^3\text{He}$  dating, radiometric  $^{14}\text{C}$  dating,  $^{137}\text{Cs}$  dating, repeat photography, and several relative dating techniques—to differentiate debris-flow surfaces, determine the ages, and estimate the magnitudes of late Holocene debris flows. The highest and oldest debris-flow deposits on the debris fan yielded a  $^3\text{He}$  date of  $3.0 \pm 0.6$  ka (1050 BC), which indicates predominantly late Holocene aggradation of one of the largest debris fans in Grand Canyon. The deposit crossed the Colorado River and raised its base level by 30 m

for an indeterminate although likely short period. Another debris flow, for which we obtained a cosmogenic  $^3\text{He}$  date of  $2.2 \pm 0.4$  ka (250 BC), also crossed the river. The youngest of 6 prehistoric debris-flow deposits inset against the oldest surface occurred no more than 500 years ago (AD 1434). Debris flows in 1939, 1954, 1955, 1963, 1966, and 1995 constricted the Colorado River between 35 and 80 percent, completely changing Lava Falls Rapid. The 1939 debris flow in Prospect Canyon is the largest known debris flow in Grand Canyon during the last 125 years. Discharges for historical debris flows ranged between about 290 and 1,000  $\text{m}^3/\text{s}$ , and boulders as heavy as 30 Mg were transported onto the debris fan. Using a log-normal flood-frequency distribution and a censored-data analysis, we calculated recurrence intervals of 15 to more than 2,000 years for debris flows from Prospect Canyon.

After a period of stability between 1872 and 1939, Lava Falls Rapid has been the most unstable reach of whitewater in Grand Canyon during the last 60 years. The configuration of Lava Falls Rapid did not change during Colorado River floods of 8,500  $\text{m}^3/\text{s}$  in 1884 and 6,230  $\text{m}^3/\text{s}$  in 1921, indicating a stable rapid unaffected by debris flows or river floods. Smaller Colorado River floods (less than 3,540  $\text{m}^3/\text{s}$ ) removed most of the deposition at the mouth of Prospect Canyon within 3 years after debris flows in 1939, 1954, and 1955. Releases in 1965 from Glen Canyon Dam that were above powerplant capacity but less than 1,640  $\text{m}^3/\text{s}$  removed most of the debris fan

deposited by the 1963 debris flow. The combination of releases from Glen Canyon Dam and a 1973 flood on the Little Colorado River removed the 1966 debris fan. Dam releases of no more than  $570 \text{ m}^3/\text{s}$  removed about  $4,800 \text{ m}^3$  of the 1995 deposit on the same day it was deposited. In March–April 1996, a controlled flood that peaked at  $1,370 \text{ m}^3/\text{s}$  significantly removed most of the remaining 1995 debris fan, and Lava Falls Rapid reverted to approximately its pre-1995, low-discharge hydraulics. Velocities on the left and right sides of Lava Falls Rapid decreased by about 50 percent, and the area and volume of the 1995 debris fan decreased by 21 and 18 percent, respectively.

Rapids similar to Lava Falls are aggradational features that reflect the net interaction of tributary and mainstem fluvial processes. Operation of Glen Canyon Dam, completed in 1963, has reduced the potential for reworking of debris fans; consequently, the rate of net aggradation at the mouths of tributary canyons, such as Prospect Canyon, has accelerated. Debris fans that formed after 1963 at Lava Falls Rapid have been mostly reworked by flows higher than typical dam releases but lower than typical pre-dam floods. Therefore, occasional high releases from Glen Canyon Dam could be scheduled as channel-maintenance flows to rework future debris-flow deposits.

## INTRODUCTION

Lava Falls, at river mile 179.4 on the Colorado River in Grand Canyon (fig. 1), is one of the most difficult navigable rapids in the continental United States (Nash, 1989; Ghiglieri, 1992; Lindemann and Lindemann, 1995) and is the standard against which all rapids in Grand Canyon National Park are judged for navigability (Stevens, 1990). Misconceptions abound concerning the origin, size, and geological significance of this rapid. The first explorers of the Colorado River—John Wesley Powell (1869–1872) and Robert Brewster Stanton (1889–1890)—believed Lava Falls was formed by the eroded remnants of Pleistocene lava dams that once spanned the inner canyon (Powell, 1875; Smith and Crampton, 1987). Indeed, the rapid is

named for the basalt flows that poured over the nearby canyon walls (Granger, 1960; Brian, 1992), and several accounts perpetuate the misconception that Lava Falls is controlled by underwater dikes or ledges of basalt (Fradkin, 1984, p. 206; Nash, 1989, p. 179). Some easily measured features of the rapid, such as its fall (about 4 m; Kieffer, 1988), have been incorrectly reported as 12 m (Stevens, 1990).

Most Colorado River rapids, including Lava Falls, flow over and around large boulders that have accumulated on debris fans at the mouths of tributary canyons (Péwé, 1968; Hamblin and Rigby, 1968; Simmons and Gaskill, 1969; Graf, 1979; Howard and Dolan, 1981; Kieffer, 1987, 1988). Cooley and others (1977), Kieffer (1985), and Webb and others (1988a, 1989) reported that debris flows from the tributary are the mechanism for transport of boulders into the Colorado River. Some of the smaller rapids and riffles are not adjacent to tributary mouths but are linked to secondary deposits, called debris bars, deposited by outwash during the reworking of debris fans (Howard and Dolan, 1981; Webb and others, 1989). In other words, frequent debris flows deposit poorly sorted particles on debris fans, forming rapids, and river floods rework these deposits to distribute cobbles and boulders in an orderly fashion downstream, forming secondary rapids and riffles.

Using a unique collection of historical photographs and Quaternary dating techniques, we demonstrate that Lava Falls has been the most unstable rapid in Grand Canyon during the last 120 years and probably during the late Holocene. Six debris flows from Prospect Canyon have substantially altered Lava Falls Rapid in the 20th century. These debris flows occurred in 1939, 1954, 1955, 1963, 1966, and 1995. We identify another eight prehistoric, late Holocene debris-flow surfaces. The largest debris flow, which occurred in about 1050 BC, is the first documented case of a debris flow having dammed the Colorado River during the late Holocene.

On many regulated rivers, such as the Colorado River in Grand Canyon, the pattern of dam releases strongly affects the stability of rapids (Graf, 1980; Kieffer, 1985; Melis and others, 1994). Before closure of Glen Canyon Dam in 1963, debris-flow deposits were eroded (completely reworked) within several years by floods in the Colorado River. Since 1963, aggraded debris fans have persisted longer. We report reworking of a 1995 debris-flow deposit by typical dam releases and the 1996 controlled flood in the Colorado



River, which was designed as a beach-building, habitat-maintenance flow for improving riverine environment in Grand Canyon (Collier and others, 1997). Reworking of the Prospect Canyon debris fan since flow regulation by Glen Canyon Dam illustrates how large dams can be operated to simulate some of the beneficial effects of large floods in unregulated, bedrock-controlled rivers.

## Purpose And Scope

The purpose of this report is to examine the history of debris flows from Prospect Canyon and to document their effect on Lava Falls Rapid. These debris flows, which have occurred more frequently in Prospect Canyon than in other tributaries of the Colorado River in the 20th century, include the largest debris flow in Grand Canyon history. The detailed history of reworking of the Prospect Canyon debris fans by the Colorado River provides important information on how releases from Glen Canyon Dam might rework aggraded debris fans at the mouths of other tributaries in Grand Canyon National Park. Documentation of navigability changes in Lava Falls Rapid provides a perspective and expectation of future alterations to the most severe whitewater in Grand Canyon. This work was partially funded by the Glen Canyon Environmental Studies Program (GCES) of the Bureau of Reclamation. A preliminary version of this report was published as Webb and others (1996), with other aspects discussed in Melis and others (1994), Webb (1996), Bowers and others (1997), Webb and others (1997), and Cerling and others (in press).

## Acknowledgments

Photographs of Lava Falls Rapid were obtained with the help of archivists at the National Archives, the Photographic Library of the U.S. Geological Survey, Special Collections at the University of Utah, the Bancroft Library of the University of California at Berkeley, the Utah State Historical Society, Special Collections at Northern Arizona University, the Study Collection at Grand Canyon National Park, the New York Public Library, and the Huntington Library. The loan of historical photographs taken by the original photographers: Bryan Brown, Kent Frost, Barry Goldwater, Don Harris, Les Jones, Martin Litton, Gretchen Luepke, Tad Nichols, P.T. Reilly, and Robert Sharp. John Cross II provided invaluable information

on changes to Lava Falls following the debris flow of 1966.

Nathan Carlton, Dar Crammond, Steve Eudaley, Cassie Fenton, Diane Grua, Jim Hasbargen, Don Jensen, Shirlee Jensen, Terry Maresca, Marker Marshall, Eric Martin, Tom Martin, Travis McGrath, Holly Metz, Elise Pendall, Dave Pratt, John Rihs, Renee Rondeau, Rachel Sobrero, Jessica Stewart, Mike Taylor, Judy Weiss, Tamara Wiggins, and Toni Yocum assisted in field work. Alan Rigby, Jan Bowers, Kelly Burke, Lauren Hammack, Richard Hereford, Alex McCord, Mimi Murov, Bill Phillips, Betsy Pierson, Robert Ruffner, and Kate Thompson contributed valuable technical expertise to this project. Mia Wise contributed greatly to all aspects of the work. Betsy Menand contributed drawings of stratigraphic sections.

Many photographers helped in replicating historical photographs of Lava Falls Rapid: Jane Bernard, Tom Brownold, Dave Edwards, Mike Grijalva, Jim Hasbargen, Liz Hymans, Dominic Oldershaw, Steve Tharnstrom, and Raymond M. Turner. The Defense Nuclear Agency provided Tharnstrom's salary for several of his trips to Lava Falls Rapid. The following professional river guides and support personnel contributed their boating skills and knowledge of the river: Jane Bernard, Steve Bledsoe, Gary Bolton, Tom Brownold, Kelly Burke, Michael Collier, Brian Dierker, Dave Edwards, Chris Geneous, Jan Kempster, Kenton Grua, Bob Grusy, Les Hibbert, Liz Hymans, Cindy Krznarich, Pete Reznick, Sue Rhodes, Glenn Rink, Rachael Running, Dennis Silva, Drifter Smith, Kelly Smith, Al Tinnes, Meg Viera, and Greg Williams. Gary Bolton, Kenton Grua, Bob Grusy, and Kelly Smith provided their interpretations of changes in Lava Falls Rapid.

Special thanks to Frank Protiva, Chris Brod, and Mark Gonzales of the GCES survey staff for assistance in preparing the topographic base for plate 1 and for their help in estimating areas, volumes, and cross-sectional areas for the Prospect Canyon debris fan. Hilary Mayes-Filmore helped prepare the topographic map of the Prospect Canyon debris fan, and Doug Wellington helped with the analyses of precipitation. Brad Dimock shared information on Buzz Holmstrom's 1938 trip. Steve Wiele of the U.S. Geological Survey, Boulder, Colorado, supplied travel times for flow in the Colorado River. Dominic Oldershaw printed most of the repeat photographs of Lava Falls Rapid, and Chuck Sternberg drafted the complex figures. Jan Bowers, Yehouda Enzel, Lauren



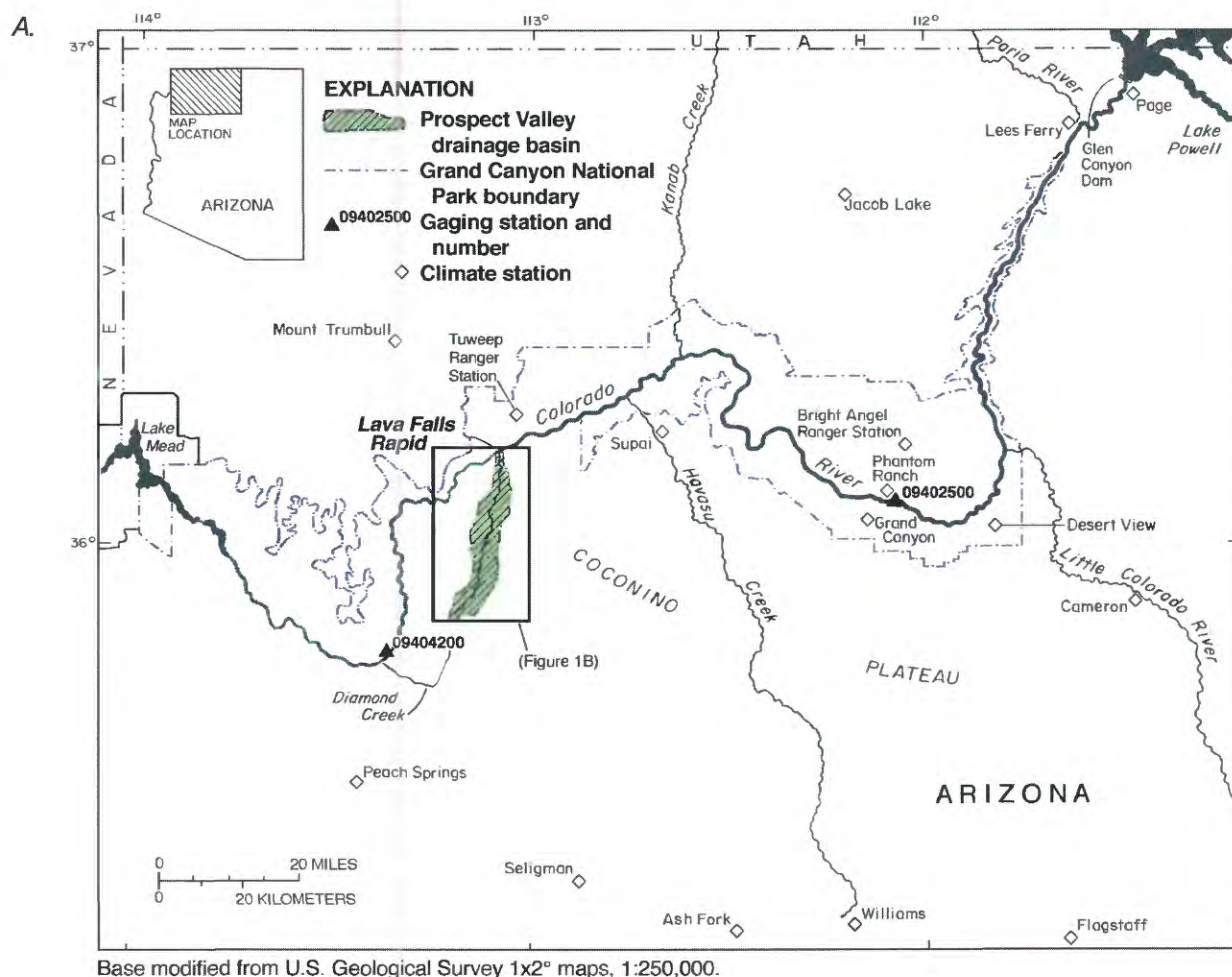


**Figure 1. A, Grand Canyon National Park.**

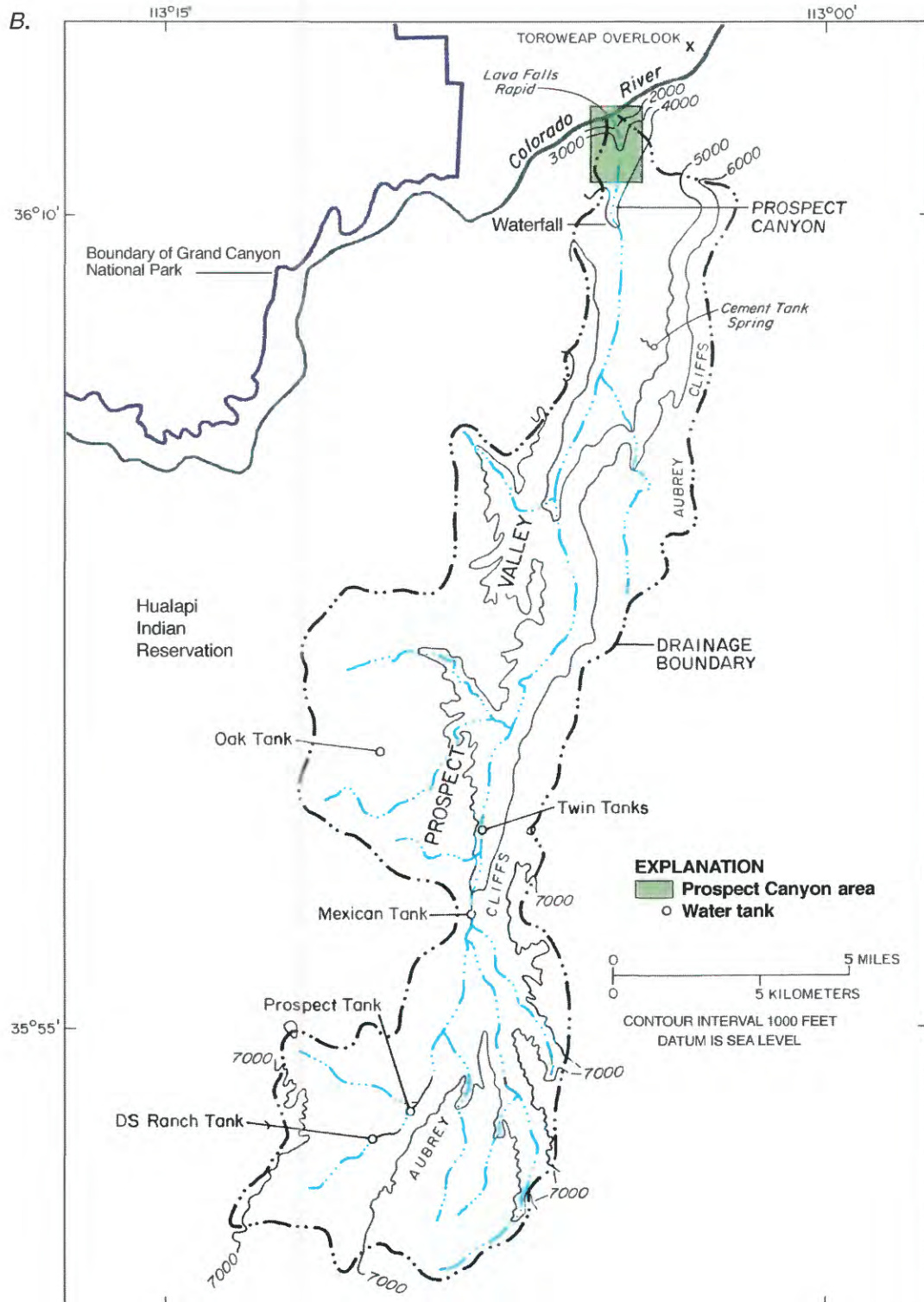
Hammack, Richard Hereford, Waite Osterkamp, Tim Randle, Jack Schmidt, and Ellen Wohl reviewed sections or all of the manuscript. We give special thanks to Dave Wegner, formerly of GCES, for his unwavering support of our research. The cosmogenic dating component of this study was funded by the National Science Foundation.

### The Debris-flow Process

Several classifications of sediment-bearing flows have been proposed on the basis of water content (Beverage and Culbertson, 1964; Pierson and Costa, 1987), depositional characteristics of sediments (Smith, 1986; Scott, 1988), and flow dynamics (Postma, 1986). We recognize two types of water-based flow in Grand Canyon tributaries (Melis and others, 1994): streamflow, which contains less than 40 percent

sediment by volume, and debris flow, which typically contains more than 80 percent sediment by volume. Although hyperconcentrated-flow deposits (Scott, 1988) are recognized in Grand Canyon (Melis and others, 1994), we include this poorly understood process with streamflow in our discussion of flow processes in Prospect Canyon.

Debris flows, water-based slurries of poorly sorted sediments (Costa, 1984; Iverson, 1997), occur in many different environments ranging from deserts (Blackwelder, 1928; Johnson and Rodine, 1984; Cooke and others, 1993) to montane forests (Sharp and Nobles, 1953; Gallino and Pierson, 1985). Most debris flows follow destabilization of landscapes by catastrophic events, such as volcanic eruptions (Pierson, 1985; Pierson and Scott, 1985; Marron and Laudon, 1986), fires (Wells, 1986, 1987; Wells and others, 1987; Wohl and Pearthree, 1991; Meyer and



Base modified from U.S. Geological Survey 7.5' topographic maps, 1:24,000.

B, The Prospect Valley drainage basin.

Figure 1. Continued.



others, 1995), extraordinary amounts or intensities of precipitation (Kaliser and Slosson, 1988; Cenderelli and Kite, 1994; Wieczorek and others, 1996), or poor land-use practices (Costa, 1984; Johnson and Rodine, 1984; Benda and Cundy, 1990). In undisturbed landscapes, debris flows can result from rapid glacial melting (Osterkamp and others, 1986) or severe rainstorms (Blackwelder, 1928; Stringfield and Smith, 1956; Glancy, 1969; Williams and Guy, 1971; Wieczorek and others, 1989; Hammack and Wohl, 1996).

Steep slopes are a prerequisite for debris-flow initiation, although threshold slope angles and lengths would be difficult to define. Many types of geologic terranes produce debris flows, particularly where dip angles of sedimentary rocks roughly coincide with slope angles. Destabilization of steep slopes may produce landslides that can mobilize into debris flows (Johnson and Rodine, 1984). Slope failures typically are associated with debris flows (Cooley and others, 1977; Kaliser and Slosson, 1988; Webb and others, 1989); landslides commonly mobilize into debris flows (Iverson and others, 1997). Lahars, or debris flows of pyroclastic material, can be produced as a part of any type of volcanic eruption but are most common in rhyolitic and andesitic terranes (Wright and Pierson, 1992). Debris flows also are common in granitic terranes (Wells and others, 1987; Whipple and Dunne, 1992).

Debris-flow frequency varies widely. Large-scale destabilization of landscapes, as from volcanic eruptions, can greatly increase debris-flow frequency for decades (Marron and Laudon, 1986). Even in the absence of disturbances, debris flows may occur in discrete periods (Jackson, 1977; Hereford and others, 1997). Before widespread logging, the recurrence interval of debris flows in forested areas may have been as low as every 1,500 and 750 years in 1st and 2nd order drainages, respectively (Benda and Dunne, 1987); frequencies after logging are much higher. In the absence of catastrophic disturbance, the frequency of debris flows probably ranges from less than one per decade to about one per millennium (Jackson, 1977; Kochel, 1987; Shlemon and others, 1987; Osterkamp and Hupp, 1987; Lips and Wieczorek, 1990). Estimates of debris-flow frequency from stratigraphic sections may underestimate the true frequency in a manner similar to "obliterative overlap" of glacial moraines (Gibbons and others, 1984).

## Characteristics Of Debris Flows In Grand Canyon

Slope failures during intense rainfall initiate debris flows in Grand Canyon. These failures are either in bedrock, typically terrestrial shales and mudstones, or in colluvial wedges that mantle steep shelves and ledges. The most common initiation mechanism, called the "firehose effect" by Johnson and Rodine (1984), consists of runoff cascading from cliffs onto colluvial wedges, causing failure (Melis and others, 1994). This failure mechanism is the most common in Prospect Canyon (Webb and others, 1996).

Historically, total rainfall associated with debris flows ranges from 27 to 355 mm (Webb and others, 1989). Instantaneous intensities are unknown, and hourly intensities range from 10 to 40 mm/hr at climate stations that typically are not in the drainage basin that has a debris flow (Melis and others, 1994; Griffiths and others, 1996, 1997). Storms that cause debris flows typically have recurrence intervals greater than 10 years, although precipitation on the day of the debris flow at nearby climate stations may not be unusual (Griffiths, 1995; Griffiths and others, 1997). Antecedent soil-moisture conditions probably affect debris-flow initiation in Grand Canyon because most historical debris flows occurred during relatively wet periods of no more than a month.

Debris flows in Grand Canyon tributaries usually travel 1 to 20 km from initiation points to the Colorado River (Webb and others, 1989). Debris flows unconfined by bedrock channels deposit levees subparallel to the flow direction (Cannon, 1989). These levees control the location of distributary channels and allow flow to continue over long distances. For 29 debris flows in Utah, Cannon (1989) concluded that the travel distance is a function of the difference between deposition and erosion rates, with termination occurring when the debris flow reached minimum thickness. In West Virginia, Cenderelli and Kite (1994) observed that debris flows scour in the upper two thirds of the drainages, which they refer to as the transport zone. Debris flows may stop, transform into streamflow floods, and remobilize downstream owing to sediment added by small tributaries or chutes (Melis and others, 1994, 1997).

Typical Grand Canyon debris flows contain 80–85 percent sediment by volume and commonly contain 2–5 percent clay and 10–30 percent sand. The silt and clay fraction greatly affects slurry behavior at high shearing rates (Major and Pierson, 1990, 1992; Major,

1993), which would occur during the transport phase from initiation point to debris fan; the amount of sand affects behavior at low shearing rates that occurs during deposition. Clay chemistry and mineralogy are also important to sustained flow (Hampton, 1975). The frequency of debris flows in Grand Canyon is strongly related to the proximity of terrestrial shale units (Griffiths and others, 1996), the major source for silt- and clay-size particles. The clay-size minerals in Grand Canyon debris flows are typically illite, kaolinite, and quartz (Griffiths, 1995).

Debris flows are a common component of flash floods in Grand Canyon (Webb and others, 1989; Melis and others, 1994; Melis, 1997). In straight, confined channels with relatively low gradients, debris flows are thought to move essentially as plug flow (Johnson and Rodine, 1984) with little internal shearing. In steeper channels, surging flow propagates as waves (Major, 1997). In both cases, considerable turbulence and shearing occurs in bends and bed-slope transitions. Melis and others (1997) described three types of debris flows in Grand Canyon. Type I debris flows consist of a single pulse of debris flow followed by a brief period of recessional flow. Type II debris flows have alternating pulses of debris flow and streamflow; the pulses may be related to the surging flow described by Major (1997). Finally, type III debris flows consist of type I or II debris flow followed by a higher-stage streamflow flood.

Debris-flow transport of very large boulders in low-gradient channels is common throughout the world (Rodine and Johnson, 1976; Johnson and Rodine, 1984; Pierson and Costa, 1987; Beatty, 1989). In Grand Canyon tributaries, debris flows commonly transport boulders with diameters greater than 3 m that weigh between 1 and 300 Mg into the Colorado River (Melis and others, 1994). A combination of factors facilitates boulder transport: (1) the accumulation of limestone and sandstone boulders in colluvial wedges; (2) the presence of terrestrial shales; (3) the steep gradients of tributary channels; and (4) the relatively short distances from initiation points to the Colorado River. Most of the boulders that form rapids are transported to the river in debris flows that consist of a single, short-duration pulse of fines and boulders. Alternating pulses of recessional streamflow and smaller debris flows may follow (Webb and others, 1988a; Webb and others, 1989; Melis, 1997; Melis and others, 1997). In contrast, tributary streamflow floods have a greater water content and generally carry finer sediments consisting

mainly of sand with cobbles or small boulders as the largest particles transported.

The presence and depth of distributary channels on alluvial fans affects the locus of deposition (Whipple and Dunne, 1992). Osterkamp and others (1986) found that the frequency of “out of channel” debris flows was lower than smaller, channelized events. Hereford and others (1993) differentiated “fan-forming” and “channelized” debris-flow deposits on large debris fans of relatively low slope in eastern Grand Canyon. Hereford and others (1996, 1997) grouped fan-forming deposits into distinct periods of debris-flow activity in the late Holocene, although they do not report recurrence intervals for specific debris flows. Using Hereford and others’ (1993) classification, some of the debris flows reported by Melis and others (1994) were “channelized,” leaving little depositional evidence on debris fans, whereas other debris flows were “fan-forming” and include the largest in the recorded history of Grand Canyon. Because the depth of channels through the debris fan determines whether a debris flow is channelized or fan-forming, these terms are not useful for describing Prospect Canyon debris flows in terms of magnitude or frequency.

Historically, debris flows in most Grand Canyon tributaries have a recurrence interval of 10–50 years (Melis and others, 1994). In contrast, debris flows in Warm Springs Draw in Dinosaur National Monument, Colorado, occur every 200–400 years (Hammack, 1994). Approximately 40 percent of Grand Canyon tributaries have not had a debris flow in the last century (Webb, 1996), possibly for hydroclimatic reasons and (or) lack of proximity to shale units (Griffiths and others, 1996). Ten percent of 59 debris fans in eastern Grand Canyon had significant aggradation between 1965 and 1973 (Howard and Dolan, 1979, 1981).

## Age Dating Of Debris Flows

The study of *in situ* produced cosmogenic isotopes has revolutionized the dating of geomorphic surfaces (Lal, 1988, 1991; Cerling and Craig 1994a; Bierman 1994; Phillips, 1997). For sites lacking appropriate organic carbon for conventional <sup>14</sup>C dating, cosmogenic isotopes offer an accurate alternative. Production rates of cosmogenic nuclides in rocks have been extensively studied in the last decade (Klein and others, 1986; Kurz, 1986; Craig and Poreda, 1986; Phillips and others, 1986; Nishiizumi and others, 1989, 1991; Cerling, 1990; Zreda and others, 1991).



Cosmogenic isotopes have been used to calculate erosion rates (Cerling, 1990; Brown and others, 1991; Nishiizumi and others, 1991; Burbank and others, 1996); to date glaciations and differentiate moraines (Lal and others, 1987; Brown and others, 1991; Nishiizumi and others, 1991; Phillips and others, 1991; Cerling and Craig, 1994a; Gosse and others, 1995a, b; Phillips, 1997); to date lava flows (Cerling, 1990; Laughlin and others, 1994), catastrophic floods (Cerling, 1990; Cerling and others, 1994c; Phillips, 1997), and meteorite impacts (Phillips and others, 1991; Nishiizumi and others, 1991); and to study a variety of other processes such as earthquake recurrence intervals (Bierman and others, 1995), ages of alluvial terraces (Phillips, 1997), and desert-pavement formation (Wells and others, 1995). After considerable research (Kurz, 1986; Nishiizumi and others, 1989; Zreda and others, 1991; Poreda and Cerling, 1992; Brown and others, 1992; Cerling and Craig, 1994b; Masarik and Reedy, 1995), the terrestrial production rates of many cosmogenic isotopes are known to within 10 percent.

Stable cosmogenic isotopes, such as  $^3\text{He}$ , have high production rates but may include  $^3\text{He}$  inherited from prior exposure. Cosmogenic  $^3\text{He}$  is retained in olivine and pyroxene but is lost from quartz and feldspar (Cerling, 1990) except occasionally under the very cold conditions of Antarctica (Brook and Kurz, 1993). Abundant olivine phenocrysts in basalts in the vicinity of Lava Falls (Wenrich and others, 1995) makes them well suited for cosmogenic  $^3\text{He}$ . The production rate of cosmogenic  $^3\text{He}$  has been well established (Cerling and Craig, 1994b), making feasible an extension of the cosmogenic  $^3\text{He}$  technique to late Quaternary basalt flows and associated alluvial deposits in western Grand Canyon.

In addition to  $^3\text{He}$ , other techniques can successfully date debris flows. Webb (1996) used repeat photography to document debris-flow frequency throughout Grand Canyon. Some researchers have used  $^{14}\text{C}$  dating for debris-flow deposits where abundant charcoal from forest fires (Meyer and others, 1995) or archaeological sites (Hereford and others, 1996) are present. Organic carbon is rare in most debris-flow deposits in Grand Canyon, making  $^{14}\text{C}$  dating appropriate mostly for young debris-flow deposits. The human-made isotope  $^{137}\text{Cs}$  is useful for distinguishing pre- and post-1952 deposition (Ely and others, 1992; Melis and others, 1994). In this study, we report  $^3\text{He}$  dates for the oldest debris-flow surfaces and

use them with  $^{14}\text{C}$  dates,  $^{137}\text{Cs}$  dating, and photographic evidence to distinguish late Holocene debris-flow surfaces and to estimate the frequency of debris flows from Prospect Canyon.

## Effects Of Debris Flows On The Colorado River

Some previous researchers have concluded that the relation between tributaries and the locations of rapids is not strong. Leopold (1969) observed that only a fraction of Grand Canyon rapids are coincident with tributary junctures and postulated that the rapids and pools are regularly spaced and maintained by quasi-equilibrium processes of flow and sediment transport in the Colorado River. Graf (1979) found that the spatial distribution of rapids in Grand Canyon is partly regular and partly random and that 79 percent of the rapids are adjacent to tributary mouths. Rapids have been interpreted as relics of past periods of wetter climate (Graf, 1979) and as landforms formed by prehistoric stream-flow floods large enough to transport boulders out of tributary canyons (Hamblin and Rigby, 1968).

In Grand Canyon, Webb and others (1988a) reported that 54 of the 57 largest rapids are located at tributary junctures and are created and maintained by debris flows from the tributary. Repeated debris-flow deposition alters the configuration of existing rapids and their controlling debris fans (Webb and others, 1989; Melis and others, 1994; Melis, 1997). In Grand Canyon, this configuration forms zones of recirculating flow (eddies) downstream from debris fans that facilitate deposition of sand bars (Howard and Dolan, 1981; Schmidt, 1990; Schmidt and Graf, 1990; Schmidt and Rubin, 1995).

Several effects of debris flows on the Colorado River are well illustrated at Lava Falls Rapid (fig. 2). Deposition of a debris fan in the river creates a rapid by constricting the width of the river and raising its bed elevation (Howard and Dolan, 1981). Similar types of deposition have caused partial or complete damming of valleys in other river systems (Stringfield and Smith, 1956; Gallino and Pearson, 1985; Benda, 1990; Miller, 1994). Local features, such as unusually large boulders or the arrangement of boulders on the bed, cause spectacular hydraulic features that impede navigation. Flow around the debris fan and through the rapid may be supercritical (Kieffer, 1987; Miller, 1994), leading to

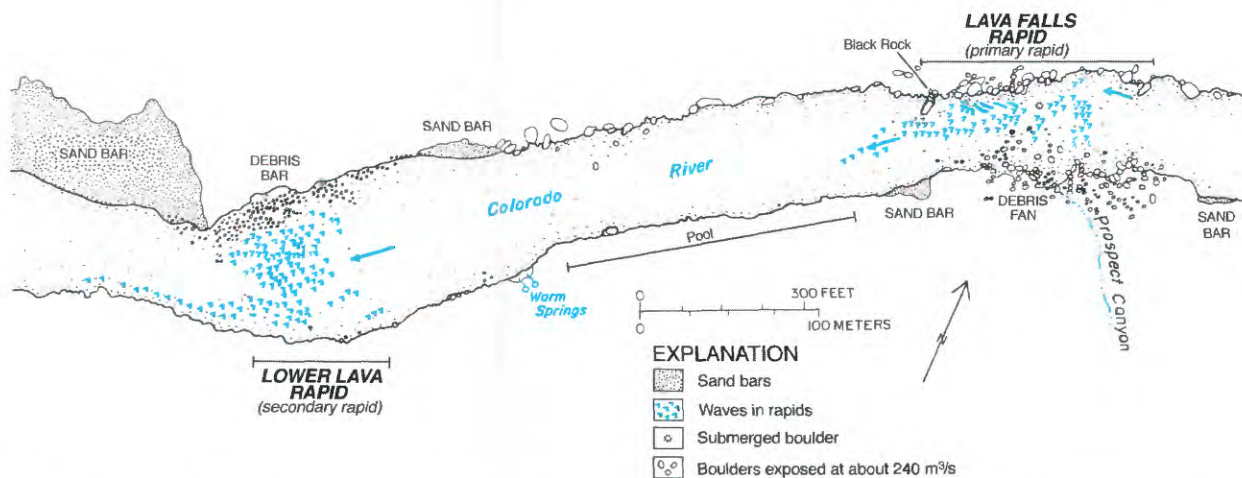


**Figure 2.** Lava Falls and Lower Lava rapids showing geomorphic features of the Colorado River. The Prospect Canyon debris fan, shaped and reworked by the Colorado River, forms a rapid-pool-rapid configuration that is typical of Grand Canyon rapids (Webb and others, 1989). The main rapid arises from the constriction and deposition of boulders on the bed of the river. The pool downstream, which has twin eddies, is a recirculation zone (Schmidt and Graf, 1990) that deposits sand bars at certain water levels. Lower Lava Rapid is controlled by cobbles and boulders that have been eroded from the Prospect Canyon debris fan, transported through the pool, and deposited as the first of a series of alternating debris bars downstream from the rapid.

hydraulic jumps that may be independent of the configuration of boulders on the channel bed (Kieffer, 1985). If reworked by a sufficiently large flood, boulders can be redistributed in an orderly fashion downstream, creating secondary rapids or riffles (Webb and others, 1989; 1997).

Most rapids in Grand Canyon are at the mouths of tributary canyons that formed along fault zones. The faults typically cross the Colorado River, and the presence of fracture zones downstream from rapids may increase downcutting rates in Grand Canyon (Dolan and others, 1978). At Lava Falls Rapid, the Toroweap Fault, a normal fault, crosses the Colorado River just upstream of the mouth of Prospect Canyon (fig. 3). Because of its position with respect to the rapid, this fault is unlikely to have the effects described by Dolan and others (1978), although offset on this fault may affect the amount of drop through the rapid. In addition, earthquakes may increase the potential for debris flows in Grand Canyon by producing abundant talus and sheared bedrock (Melis and others, 1994).

The unregulated Colorado River periodically widened constricted rapids by eroding boulders and debris-flow matrix from debris fans during floods that regularly exceeded  $2,800 \text{ m}^3/\text{s}$  (Kieffer, 1985). Reworked debris fans developed residual surfaces composed of cobbles and boulders lying near their

original depositional sites and sand deposited by the Colorado River (Howard and Dolan, 1981). Graf (1980) stated that flow regulation reduces reworking in the Colorado River system, leading to aggradation on debris fans and in rapids. Many rapids, including Lava Falls, have been altered by debris-flow deposition since 1963 (Howard and Dolan, 1979, 1981; Melis and others, 1994; Webb, 1996) because debris-fan constrictions and their boulder deposits have not been totally removed by typical releases from Glen Canyon Dam (typically less than  $850 \text{ m}^3/\text{s}$ ). Because severity of rapids depends on the arrangement of boulders and waves, the navigational difficulty of rapids is not necessarily increased by debris-flow deposition (Webb, 1996).

During the reworking process, sediment eroded from the debris fan is deposited on downstream debris bars. Debris bars can be either low-water islands or alternating bars and are composed of well-sorted and imbricated gravel, cobbles, or boulders. They commonly form secondary rapids downstream from the larger, primary rapids at tributary mouths. One such secondary rapid—Lower Lava Rapid—is about 200 m downstream from Lava Falls Rapid (fig. 2). Others are found downstream from major rapids such as Hance, Granite, and Crystal (at river miles 77, 93.5, and 98.3, respectively; Stevens, 1990).



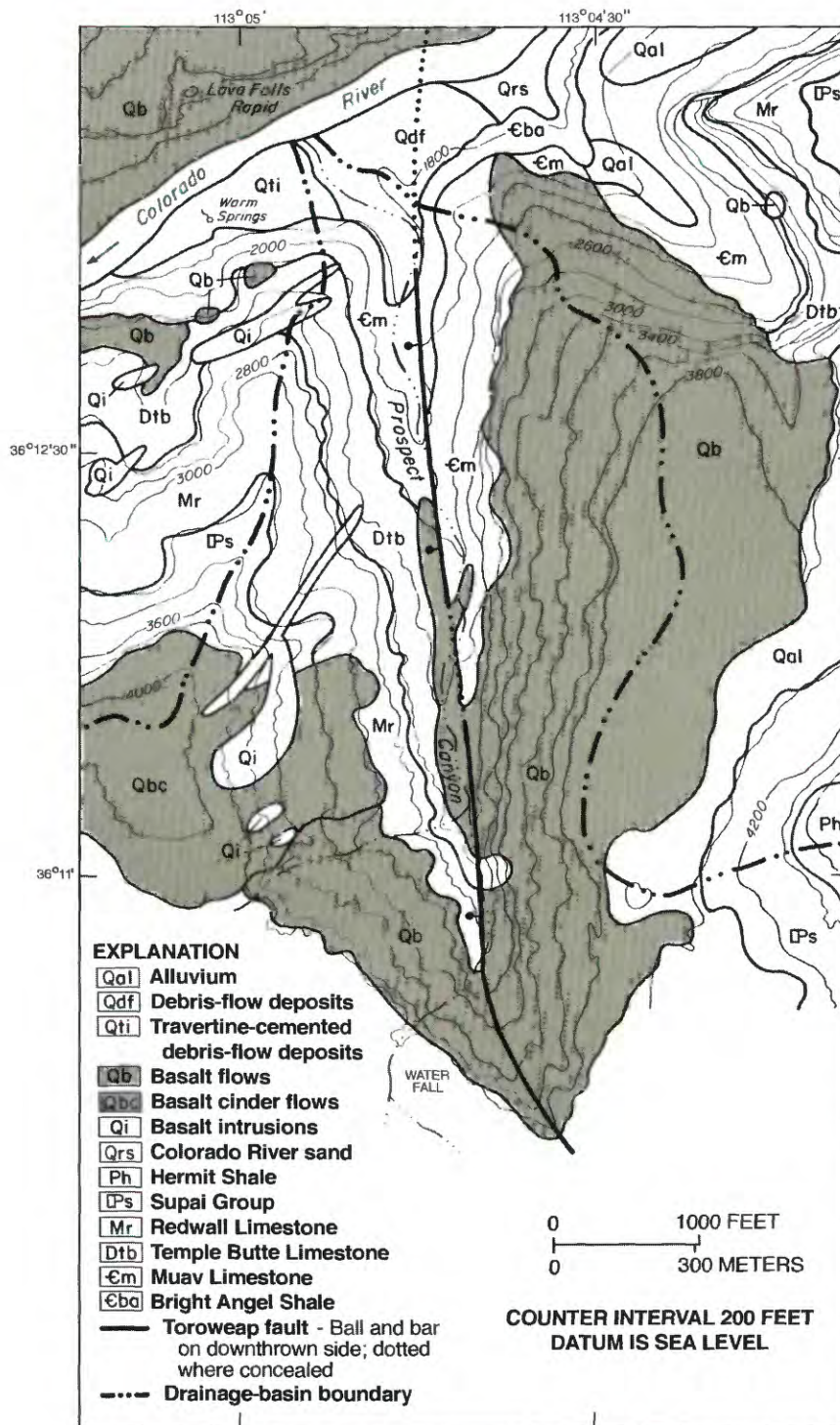


**Figure 3.** Geology of Prospect Canyon.



## METHODS

### The Prospect Valley Drainage Basin

In remote northwestern Arizona, names commonly are lacking for stream channels and other drainage features. The basin that drains northward into the Colorado River at Lava Falls Rapid was named Prospect Valley (fig. 1B) by prospectors in the late 19th century (Granger, 1960; Brian, 1992); the watercourse is unnamed. The Prospect Valley drainage basin includes 257 km<sup>2</sup> of forests, grasslands, and desert scrub south of Grand Canyon (fig. 1A). It is the ninth largest of 529 debris-flow producing tributaries in Grand Canyon (Melis and others, 1994). Although the highest point in the drainage basin is 2,367 m, most of the upper part lies between 1,450 and 1,950 m.

Prospect Valley abruptly becomes a small gorge informally called Prospect Canyon (fig. 1B) at the point where a 325-m fall occurs in a horizontal distance of approximately 250 m. The rocks exposed in Prospect Canyon are Paleozoic sedimentary strata and Quaternary basalts extruded from local vents (fig. 3). The Toroweap Fault, which is downthrown to the west, trends south across the Colorado River and through Prospect Canyon (Billingsley and Huntoon, 1983; Jackson, 1990a, b). The drainage of Prospect Valley and Prospect Canyon formed along and to the west of this fault. The upper Paleozoic strata of Grand Canyon are exposed in the Aubrey Cliffs, which line the east side of Prospect Valley (fig. 1B).

The Toroweap Fault is thought to be the most active fault in Arizona (Jackson, 1990b). Offset on the fault is greatest in Prospect Canyon, where Holocene alluvial fans are displaced by about 5 m (Billingsley and Huntoon, 1983). Jackson (1990a, b) reports that the most recent, surface-rupturing earthquake, of magnitude 7.1 to 7.2 on the Richter scale, occurred about 3.1 ka. This earthquake caused 2.2 m displacement on the fault scarp in Prospect Canyon.

Prospect Valley formed after Quaternary basalt flows filled the ancestral Prospect Canyon from 1.2 Ma to 140 ka (Hamblin, 1994a, b). These flows formed 5 dams across the Colorado River near the mouth of Prospect Canyon; the lake impounded by the tallest dam reportedly extended upstream to Moab, Utah (Hamblin, 1990). The ancestral Prospect Canyon was filled by the lava flow that produced the Prospect Dam (Hamblin, 1990, 1994b). Contemporary Prospect Canyon occupies part of the former canyon, which

joined the Colorado River upstream of the current mouth.

The waterfall separating Prospect Valley from Prospect Canyon causes an abrupt change in fluvial process from streamflow in Prospect Valley to debris flow in Prospect Canyon. Debris flows in Prospect Canyon are generated when floods in Prospect Valley flow over the waterfall onto unconsolidated colluvium (the firehose effect). There is no evidence of past debris flows on the floor of Prospect Valley; stratigraphic evidence of debris flows begins at the foot of the waterfall into Prospect Canyon. Although the gradient of Prospect Valley (0.041) is relatively low in comparison to other Grand Canyon tributaries, the gradient through Prospect Canyon (0.315) is steep enough to provide considerable potential energy for debris flows. The largest sources of colluvium in Prospect Canyon are rockfall from a headwardly eroding cinder cone on the western rim and talus from the steep slopes of Prospect Canyon (fig. 3).

### Mapping of Debris-flow Surfaces

Between 1991 and 1994, we surveyed the Prospect Canyon debris fan, produced a topographic map, and mapped the surficial geology (pl. 1). The map of the Prospect Canyon debris fan (pl. 1) delineates geomorphic surfaces, not stratigraphic units as depicted on other surficial geology maps of parts of Grand Canyon (Hereford, 1996). The history of debris-flow deposition is inherently difficult to interpret from deposits (Major, 1997), and fortuitous channel exposures are probably inadequate to determine the complete history of events. Some of the surfaces on the Prospect Canyon debris fan have complex depositional histories that are adequately expressed, mappable deposits. Other surfaces are terraces with superimposed snouts or push-out lobes of potentially different ages. The geomorphic surface map also allows delineation of colluvial and reworking processes that could not be distinguished on a stratigraphic unit map.

We used approximately 1,400 points to develop our topographic base map. These data were combined with 1:2,400 scale digital contour data calculated from 1990 aerial photography using image processing. The 1990 data have a horizontal accuracy of  $\pm 1.3$  m and a vertical accuracy of  $\pm 0.25$  m on flat slopes and  $\pm 1$  m on steep slopes (F. Protiva, GCES, written commun., 1996). Combining the topographic data required absolute elevation and topographic control, which we

obtained using a global positioning system (GPS) with a horizontal and vertical accuracy of  $\pm 0.4$  m, owing to discrepancies between the 1990 control points and subsequent GPS measurements. For consistency, we rounded all surveyed areas to the nearest  $100 \text{ m}^2$  (implied accuracy of  $\pm 50 \text{ m}^2$ ), all volume measurements to the nearest  $100 \text{ m}^3$  (implied accuracy of  $\pm 50 \text{ m}^3$ ), and all distance measurements to the nearest 1 m (implied accuracy of  $\pm 0.5$  m), although the survey data is of considerably higher accuracy than is implied by these uncertainties.

Contours were calculated using Terramodel for DOS software. Surficial geology was mapped on an enlarged aerial photograph (1:3,000 scale) taken in October 1989 and transferred to the base map. Historical photography greatly facilitated differentiation of geomorphic surfaces, particularly those deposited in the 20th century, and enabled us to ascribe small surfaces to specific debris flows or floods.

## Age Dating of Debris Flows

### Repeat Photography

Repeat photography was the most important tool we used to document 20th century debris flows in Prospect Canyon. Early expeditions on the Colorado River included photographers, and numerous photographs and movies have been made of Lava Falls Rapid, beginning with stereoscopic views made by the Powell Expedition in 1872 (Stephens and Shoemaker, 1987). The downstream view from Toroweap Overlook, which towers 1,000 m above the river on the northwestern rim of the canyon (fig. 1B), has been frequently photographed as well. We examined 232 historical views of Lava Falls Rapid made between 1872 and 1984: 48 oblique aerial views, 17 vertical aerial photographs, 129 views taken at or near river level, and 38 views from Toroweap Overlook. We replicated 121 of these photographs from February 1990 to March 1995. All camera stations are assigned a unique stake number, and negatives and prints are stored in the Desert Laboratory Collection of Repeat Photography in Tucson, Arizona.

Photographic coverage was sparse from 1872 through 1938, when commercial river running began (Lavender, 1985). Photographs were available for 18 dates from 1872 through 1939, including 14 of 68 years; these photographs were taken primarily by parties conducting scientific exploration and surveys of

the river. Because river running was a luxury during World War II, only 12 photographs were available from 1940–1947. Beginning in the 1950's, the photographic record of Lava Falls expanded greatly thanks to a new generation of river runners. We obtained photographs for 30 dates in the 1950s and 29 dates in the 1960s. Vertical aerial photographs are available for several years from 1980 through 1995, but in this study we only used vertical photographs to document the effects of the 1995 debris flow.

### $^3\text{He}$

The basalt clasts in Prospect Canyon debris flows contain olivine phenocrysts (Hamblin, 1994b; Wenrich and others, 1995), which are efficient traps for cosmogenically produced helium, termed  $^3\text{He}_c$  (Kurz, 1986; Cerling, 1990; Cerling and Craig, 1994a). The clasts are mostly from the Prospect Dam lava flows that form a near-vertical wall at the head of Prospect Canyon (shown as  $Q_b$  in fig. 3).  $^3\text{He}_c$  in the massive basalt is minimal because the high cliffs in the narrow canyon shield the basalt from cosmic-ray bombardment. Slope failures that cause debris flows produce previously unexposed basalt clasts, and the short transport distance between source and debris fan (1.6 km) offers little opportunity for long-term cosmogenic exposure of boulders in the channel of Prospect Canyon. Surface erosion after deposition, which produces anomalously young cosmogenic dates (Cerling and Craig, 1994a), is minimal on the Prospect Canyon debris fan. The amount of pitting on limestone clasts indicates primary depositional surfaces (Hereford and others, 1997).

We sampled basalt boulders over a relatively small area on the Prospect Canyon debris fan (pl. 1). We chose boulders that were at least 1 m in diameter for cosmogenic  $^3\text{He}$  dating (Cerling and others, in press). All samples had abundant phenocrysts with few vesicles, indicating that they were derived from the interior of their respective lava flows. The outer 4 cm rind of the boulder was crushed and sieved to less than 20 mesh. Olivine separates were prepared by magnetic separation, heavy liquids, and hand picking. Samples were crushed under high vacuum to release mantle helium contained in inclusions for separate analyses.

Powders and uncrushed phenocrysts were melted at  $1,800^\circ\text{C}$  in a modified Turner-type furnace, and the liberated gas was purified using getters and cryogenic traps. Isotope measurements were made on a VG 5400 mass spectrometer fitted with electron multiplier and pulse-counting electronics.  $^3\text{He}/^4\text{He}$  ratios

were standardized against the SIO-MM standard at 16.45  $R_a$  (where  $R_a$  is the atmospheric  $^3\text{He}/^4\text{He}$  ratio). All values were corrected for interference peaks and instrumental and extraction blanks (Poreda and Cerling, 1992; Poreda and Farley, 1992).

Corrections were made for contamination, radiogenic  $^4\text{He}$ , and local shielding.  $^4\text{He}$ ,  $R/R_a$  (melt), and  $R/R_a$  (crush) were corrected for air contamination using measured  $^{22}\text{Ne}$  concentrations, assuming that all  $^{22}\text{Ne}$  was from air. Samples were corrected for the mantle component of  $^3\text{He}$  using the  $R/R_a$  value determined from crushed phenocrysts. Occasionally, crush values gave  $R/R_a$  ratios less than 1 indicating contamination of a highly radiogenic component. If after correction for blanks and air contamination the  $R/R_a$  ratio was lower than the crush value, we assumed that the residual  $^4\text{He}$  was radiogenic. Background values for  $^3\text{He}$  and  $^4\text{He}$  are  $13,500 \pm 5,000$  atoms and 0.1 ncc, respectively, and hot blank values for  $^3\text{He}$  ranged between 0.01 and  $0.07 \cdot 10^6$  atoms per run over the 2-year period of analysis.  $^3\text{He}_c$  values were corrected to the surface ( $z=0$ ), and local production rates at  $z=0$  were corrected for skyline shielding ( $P^*_{z=0}$ ) using the relation of Nishiizumi and others (1989). Replicate samples of  $^3\text{He}$  from the well-dated Tabernacle Hill basalt (17.4 ka) yield 6.2 at/gm, and our calibration is based on a high latitude (greater than  $60^\circ$ ) and sea level  $^3\text{He}_c$  production rate of 115 at  $\text{gm}^{-1} \text{yr}^{-1}$  (Cerling and Craig, 1994a). No corrections were made for changes in the  $^3\text{He}_c$  production rate due to changes in secular variation or in the strength of the Earth's magnetic field because accurate data are not available. Age is given as the absolute age in ka, calculated from calibrated  $^{14}\text{C}$  years before present. Sample localities and shielding information are given in table 1 and Cerling and others (in press).

## $^{14}\text{C}$

We used radiocarbon ( $^{14}\text{C}$ ) analyses to date debris-flow deposits on the Prospect Canyon debris fan. We gathered and analyzed various types of organic detritus, including pieces of driftwood and small twigs, from the top of several debris-flow surfaces (table 2). In terms of association between the organic material and the transporting event, the samples most suitable for dating appeared to be fine organic debris wrapped around or pinned beneath cobbles and boulders in debris-flow levees. Woody detritus, particularly driftwood, was abundant on debris-flow surfaces, but a firm link between the wood and a transporting debris flow

usually was difficult to establish. No organic material was observed at depth in the debris-flow deposits. The resulting radiocarbon ages older than AD 1950 were converted to calibrated calendar years using computer routines (Stuiver and Becker, 1993; Stuiver and Reimer, 1993). For post-bomb dates, we used or extrapolated calibration curves presented in Baker and others (1985) and Ely and others (1992).

## $^{137}\text{Cs}$

$^{137}\text{Cs}$  is a human-produced isotope that was injected into the atmosphere during above-ground nuclear testing, mostly from 1952 to 1963 (Ely and others, 1992). Fallout distributed  $^{137}\text{Cs}$  worldwide, and in alkaline environments,  $^{137}\text{Cs}$  delivered in rainfall quickly sorbed to clays and other sediments in the upper soil horizons. We evaluated  $^{137}\text{Cs}$  activities in prehistoric colluvial wedges and in the oldest debris-flow surface as part of this study.  $^{137}\text{Cs}$  has a half-life of 38 years and remains measurable in atmospheric fallout. We used  $^{137}\text{Cs}$  dating to distinguish pre- and post-1952 deposition, following Ely and others (1992). Sediment samples containing particles less than 2 mm in diameter were collected from each of the debris-flow deposits, at three levels in a deposit of Holocene age, and from a colluvial wedge at the head of Prospect Canyon (table 3). In one case, a less than 63- $\mu\text{m}$  fraction was analyzed.

## Pedogenic Calcium Carbonate

Soils on the oldest surfaces are weakly developed but contain pedogenic calcium carbonate, which is reflective of the age of the soil and the underlying parent material (Birkeland, 1984). The greatest accumulation of  $\text{CaCO}_3$  in soils on the Prospect Canyon debris fan is Stage I carbonate morphology (see Machette, 1985, for a description of carbonate stages) with a maximum accumulation at about 0.50 m depth. In the hot desert soils of the southwestern United States, this amount of accumulation generally occurs in surfaces deposited in the latest Pleistocene or Holocene (Machette, 1985, table 2). Hereford and others (1996) also used soil carbonate to differentiate the ages of debris flows in Grand Canyon.

Models of carbonate accumulation in desert soils help constrain the rates of soil formation in deserts (McFadden and Tinsley, 1985). These models of soil-forming processes do not completely apply given the semiarid and hot conditions of the Prospect Canyon

**Table 1.** Data for cosmogenic  $^3\text{He}$  analyses of basalt samples from the Prospect Canyon debris fan (from Cerling and others, in press). The surfaces are shown in Plate 1. The age given in parentheses is an average of the sample data; see text for details.

Boulder number	$^3\text{He}$ blank (percent)	$^4\text{He}$ (ncc gm $^{-1}$ )	R/R $_a$ melt	$^3\text{He}_c$ (percent)	$^3\text{He}_c$ (10 $^6$ at gm $^{-1}$ )	$^3\text{He}_c$ (x=0) (10 $^6$ at gm $^{-1}$ )	P* (at gm $^{-1}$ yr $^{-1}$ )	Age (ka $\pm$ error)
Surface tua (3.0 $\pm$ 0.6 ka)								
tfa 1	11.2	1.97	12.0	47.0	0.481 $\pm$ 0.063	0.500 $\pm$ 0.065	152	3.30 $\pm$ 0.43
tfa 1	2.0	2.59	8.1	31.6	0.254 $\pm$ 0.041	0.264 $\pm$ 0.042	152	1.74 $\pm$ 0.28*
tfa 4	9.1	1.59	7.0	83.9	0.416 $\pm$ 0.031	0.433 $\pm$ 0.032	152	2.84 $\pm$ 0.21
tfa 6	6.7	0.31	78.6	85.2	0.859 $\pm$ 0.050	0.893 $\pm$ 0.051	153	5.86 $\pm$ 0.34*
tfa 6	2.9	1.41	11.0	49.2	0.294 $\pm$ 0.035	0.306 $\pm$ 0.036	153	2.01 $\pm$ 0.24
tfa 8	4.2	0.48	51.6	83.6	0.821 $\pm$ 0.045	0.854 $\pm$ 0.047	151	5.64 $\pm$ 0.31 $\tau$
tfa 9	13.5	1.11	14.6	48.5	0.378 $\pm$ 0.058	0.506 $\pm$ 0.049	137	3.69 $\pm$ 0.36
tfa 12	12.8	0.37	30.9	69.2	0.353 $\pm$ 0.030	0.367 $\pm$ 0.031	137	2.67 $\pm$ 0.23
tfa 14	8.9	3.09	3.7	83.1	0.425 $\pm$ 0.033	0.442 $\pm$ 0.034	124	3.58 $\pm$ 0.28
tfa 15	2.8	0.88	15.8	61.0	0.339 $\pm$ 0.032	0.353 $\pm$ 0.033	124	2.86 $\pm$ 0.27
tfa 15	14.7	1.46	11.7	65.0	0.342 $\pm$ 0.039	0.356 $\pm$ 0.040	124	2.88 $\pm$ 0.33
tfa 15	11.1	0.48	50.2	76.3	0.812 $\pm$ 0.065	0.844 $\pm$ 0.067	124	6.84 $\pm$ 0.55*
Surface tia (2.2 $\pm$ 0.6ka)								
tia 24	18.8	1.58	3.9	81.1	0.232 $\pm$ 0.027	0.241 $\pm$ 0.028	136	1.78 $\pm$ 0.21
tia 25	13.9	1.91	4.8	85.8	0.341 $\pm$ 0.030	0.355 $\pm$ 0.031	136	2.61 $\pm$ 0.23
Surface tib (2.2 $\pm$ 0.4ka)								
tib 22	17.3	0.98	6.7	73.2	0.244 $\pm$ 0.029	0.254 $\pm$ 0.030	133	1.90 $\pm$ 0.23
tib 23	26.9	0.13	70.1	63.7	0.314 $\pm$ 0.054	0.327 $\pm$ 0.056	133	2.45 $\pm$ 0.42
Surface tig (1939)								
tig 16	40.1	0.12	19.3	48.7	0.084 $\pm$ 0.030	0.087 $\pm$ 0.031	126	0.69 $\pm$ 0.25
tig 17	21.6	0.92	5.2	65.0	0.180 $\pm$ 0.025	0.187 $\pm$ 0.026	126	1.48 $\pm$ 0.21
tig 18	54.4	2.15	0.9	36.6	0.077 $\pm$ 0.048	0.080 $\pm$ 0.050	126	0.63 $\pm$ 0.40

Notes: Age is given as the absolute age in ka from calibrated  $^{14}\text{C}$  yrs B.P. The R/R $_a$  ratio for crushed samples is 5.5. \*, data rejected on the basis of choice of duplicate sample; t, data possibly should be rejected because its value is high and may indicate a prior exposure history.

debris fan. Nonetheless, they predict substantial carbonate deposition in Holocene soils. In the case of a semiarid, thermic climate, the maximum accumulation of carbonate is at 0.25 to 0.70 m depth for soils about 3,000 years old (McFadden and Tinsley, 1985).

The soil carbonate stage for debris-flow deposits on the Prospect Canyon debris fan are not sufficient for determining absolute ages or distinguishing the ages of surfaces. However, the carbonate stages indicate that all surfaces are Holocene.

## Desert Plant Assemblages

Desert vegetation on the Prospect Canyon debris fan, which is similar to the common vegetation assemblages of the Mojave Desert (Phillips and others, 1987), was used to estimate relative ages of surfaces. Webb and others (1987, 1988b) and Bowers and others (1997) have shown that the species composition of desert vegetation on debris-flow deposits is related to the age of the deposit. Long-lived species such as creosote bush (*Larrea tridentata*), for example, do not

**Table 2.** Radiocarbon dates of organic material collected from debris-flow deposits at the mouth of Prospect Canyon. Known years of debris flows are given in parentheses.

Surface	Sample number	Type of organic material	Radiocarbon date $\pm$ 1 SD	Calendar date (AD)	2 $\sigma$ range in date (AD)
tif (Prehistoric)	GX-19925	Wood	485 $\pm$ 90	1434	1296–1640
tig (1939)	GX-19326	Wood	460 $\pm$ 75	1439	1327–1638
tih (1955)	GX-19320	Wood	365 $\pm$ 90	1494, 1601, 1616	1410–1954
	GX-19324	Twigs	190 $\pm$ 95	1674, 1779, 1801, 1943, 1954	1488–1955
	GX-19325	Wood	635 $\pm$ 80	1319, 1369, 1386	1259–1438
tii (1963–66)	GX-19321	Twigs	153.8 $\pm$ 1.5 PMC	1963 or 1969	n.a.
	GX-19322	Twigs	141.1 $\pm$ 1.1 PMC	1962 or 1974	n.a.
rwg (1993)	GX-19323	Twigs	127.7 $\pm$ 1.3 PMC	1959, 1961, or 1981	n.a.
tij (1995)	GX-20788	Twigs	117.5 $\pm$ 1.0 PMC	1958, 1995	n.a.

*Notes:* All  $^{14}\text{C}$  analyses were performed by Geochron Laboratories. The raw dates are in years before 1950 (yrs BP), except for those labelled with PMC (percent of modern carbon), which are post-1950. All raw values are  $\pm 1$  standard deviation. Calendar age and 2 $\sigma$  range are calculated using the calibration curves presented in Stuiver and Becker (1993) and incorporated in a computer program (Stuiver and Reimer, 1993). Post-bomb ages determined using extrapolated calibration curves given in Baker and others (1985) and Ely and others (1992). The range in age for post-1950  $^{14}\text{C}$  ages is very small. n.a., not applicable.

become established until many decades after the surface formed. The proportion of long-lived versus short-lived species increases consistently on progressively older geomorphic surfaces (Webb and others, 1988b; Bowers and others, 1997).

### Clonal Rings of Creosote Bush

Creosote bush forms clonal rings (Vasek, 1980). As the plant ages, the center of the root crown dies and the outer segment of the root crown splits into genetically identical clones. The diameter of the clonal ring that forms continues to expand radially at the average rate of 0.66 mm/yr (Vasek, 1980). The diameter of a creosote bush clonal ring, therefore, reflects the establishment date for the plant and gives a minimum age for the surface on which it is growing.

### Climatic and Hydrologic Data

No climate stations are located in the Prospect Valley drainage basin. Stations in the Grand Canyon region (fig. 1A) are 40 to 100 km from the center of the drainage (table 4). These stations have mean annual precipitation that ranges from 216 to 646 mm; the average of the 8 stations is 334 mm. Two of the stations—Tuweep Ranger Station and Grand Canyon National Park—have recording rain gages and report hourly precipitation (U.S. Department of Commerce, 1966). About 45 percent of precipitation in the Grand Canyon region occurs in winter (November–March), 43 percent in summer (July–September).

Seasonal precipitation was standardized following an existing technique (Hereford and Webb, 1992) to examine the effects of antecedent soil moisture on

**Table 3.**  $^{137}\text{Cs}$  activities of sediment collected from historical debris-flow deposits on the Prospect Canyon debris fan.

Surface (date)	Part of deposit	Activity of $^{137}\text{Cs} \pm 1 \text{ SD}$ (pCi/g)	Meaning of result	Expected result
Colluvial wedge	Surface	0.196±0.015	Detection	Detection
	15 cm	0.000±0.014	No detection	No detection
tua (1050 BC)	0-5 cm	0.917±0.053	Detection	Detection
	10-15 cm	0.075±0.009	Detection	No detection
	45-50 cm	0.009±0.003	No detection	No detection
tig (1939)	Surface	0.109±0.008	Detection	Detection
	Under rock	0.08±0.01	No detection	No detection
	Interior	0.0±0.1	No detection	No detection
	Interior	0.009±0.003	No detection	No detection
	30 cm	0.067±0.009	Detection	No detection
	30 cm	0.014±0.005	Detection	No detection
	30 cm	0.013±0.013	No detection	No detection
tih (1955)	Under rock	1.02±0.05	Detection	Detection
	Under rock	0.000±0.003	No detection	Detection
	30 cm	0.010±0.006	No detection	Detection
tii (1963/1966)	Under rock	0.2±0.1 <sup>1</sup>	Detection	Detection
	Under rock	2.43±0.11	Detection	Detection
	Under rock	0.0±0.1	No detection	Detection
	Under rock	0.0±0.1	No detection	Detection
	Under rock	0.0±0.1	No detection	Detection
	Surface	0.299±0.017	Detection	Detection
	Interior	0.000±0.005	No detection	Detection
	Interior	0.069±0.007	Detection	Detection
	30 cm	0.076±0.010	Detection	Detection
	30 cm	0.043±0.008	Detection	Detection
	30 cm	0.046±0.005	Detection	Detection
rwc (1993)	Surface	0.09±0.01	Detection	Detection
	Surface	0.050±0.006	Detection	Detection
tij (1995)	Surface	0.021±0.006	Detection	Detection

Notes: All analyses were performed on <2 mm fraction except (<sup>1</sup>), which was performed on <0.063 mm fraction. All values are ±1 standard deviation. Detection indicates post-1952 deposition or contamination; no detection indicates pre-1952 deposition or dilution of post-1952 sediments.

**Table 4.** Characteristics of climate stations in the vicinity of Prospect Canyon. Locations of climate stations are shown in figure 1.

Station name	Distance from centroid of Prospect Canyon (km)	Elevation (m)	Record length (month/year)	Mean annual precipitation (mm)	Summer precipitation (percent)	Winter precipitation (percent)
Bright Angel Ranger Station	100	2,726	7/48-3/95	646	29	60
Grand Canyon	90	2,204	10/04-3/95	403	42	46
Mount Trumbull <sup>1</sup>	51	1,818	10/20-12/78	297	49	37
Peach Springs	56	1,613	7/48-3/95	280	45	43
Phantom Ranch	96	834	8/66-3/95	234	39	49
Seligman	75	1,704	12/04-3/95	293	49	40
Supai <sup>1</sup>	50	1,039	6/56-2/87	216	46	41
Tuweep Ranger Station <sup>2</sup>	40	1,551	7/48-12/86	306	42	43

*Notes:* <sup>1</sup>Station discontinued. <sup>2</sup>In 1986, Tuweep Ranger Station was discontinued as a cooperative observer station, which records rainfall in 0.01 in. accuracy and reports in increments of daily rainfall. A tipping-bucket recording rain gage, which records rainfall in 0.10 in. increments and reports hourly as well as daily rainfall (for example, U.S. Department of Commerce, 1966), remains in operation.

debris-flow initiation. We identified the two seasons of summer (July–September) and winter (November–March). For winter precipitation, November and December totals were considered part of the following year. For each climate station (table 4), we calculated the standardized seasonal precipitation,  $P_s$ , by

$$P_s = \sum[(x_i - \mu_i)/\sigma_i]/N, \quad (1)$$

where  $x_i$  = annual seasonal rainfall for climate station  $i$  (mm);  $\mu_i$  = the mean;  $\sigma_i$  = the standard deviation of seasonal rainfall for climate station  $i$  (mm); and  $N$  = the number of climate stations with data.

We estimated the probability of daily precipitation and storms on known or probable dates of debris flows. We considered the duration of a storm to be the number of consecutive days with rainfall irrespective of the number of sources of precipitable moisture. We used a modified Gringorten plotting position (U.S. Water Resources Council, 1981):

$$p = ((m - 0.44)/(n + 0.12)) \cdot d, \quad (2)$$

where  $p$  = probability of the daily precipitation or storm ( $\text{yr}^{-1}$ ),  $m$  = the ranking of the event,  $n$  = the number of days in the record (days), and  $d$  = the number of days in the season (days/yr). The recurrence interval,  $R$  (yrs), is

$$R = 1/p. \quad (3)$$

Streamflow data were obtained for two gaging stations on the Colorado River (fig. 1): the Colorado River near Grand Canyon, Arizona (09402500; Garrett and Gellenbeck, 1991) and the Colorado River above Diamond Creek near Peach Springs, Arizona (09404200; unpublished data). Flood frequency for the Colorado River near Grand Canyon was estimated using the log-Pearson type III distribution (U.S. Water Resources Council, 1981). Data from the gaging station above Diamond Creek were used to estimate discharges in the Colorado River immediately after the 1995 debris flow using a travel time of 9 hrs in the intervening reach (S. Wiele, U.S. Geological Survey, written commun., 1995).

Streamflow is not measured in either Prospect Valley or Prospect Canyon. On the basis of regional regression equations (Region 10; Thomas and others, 1994), we estimated the streamflow flood frequency for Prospect Valley. The estimated 2-year flood is only  $6 \text{ m}^3/\text{s}$ , but the estimated 50- and 100-year floods are 500 and  $800 \text{ m}^3/\text{s}$ , respectively. The actual long-recurrence interval discharges in Prospect Canyon may be less than the estimated discharges because of attenuation of flow through the meandering, braided channel of Prospect Valley. Also, the main channel and its tributaries are dammed by six small stock tanks (five stock tanks are shown in fig. 1B), which would reduce runoff reaching Prospect Canyon.



## Characterization of Debris Flows and Debris Fans

Particle-size distributions for debris-flow surfaces and fresh debris-flow deposits were estimated using several techniques. Point counts (Wolman, 1954; Melis and others, 1994; Rice and Church, 1996) were made every 1–2 m, depending on the size of particles, along a tape measure stretched across the surface; the sizes of all particles with an intermediate (b-axis) diameter greater than 2 mm were recorded. We chose at least 100 particles in each point count, which theoretically would result in standard errors of estimate of less than  $\pm 20$  percent (Rice and Church, 1996). In one pit dug in the 1995 debris-flow deposit, we recorded all particles greater than 16 mm collected from a 1 m<sup>3</sup> volume. In most cases, a sample was collected and dry sieved to determine the size distribution of particles smaller than 16 mm. Point count and sieve data were combined by weighting the data obtained by sieve analysis relative to the percentage of particles less than 16 mm determined by point counts (fig. 4). We use the standardized size classes for sediment (Folk, 1974; Friedman and Sanders, 1978), except we prefer the term gravel instead of pebbles for particles between 2 and 64 mm diameter.

For all particles greater than 2 mm measured with point counts, the source geologic units for particles was identified and categorized into 6 groups: basalt; sandstones from the Supai Group; Redwall Limestone (including Temple Butte Limestone); Muav Limestone; and undifferentiated limestone, which includes the Kaibab Limestone and Toroweap Formation, limestones from the Supai Group, and indistinctive particles from the Redwall, Temple Butte, and Muav Limestones (fig. 5). All particles that could not be classified into one of these groups were assigned to an unknown-source group. We estimated the weight of the largest boulders transported in Prospect Canyon and deposited on several debris-flow surfaces (Melis and others, 1994; Melis, 1997). An arbitrary number of boulders—usually 10—were selected. The boulder shape determined how the weight was estimated. For example, we measured length, width, and height of rectangular particles but only the diameter of spherical particles. We then calculated the volume of each particle and estimated its weight using a density of 2,650 kg/m<sup>3</sup> for limestone and sandstone and 2,700 kg/m<sup>3</sup> for basalt.

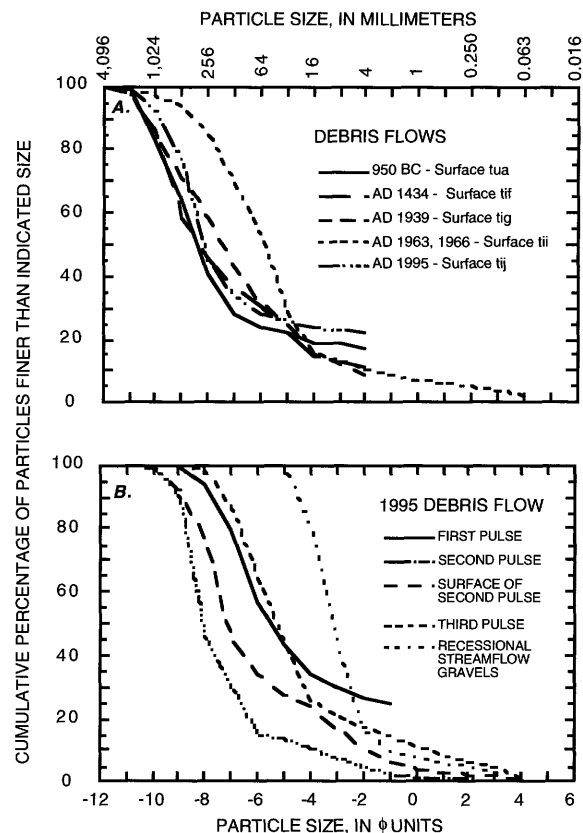


**Figure 4.** Particle-size distributions for debris flows in Prospect Canyon. A, Prehistoric and historical debris flows (see pl. 1 for unit descriptions). B, Pulses of debris flow and recessional flow during the 1995 event.

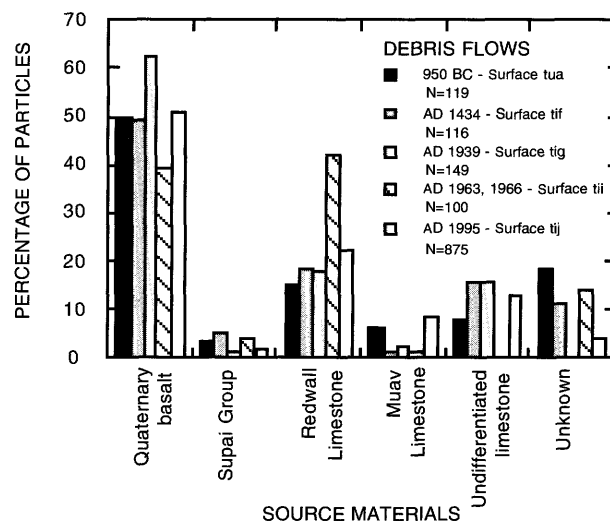


**Figure 5.** Source materials transported by five debris flows in Prospect Canyon.

We estimated the discharge of three historical Prospect Canyon debris flows from depositional and photographic evidence along or upstream from section A - A' (fig. 6, pl. 1). The surface of a moving fluid typically rises on the outside of a bend and drops on the inside. The difference in flow elevation is attributable to centrifugal forces exerted on the fluid mass and is termed "superelevation" (Apmann, 1973). The mean velocity ( $V_s$ ) is related to the difference between the flow elevations on the outside and inside of the bend by

$$V_s = (g \cdot R_c \cdot \Delta H_s / T_c)^{0.5}, \quad (4)$$

where  $g$  = acceleration due to gravity ( $9.8 \text{ m/s}^2$ ),  $R_c$  = the radius of bend curvature along the channel centerline (m),  $\Delta H_s$  = the elevation difference at the point of maximum superelevation (m), and  $T_c$  = channel width (m). We estimated discharges using

$$Q = A \cdot V_s, \quad (5)$$

where  $A$  = cross-sectional area ( $\text{m}^2$ ). However, Webb and others (1989) and Melis and others (1994) report significant overestimation of discharge using  $V_s$  and the area of the cross section measured in the bend. To obtain  $A$ , the water surface described by  $\Delta H_s$  is assumed linear, although it is likely non-linear (S-shaped). A more accurate discharge estimate is obtained using the cross-sectional flow area slightly downstream from  $A - A'$  where  $\Delta H_s = 0$ .

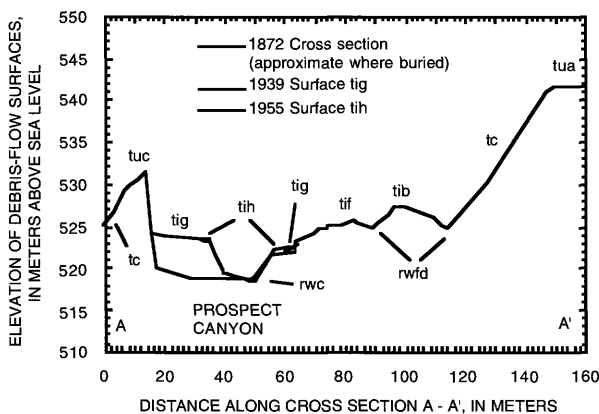


**Figure 6.** Cross section showing the relative elevations and positions of the upper and inset debris-flow surfaces along section A - A' (see pl. 1).

We estimated the water content of the less than 16 mm fraction by gradually adding water to a 5-kg sediment sample in a laboratory tray and observing the point when its flow properties became debris-flow like (Melis and others, 1994). Our method differs from other volumetric approaches (Johnson and Rodine, 1984; Cannon, 1989) because large boulders make accurate estimation of sample volumes prohibitively difficult. Rehydrated samples from debris-flow deposits typically exhibited debris-flow behavior (for example, particle support and levee formation) over a 1-2 percent range in water content, whereas rehydrated samples from hyperconcentrated-flow deposits did not exhibit debris-flow behavior at any water content.

Unit stream power is estimated from

$$\omega = \gamma \cdot Q \cdot S/T_{ave}, \quad (6)$$

where  $\omega$  = the stream power per unit width of channel ( $\text{W/m}^2$ ),  $\gamma$  = the unit weight of the flow ( $\text{N/m}^3$ ),  $Q$  = the discharge ( $\text{m}^3/\text{s}$ ),  $S$  = the energy slope of the flow (dimensionless), and  $T_{ave}$  = the width of the flow (m). For a debris flow,  $\gamma$  is a function of water content and particle-size distribution.

### Debris-fan Area and Volume

The volume of sediment deposited by Holocene and historical debris flows was estimated using a combination of surveys, image processing, and slope projection. Some deposits, such as the debris fans present in 1993 and deposited in 1995, were surveyed and areas and volumes were calculated from digital-elevation models. Others, including the debris fans in 1954, 1955, 1963, and 1964, appear in oblique aerial photographs. We used surveyed control points and the Map and Image Processing Software (MIPS) to rectify oblique aerial and ground photographs.

The accuracy of image processing varied among the debris fans on the basis of the amount of distortion in the aerial photographs, the accuracy of surveyed or orthophotograph controls, the clarity of the image, and the choice of borders between debris fans, sandbars, and water surface in the Colorado River. The river discharge at each debris fan was not the same in the before- and after-flood aerial photographs and is a source of error. Although the pixel resolution for the rectified images ranged from 0.1 to 0.5 m, rectification involved the alteration of pixel locations by as many as several meters. For consistency, we rounded all debris-

fan areas to the nearest 100 m<sup>2</sup> (implied accuracy of  $\pm 50$  m<sup>2</sup>) and all distance measurements to the nearest 1 m (implied accuracy of  $\pm 0.5$  m).

We used the topographic information in plate 1 to reconstruct the area and volume of primary debris-fan deposition. For debris fans with no photographic documentation, we projected the slope of remnant deposits toward the Colorado River until its projected elevation either intersected the water-surface profile of the river at a stage corresponding to 140 m<sup>3</sup>/s or touched the right bank. The assumption of a linear slope is justified by our direct observations of the evenness of the 1995 debris fan and other surfaces, especially surface tua (pl. 1).

Thickness of debris fans was estimated using several techniques. The depth of the 1995 debris flow was easily determined by comparison with the 1993 survey of the debris fan. The existing surface of the 1939 deposit was projected over the 1993 debris fan, and photographic evidence was used to identify points on the 1939 debris fan that had not been eroded or buried by the debris flows of 1954, 1955, 1963, and 1966. Boulders on the 1872 debris fan that were covered by 20th century debris flows but not moved by subsequent Colorado River floods provided minimum thicknesses for the deposits. We could not estimate the accuracy of the estimated thicknesses.

### Debris-fan Frequency

We used the volumes of debris flows from Prospect Canyon to estimate recurrence intervals by assuming the frequency of debris-fan production at the mouth of Prospect Canyon could be approximated using a log-normal distribution. We assumed that oblitative overlap (Gibbons and others, 1984) is not a factor in the preservation of debris flows in the late Holocene. Because debris fans do not form every year, and years with zero volume are difficult to model using log-transformed data (Kite, 1988), we chose a minimum censoring threshold volume of 3,000 m<sup>3</sup>, which also minimizes the effects of oblitative overlap of the smallest debris flows. We then used a maximum-likelihood procedure (Stedinger and Cohn, 1986; Stedinger and others, 1988) to fit a log-normal distribution to the volume data.

### Constrictions of the Colorado River

Historical debris flows from Prospect Canyon significantly constricted the Colorado River at Lava

Falls Rapid. Kieffer (1985, 1990) defined the constriction ratio as the ratio of rapid width to upstream channel width. According to Kieffer (1990), the average major rapid constricts the Colorado River by 50 percent; Melis (1997) determined the average constriction of 444 debris fans to be 42 percent. Similarly, Schmidt (1990) and Schmidt and Graf (1990) report an expansion ratio, which is the ratio of the downstream channel width to rapid width, for 70 debris fans in eastern Grand Canyon. Webb and others (1996, 1997) defined the constriction,  $C_w$ , as:

$$C_w = [1 - W_{r(ave)} \cdot (1/W_u + 1/W_d)/2] \cdot 100, \quad (7)$$

where  $W_{r(ave)}$  = the average width of the constricted channel in the rapid,  $W_u$  = the upstream channel width, and  $W_d$  = the downstream channel below the expansion zone. For the maximum  $C_w$ ,  $W_r$  is the narrowest width of the rapid.

Channel widths upstream and downstream from Lava Falls Rapid are not equal and change with stage of the Colorado River, as do rapids at other Grand Canyon debris fans (Schmidt, 1990). Because river banks typically are steep and the debris fan has a low slope,  $C_w$  increases as the discharge decreases below the stage where a significant area of the debris fan is exposed. At Lava Falls Rapid,  $C_w$  increases substantially below a discharge of about 150–200 m<sup>3</sup>/s regardless of the recent depositional history. Because of the uncertainty in image rectification and change in constriction with stage, we rounded  $C_w$  to the nearest 5 percent.

### River Velocities and Reworking

We measured surface velocities at various times in Lava Falls Rapid. For measurements during the 1996 controlled flood, we timed the movement of tetherballs released either from shore or from boats down the left and right sides of the rapid. The configuration of the tetherball float did not affect the velocity measurement; the velocities obtained with partially deflated balls, fully inflated balls, and balls with carabinier clips attached for retrieval purposes were statistically identical. River velocity was measured at times when wind velocity was minimal. The length of the velocity test was determined with tape measures stretched along the shore (an accuracy of  $\pm 1$  m over a distance of 40–70 m), and timing was to the nearest 0.1 s. Therefore, we estimated the accuracy of velocity

measurements under ideal conditions to be on the order of 0.1 m/s. Before the 1996 flood, we used various objects, including driftwood and rescue devices, to measure surface velocity and found no significant differences on the basis of object type (Webb and others, 1997).

Before the 1996 controlled flood, radio transmitters (tags) were embedded into 9 selected particles to allow tracking. We used specially built radio tags transmitting in the 40-Mhz waveband with a battery life of 30 days for maximum transmission power (Lee Carstenson, Smith-Root Incorporated, oral commun., 1996). All particles were in positions on the left side of the rapid that would be inundated by discharges between 250–280 m<sup>3</sup>/s. A radio tag was attached to the outside of a 10th particle. Three of the 10 particles were cobble size (b-axis diameter less than 256 mm); the rest were boulders (b-axis diameter greater than 256 mm).

We determined that the particles had moved on the basis of loss of signal strength received by the directional antennae. The time of initial motion during the flood was documented using both a scanning receiver attached to a data logger and an audible receiver. Radio signals from dislodged particles were faint during the controlled flood because of signal attenuation in the deep water. Weak to strong signals were detected during the steady low discharges after the flood. By triangulation with manual receivers, we located 8 of 10 radio-tagged particles after the flood. We could relocate a particle within at least a 5 m radius after the flood. The accuracy of our relocation varied with water depth, which we did not determine.

## **SURFICIAL GEOLOGY OF THE PROSPECT CANYON DEBRIS FAN**

### **General Characteristics of Debris Fans**

The Prospect Canyon debris fan (fig. 7) has a plan area of 9.2 ha and a minimum volume of 1.9 million m<sup>3</sup> above the 140 m<sup>3</sup>/s stage of the Colorado River. Of Holocene-age debris fans in Grand Canyon, the Prospect Canyon debris fan has the largest volume and second largest area; only the Kwagunt Creek debris fan has a larger area (table 5). With an average thickness of 28 m, the Prospect Canyon debris fan is the third thickest debris fans of probable Holocene age. In contrast, the Crystal Creek debris fan, which controls the second most difficult rapid in Grand

Canyon (Nash, 1989; Stevens, 1990), ranks 58th in area and 13th in volume (table 5).

In general, the Prospect Canyon debris fan is composed of two distinct types of debris-flow surfaces and several types of deposits related to other processes. The oldest and highest deposits form the overall shape of the debris fan, and we refer to these as the upper debris-flow surfaces. Subsequent erosion cut a wide channel through the debris fan, giving rise to depositional sites for inset debris-flow deposits. Inset deposits are somewhat similar to those termed channelized debris flows by Hereford and others (1993), although the magnitude of the Prospect Canyon debris flows appears to be considerably larger. Other surfaces arise from colluvial processes and reworking by the tributary and (or) the Colorado River.

Surficial deposits on the Prospect Canyon debris fan are poorly sorted mixtures of particles that range in size from clay to boulders (fig. 4A). In general, deposits from Prospect Canyon debris flows are 10 percent sand or finer; typically only 1–2 percent of the particles are silt and clay. The amount of fine-grained sediment is low compared with most debris flows in Grand Canyon, which typically have 5–10 percent silt and clay and 20–30 percent sand (Melis and others, 1994). Basaltic source material accounts for the coarseness of the deposits. Much of the sand is either suspended sediment eroded from Prospect Valley or ash from tuffs or the cinder cone on the west side of Prospect Canyon (fig. 3).

The Hermit Shale, which contributes clay to most debris flows in Grand Canyon (Griffiths, 1995), is not exposed in Prospect Canyon but is exposed in Prospect Valley. Clay particles in Prospect Canyon debris flows are mostly illite and kaolinite; their abundances are similar to those in other Grand Canyon debris flows (table 6) and the mineralogy of the Hermit Shale. Colluvium in Prospect Canyon has a similar mineralogical signature as the debris-flow deposits on the Prospect Canyon debris fan. The colluvium also contains detectable <sup>137</sup>Cs at the surface and no detectable activity at 0.15-m depth (table 3).

Between 39 and 63 percent of the clasts present in debris flows from Prospect Canyon are Pleistocene basalts (fig. 5). The lithologies of particles on debris fans vary by reach according to bedrock exposures in tributary canyons; we have not found extra local particles on Holocene debris fans in Grand Canyon. Typical Grand Canyon debris-flow deposits are dominated by clasts from the Redwall and Muav



**Figure 7.** View of the Prospect Canyon debris fan on March 7, 1995 (S. Tharnstrom). Surface tua dominates the left center of the view, with the vegetated inset surfaces appearing adjacent to the active channel. Deposition from the 1995 debris flow appears at right center adjacent to the rapid.

Limestones, as well as other Paleozoic units (Melis and others, 1994; Melis, 1997). The reason for the abundance of basalt is the large amount of locally derived Quaternary basalt in Prospect Canyon, especially in the vicinity of the waterfall (fig. 3).

### Upper Debris-flow Surfaces

#### tua

The highest surface on the Prospect Canyon debris fan, surface tua (figs. 6, 7, pl. 1), is composed of mid-Holocene debris-flow deposits. The area of this surface, the largest on the debris fan, is 4.38 ha. Surface tua accounts for about 48 percent of the entire Prospect Canyon debris fan. Although individual lobes and

snouts have surface expressions on surface tua, the surficial deposits appear to be of uniform age. Internal drainage channels, developed after debris-flow deposition, slightly dissect this surface. The average height of the surface is 28 m, but at its maximum height surface tua is about 24 m above the channel of Prospect Canyon and 33 m above the Colorado River (pl. 1). Three distinct strata appear in the vertical exposures, each of which represents deposition by an unknown number of debris flows (fig. 8). The lower strata have no preserved soils, suggesting that deposition of the main body of the debris fan occurred in one massive pulse or at a faster rate than soil-forming processes.

We analyzed  $^3\text{He}_c$  concentrations in olivine phenocrysts in 15 samples from 8 basalt boulders on surface tua (Cerling and others, in press). Young age of

**Table 5.** Rankings of the area and volume of the largest debris fans of probable Holocene age on the Colorado River in Grand Canyon National Park (after Melis, 1997).

Debris-fan name	River mile	River side	Area (ha)	Area rank	Average thickness (m)	Thickness rank	Volume (10 <sup>6</sup> m <sup>3</sup> )	Volume rank
Kwagunt Creek	56.0	R	23.5	1	23	4	1.6	2
Prospect Canyon	179.3	L	15.6 <sup>1</sup>	2	28	3	1.9	1
Nankoweap Creek	52.2	R	11.3	3	11 <sup>2</sup>	61	0.12	20
194-Mile Canyon	194.5	L	9.5	4	n.d.	n.d.	n.d.	n.d.
Whitmore Wash	188.1	R	8.2	5	7	92	0.087	26
Palisades Canyon <sup>3</sup>	65.5	L	7.5	6	8	86	0.96	3
Fossil Canyon	125.0	L	6.2	7	17	21	0.18	11
Gateway Canyon	171.5	L	6.2	8	9	74	0.14	15
Basalt Canyon	69.6	R	6.2	9	17	20	0.26	7
Espejo Creek	66.8	L	5.2	10	n.d.	n.d.	n.d.	n.d.
192-Mile Canyon	191.8	L	5.0	11	n.d.	n.d.	n.d.	n.d.
Tanner Canyon	68.5	L	4.9	12	n.d.	n.d.	n.d.	n.d.
220-Mile Canyon	220.0	R	4.4	13	n.d.	n.d.	n.d.	n.d.
Unnamed	49.8	R	4.3	14	14	37	0.11	21
Soap Creek	11.2	R	4.2	15	14	36	0.26	8
Crystal Creek	98.2	R	2.3	58	8	87	0.026	59
Unnamed	23.5	L	.62	217	33	2	0.21	9
Unnamed	139.5	R	.32	314	37	1	0.16	13

*Notes:* n=529 for area, n=144 for thickness, n=140 for volume. All values are for debris fans above about 140 m<sup>3</sup>/s discharge in the Colorado River and only include the area of Holocene debris-flow deposition. Areas of sand bars, debris bars, and colluvium are not included. Debris fans reported in Hereford and others (1996) in eastern Grand Canyon are not included, with the exception of the Palisades Creek debris fan, which is of late Holocene age. The entire Nankoweap Canyon debris fan is possibly the largest in Grand Canyon but the highest section is at least 200 ka old (Hereford and others, 1997). Data is unavailable for the entire Unkar Creek debris fan; only the most recently active section is included in Melis (1997). The Comanche Creek debris fan, which appears to be mostly of Pleistocene age, would probably rank third in area. n.d., no data.

<sup>1</sup>Includes greater downstream area than 9.2 ha area cited in text and shown on plate I (from Melis, 1997). For consistency in the other debris-fan areas from Melis (1997), we used this value.

<sup>2</sup>Estimated from Hereford and others (1997).

<sup>3</sup>From Hereford (1996).

deposition, combined with the low elevation of the site and shielding by canyon walls, yielded relatively small amounts of cosmogenic <sup>3</sup>He<sub>c</sub> and therefore complicated the dating. These samples had relatively low blank values (in one case, the R/R<sub>a</sub> for the melt was less than 1.0), but some of the splits had R/R<sub>a</sub> ratios for the melt that were lower than the crush values after correction for blanks and air, which is indicative of a radiogenic <sup>4</sup>He component (for example, sample 14 from tua; samples 24 and 25 from tia; samples 17 and 18 from tig; table 1). Because the correction for inherited <sup>3</sup>He is based on the measured <sup>4</sup>He concentration, this introduces some uncertainty into the analysis. For the samples in this study, the maximum difference in the calculated cosmogenic <sup>3</sup>He concen-

trations was 0.3 · 10<sup>6</sup> at/gm or less. An uncertainty of this magnitude is small for old samples, but is significant in this study where the total <sup>3</sup>He<sub>c</sub> is on the order of 0.5 · 10<sup>6</sup> at/gm or less.

The 12 analyses from surface tua yielded an average <sup>3</sup>He<sub>c</sub> age of 3.7 ka (table 1). Of these analyses, six yielded <sup>3</sup>He<sub>c</sub> ages between 2.6 and 3.6 ka; two analyses gave younger ages and four yielded older ages. Several of the duplicate samples showed significantly older or younger dates than the remainder for the same boulder; for example, for sample 15 we obtained <sup>3</sup>He<sub>c</sub> ages of 2.86, 2.88, and 6.84 ka (table 1), which suggests the 6.84 ka date should be discarded. Eliminating the three incongruous duplicate samples (two high, one low; table 1), we obtained a date of 3.3±1.0



**Table 6.** Mineralogy of the clay-size fraction of Prospect Canyon debris flows compared with other Grand Canyon debris flows.

Sample	Illite	Kaolinite	Smectite	PERCENT OF PARTICLES		
				Quartz	Carbonate	Other
		Grand Canyon debris flows <sup>1</sup>				
Mean	46	28	5	7	5	9
SD	15	10	12	4	5	13
		Prospect Canyon debris flows				
Colluvium	36	24	2	13	21	4
AD 1939	21	28	12	8	18	13
AD 1995	34	38	4	7	15	2

Notes: Semiquantitative clay mineralogy analyses were done by X-ray diffraction techniques and are accurate to  $\pm 20$  percent.

<sup>1</sup>Statistics are for 12 historical debris flows in Grand Canyon (P.G. Griffiths and R.H. Webb, unpubl. data).

ka. For sample 8, we obtained an age of 5.64 ka with no duplicate, and eliminating this analysis yielded an average age of  $3.0 \pm 0.6$  ka. Given these uncertainties, we believe that the most parsimonious estimate of the cosmogenic exposure age of surface tua is about 3.0 ka, which we consider to be the maximum age of the debris fan surface.

No organic material suitable for  $^{14}\text{C}$  was found on surface tua or within the deposit. As expected, samples from the prehistoric terrace had detectable activities of  $^{137}\text{Cs}$  in the surface and at 0.10- to 0.15-m depth, but no detectable activity at 0.5 m depth (Table 3).

Soils are weakly developed on surface tua. Although desert pavement is not well developed, cryptobiotic crusts are common in the fine-grained soil between the boulders indicating a relatively stable surface. The soil has a thin and weakly developed A horizon, Stage I carbonate accumulations on particles in the C horizons, and no cambic development in the profile. The maximum carbonate accumulation is at 0.50 m depth. Such soil profile is indicative of a surface of Holocene age. The Toroweap Fault crosses the Prospect Canyon debris fan (fig. 3) without a rupture in surface tua (Jackson, 1990a, b). Using regional correlation of soil morphology, Jackson (1990a) estimated the age of the most recent rupture in Prospect Valley at 3.1 ka, which suggests that the  $^3\text{He}$  age is a reasonable maximum estimate.

The soil parent material on surface tua is very poorly sorted with  $D_{50} = 0.35$  m (fig. 4A) and boulders up to 3 m in diameter; larger boulders up to 5 m in diameter have fallen from the side of the deposit onto lower surfaces. The larger particles, which are suban-

gular to rounded, consist of basalt (50 percent), limestones (25 percent), sandstones from the Supai Group (4 percent), and unknown rock types (21 percent) (fig. 5). The limestone and sandstone clasts are highly weathered with slight to moderate coatings of desert varnish, and the undersides of basalt clasts have a slight orange coloration.

The desert plant assemblage on surface tua is dominated by creosote bush with 19 percent cover (Bowers and others, 1997). Mormon tea (*Ephedra nevadensis*) and Engelmann's prickly pear (*Opuntia engelmannii*) also contribute significant cover. Barrel cactus (*Ferocactus cylindraceous*) is very prominent on this and the other upper debris-flow deposits. Creosote bush forms distinct clonal-ring structures between 1.02 and 1.35 m in diameter on this surface. Using Vasek's (1980) relation, we determined that the original plants were established between AD 0 and 500, which suggests a minimum age of 1.5 ka for surface tua.

## tub

Surface tub is a poorly defined swale of about 0.15 ha between units tua and tuc on the downstream side of the Prospect Canyon debris fan (pl. 1). The deposit appears to be the remnant of a late Holocene debris flow that lapped onto and is inset into surface tua. Exposures of the deposit underlying surface tub show poorly sorted sediment; most of the largest particles are cobbles, although some boulders are present. The vegetation on surface tub is similar to that on tua, except that Engelmann's prickly pear forms dense stands at the distal end of the surface.



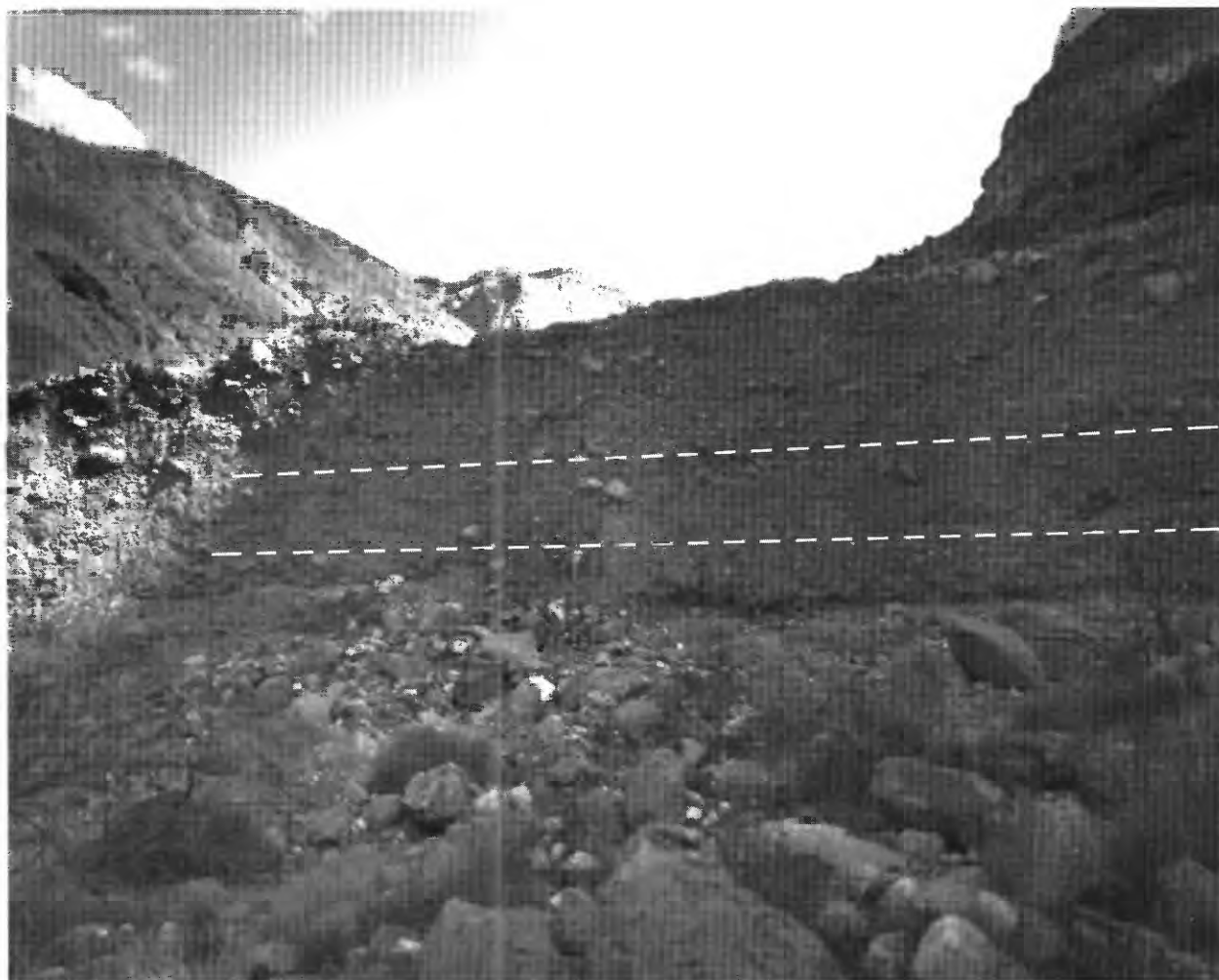


**Figure 8.** View showing the stratigraphy of surface tua (1050 BC) on the Prospect Canyon debris fan. Note the person standing with a stadia rod in the center of the view. Dashed lines indicate the approximate contact points between stratigraphic layers.

## tuc

This surface is inset against surfaces tua and tub at about the same elevation (pl. 1). The deposit consists of poorly sorted sediments with boulders up to 3 m in diameter. One or more beds of very poorly sorted, subangular to rounded clasts of basalt, limestone, and sandstone are present. Larger clasts have Stage I calcium carbonate coatings that are maximum on bottoms but also present on the sides and top. Surface weathering of limestone boulders is less intense on this surface than on tua, possibly owing to greater erosion of the smaller surface tuc. The deposit has a vertical exposure of approximately 8 m. The desert plant assemblage on this surface, which has an area of only 364 m<sup>2</sup>, is similar to that on surface tua.

## Inset Debris-flow Surfaces

### tia

This triangular-shaped remnant of a debris-flow levee is the oldest of the inset debris-flow deposits on the Prospect Canyon debris fan. The surface, which has an area of 800 m<sup>2</sup>, consists of poorly sorted deposits with occasional boulders that have fallen from surface tua. Unlike other inset surfaces, large open areas with fine-grained sediment characterize this surface; cryptobiotic crusts are common. The larger particles are subangular to rounded clasts of moderately varnished basalt and moderately weathered limestone and sandstone. Most clasts of Redwall Limestone show

moderate pitting and some sandstone clasts have disintegrated.

$^3\text{He}_c$  concentrations in olivine phenocrysts in two basalt samples from surface tia (table 1) indicate an average age of  $2.2 \pm 0.6$  ka (250 BC). The selection of boulders for cosmogenic work on surface tia is more limited than on surface tua because the fan area is much smaller and there is potential for contamination by boulders fallen from surface tua. We avoided boulders that appeared to be talus and only collected two boulders from surface tia; hence, the uncertainty in the cosmogenic age may be much greater than indicated by statistics. The  $^3\text{He}_c$  age is younger than surface tua, which is in accord with the inset stratigraphic relation between the two surfaces.

The soil on surface tia has a weak A horizon and Stage I carbonate on clasts similar to surface tua. Maximum carbonate development is at 0.50 m; below a depth of 1.0 m, carbonate coatings on clasts are very weak. The vegetation is mostly creosote bush with scattered shrubs and barrel cacti; the creosote bush clonal rings range in diameter from 0.60 to 1.50 m, which indicates establishment between 300 BC to AD 1100, and a minimum age range of 0.8 to 2.3 ka.

#### tib

This surface, with an area of 0.28 ha, is the largest of the inset surfaces of Prospect Canyon (pl. 1) and is inset against surface tua (fig. 6). An internal drainage channel bisects the surface into eastern and western segments. Sediment is poorly sorted with boulders up to 3 m in diameter. Larger boulders that fell from surface tua lie on the surface. Clasts on surface tib are weathered and varnished slightly less than similar clasts on surface tia, and some appear to have faint percussion marks.

$^3\text{He}_c$  concentrations (table 1) indicate an age of  $2.2 \pm 0.4$  ka (250 BC) for surface tib. As with surface tia, the selection of boulders for cosmogenic  $^3\text{He}_c$  analyses was limited by the small fan area and the potential for contamination by fallen boulders. We selected two boulders that could not have fallen from surface tua. The  $^3\text{He}_c$  age of surface tib is younger than surface tua and equal to the age of surface tia. Based on the geometry of the surfaces, surface tib is younger than surfaces tua or tia.

The soil developed on surface tib has a weakly developed A horizon and Stage I carbonate that is similar to the soil developed on tia. Creosote bush dominates the desert plant assemblages; most clonal

rings range between 0.10 and 0.60 m in diameter, indicating establishment between AD 1100 and 1800. Mormon tea and California buckwheat (*Eriogonum fasciculatum*) are common shrubs on this surface, and barrel cacti are particularly large and numerous.

#### tic

Surface tic, a large push-out lobe superimposed on surface tib, occupies 314 m<sup>2</sup> near the apex of the Prospect Canyon debris fan (pl. 1). The downslope side of the surface appears to be a relict snout. The soil development and weathering of clasts are similar to those of surfaces tia and tib. Several of the largest boulders on this surface fell from surface tua. The creosote bush on this small surface form small clonal rings 0.30 to 0.50 m in diameter, which indicates they became established between AD 1240 and 1540.

#### tid

The morphology of surface tic suggests that this small, arcuate surface at the apex of the Prospect Canyon debris fan is a push-out lobe over surface tic. On its upstream side, erosion by recent Prospect Canyon debris flows—particularly the 1939 event—has created a vertical exposure of about 4 m. Because of poor sorting, lack of imbrication, and lack of soil development, a stratigraphic break could not be distinguished between surfaces tic and tid. Few plants grow on this surface because it has an area of only 190 m<sup>2</sup>. Surfaces tic and tid may have been deposited during the same debris flow, but we do not have sufficient evidence to make this conclusion.

#### tie

This small (43 m<sup>2</sup>), lobate surface overlaps surface tib. The soil properties, surface weathering, and desert varnish on surface tie indicate an age slightly younger than surface tib but perhaps similar to tic and tid. The particle-size distribution and source material for this surface are similar to other inset debris-flow deposits. This surface could be contemporaneous with surface tid; the two surfaces have no distinguishing characteristics, other than their morphology as push-out lobes, to determine their genetic link.

#### tif

Debris-flow sediments form a prominent surface along the right (east) side of Prospect Canyon (fig. 6)

and the downstream side of Lava Falls Rapid. Driftwood collected from under cobbles on surface tif yielded a radiocarbon age of  $485 \pm 90$  years BP, which corresponds to a calendar date of AD 1434 and a range of AD 1296 to 1640 (table 2). The deposit is poorly sorted with  $D_{50} = 0.35$  m (fig. 4A) and boulders up to 2.7 m in b-axis diameter (Webb and others, 1996). Snouts and boulder-strewn levees are prominent on this irregular surface. About 49 percent of the clasts are basalt and 35 percent are limestone (fig. 5). Boulders are lightly varnished, and percussion marks remain prominent.

The desert plant assemblage reflects the late Holocene age of this 0.18-ha surface. The dominants are catclaw (*Acacia greggii*), with 19.5 percent cover, and Mormon tea, with 11.5 percent cover (Bowers and others, 1997); both are long-lived species. Young barrel cacti are abundant, and California buckwheat is common around the margins of this deposit. Creosote bush are rare.

#### tig

Using photographic evidence (see below), we identified five debris flows that occurred in the 20th century. Deposits from the 1939 debris flow form extensive surfaces that are inset against surface tuc on the west and surfaces tie and tif on the east side of Prospect Canyon (fig. 6). Levee deposits on both sides have a maximum thickness of about 4 m and an area of 0.65 ha. Internal drainage between surfaces tig and tib, tic, and tid (pl. 1) is composed mostly of sand and gravel at the surface and was a conduit for recessional flow or dewatering of the 1939 deposit. Deposits underlying surface tig on the left (west) side of Prospect Canyon are 1–2 m thick over an older surface, possibly tif.

$^3\text{He}_c$  ages for boulders from surface tig are several hundred years old, averaging  $0.9 \pm 0.5$  ka (table 1). However, the  $^3\text{He}$  blank correction is as much as 50 percent of total measured  $^3\text{He}$ , a much higher blank correction than was associated with the other boulders from surfaces tua, tia, and tub. The samples from this young flow show the resolution limit of cosmogenic  $^3\text{He}$  dating. The cosmogenic ages of these boulders, on the order of 600 years or more, may be the correction that needs to be applied to the older fan surfaces for cosmogenic  $^3\text{He}$  inherited from a previous exposure history, or they may illustrate the consequences of exceeding the minimum-age analytical bounds of the  $^3\text{He}_c$  technique.

Driftwood on top of the 1939 deposit yielded a calendar date range of AD 1327–1638 (table 2), indicating a substantial residence time for woody detritus in the Prospect Valley drainage basin. The activity of  $^{137}\text{Cs}$  was inconsistent in the 1939 debris-flow deposits (table 3). Three of seven samples had detectable activities of  $^{137}\text{Cs}$ ; although one of these samples was from the surface and was therefore exposed to fallout, the other two samples were from 0.30 m depth.

Surface tig is poorly sorted with  $D_{50} = 180$  mm (fig. 4A) and boulders with a b-axis diameter of 2.7 m (Webb and others, 1996). Sixty-two percent of the clasts are basalt (fig. 5), the highest of any Prospect Canyon debris flows. The 1939 deposit consists of at least two beds of debris-flow strata separated by tributary streamflow deposits (fig. 9). The stratigraphy represents several pulses of debris flow during a single period of runoff, which is consistent with observations elsewhere in Grand Canyon (Webb and others, 1989).

On the remnant of surface tig on the west side of Prospect Canyon, boulders are deposited around mature catclaw trees, and long-lived perennial shrubs are present downstream from most boulder piles. These plants likely pre-date the 1939 debris flow; if so, the 1939 deposit was relatively thin. Boulders on the surface show slight weathering with prominent percussion marks. Other desert plants have colonized surface tig; sweet bebbia (*Bebbia juncea*), a short-lived species, contributes 10.1-percent cover, and five other short-lived species contribute significant cover (Bowers and others, 1997). The edges of this surface were eroded during debris flows in 1955, 1963, and 1966.

#### tih

Deposits from the 1955 debris flow are preserved as eroded remnants that form small surfaces along the east and west sides of Prospect Canyon. The deposits appear superelevated along the left side of Prospect Canyon at cross section A - A' (pl. 1) and lap onto surface tig (fig. 6). The deposits consist of poorly sorted sediments approximately 0.5–2-m thick inset against, and in some cases on top of, surface tig (fig. 10). Much of the surface, which had an area of  $800 \text{ m}^2$  when it was mapped in 1993, was covered with sand and gravel that appeared to have been deposited during the recessional flow of 1955.

Three samples of driftwood and twigs on the 1955 deposit correspond to calendar age ranges of AD

1259–1438, 1410–1954, and 1488–1955, respectively (table 2), again indicating long-term storage of woody detritus in the drainage. One  $^{137}\text{Cs}$  sample collected from the 1955 deposit had a significant, high activity of  $^{137}\text{Cs}$ , as expected, but two other samples had no detectable  $^{137}\text{Cs}$  (table 3). Desert vegetation on surface tih consists of occasional catclaw and short-lived species such as poreweed (*Porophyllum gracile*). Much of surface tih that we mapped in 1993 and 1994 was eroded during the 1995 debris flow.

#### tii

The surfaces formed by deposition from the 1963 and 1966 debris flows were not differentiated on the Prospect Canyon debris fan. The undifferentiated deposits form a surface tii that has relatively fine-grained particle-size distribution, with  $D_{50} = 64$  mm (fig. 4A). This surface has poorly sorted, subangular to rounded clasts that are 39-percent basalt and 43-percent Redwall Limestone (fig. 5). Two samples of twigs from the undifferentiated 1963/1966 deposits provided post-bomb  $^{14}\text{C}$  activities that correspond to calendar date ranges of AD 1963 or 1969 and 1962 or 1974, respectively, suggesting either we selected better samples or that woody detritus may have been flushed from the drainage by previous 20th century debris flows. The activity of  $^{137}\text{Cs}$  in the undifferentiated 1963/1966 deposits was equivocal; of 11 samples, 7 had detectable activities, as expected, but 4 samples had no detectable activity (table 3). Long-leaf brick-ellbush (*Brickellia longifolia*) and other short-lived species colonized these small surfaces, which had a total area of 385 m<sup>2</sup> in 1993. Surface tii was almost totally removed during the 1995 debris flow.

#### tij

The 1995 debris flow deposited a debris fan in the Colorado River with an area of 0.56 ha. This debris flow did not create a distinct surface on the Prospect Canyon debris fan and for that reason is not included on plate 1. Most deposition was in or adjacent to the channel of the Colorado River (fig. 11A), and the large volume of recessional streamflow eroded most of the initial deposit. In addition, most of the deposits of surfaces tih and tii were removed, and the edge of surface tig was eroded in places by 1 m.

The aggraded debris fan (pl. 1) had four distinct areas of deposition and erosion that represent the different phases of the 1995 event. The first pulse of

relatively fine-grained ( $D_{50} = 50$  mm) sediments were deposited on the downstream side of the debris fan (fig. 4B). The second, or main pulse of debris flow pushed directly towards the center of Lava Falls Rapid. These sediments, with  $D_{50} = 350$  mm (fig. 4B) and boulders up to 1.6 m in b-axis diameter, composed most of the aggraded debris fan. Particles in the main pulse were 50 percent basalt and 21 percent Redwall Limestone (fig. 5). The recessional pulse of debris flow was relatively fine grained ( $D_{50} = 40$  mm; fig. 4B). The recessional streamflow deposited gravels and well-sorted sand ( $D_{50} = 10$  mm; fig. 4B) in the channel and on the debris fan.

Driftwood deposited by a small flood in 1993 (Webb and others, 1996) and the 1995 debris flow had post-bomb  $^{14}\text{C}$  activities that correspond to a calendar dates of AD 1959, 1961, or 1981 and 1958 or 1995, respectively (table 2). Two samples of sand-and-finer sediment from the 1993 flood deposit and the 1995 debris-flow deposit had detectable  $^{137}\text{Cs}$ , as expected (table 3).

### Colluvium and Steep Slopes

#### tc

Colluvium and steep slopes compose 1.12 ha of the Prospect Canyon debris fan. Unconsolidated talus displaced from nearly vertical exposures of surfaces tua and tuc (fig. 6) forms steep slopes within the incised channel of the Prospect Canyon debris fan and between the distal edge of tua and tuc and the Colorado River. The deposits consist of relatively well-sorted boulders, which are mostly basalt clasts that have fallen from near-vertical exposures. This deposit partially covers older, inset deposits along the right side of Prospect Canyon; in particular, surface tic has many boulders up to 5–6 m in diameter on its top that are part of surface tc.

### Reworked Debris-flow Deposits

#### rwr

This surface is mostly residual boulders that were the largest clasts transported by several undifferentiated Prospect Canyon debris flows. These boulders were deposited in or adjacent to the Colorado River and were exposed but were not removed by subsequent river floods. Between 1939 and 1995, these floods had discharges up to 3,540 m<sup>3</sup>/s. This deposit has an area of

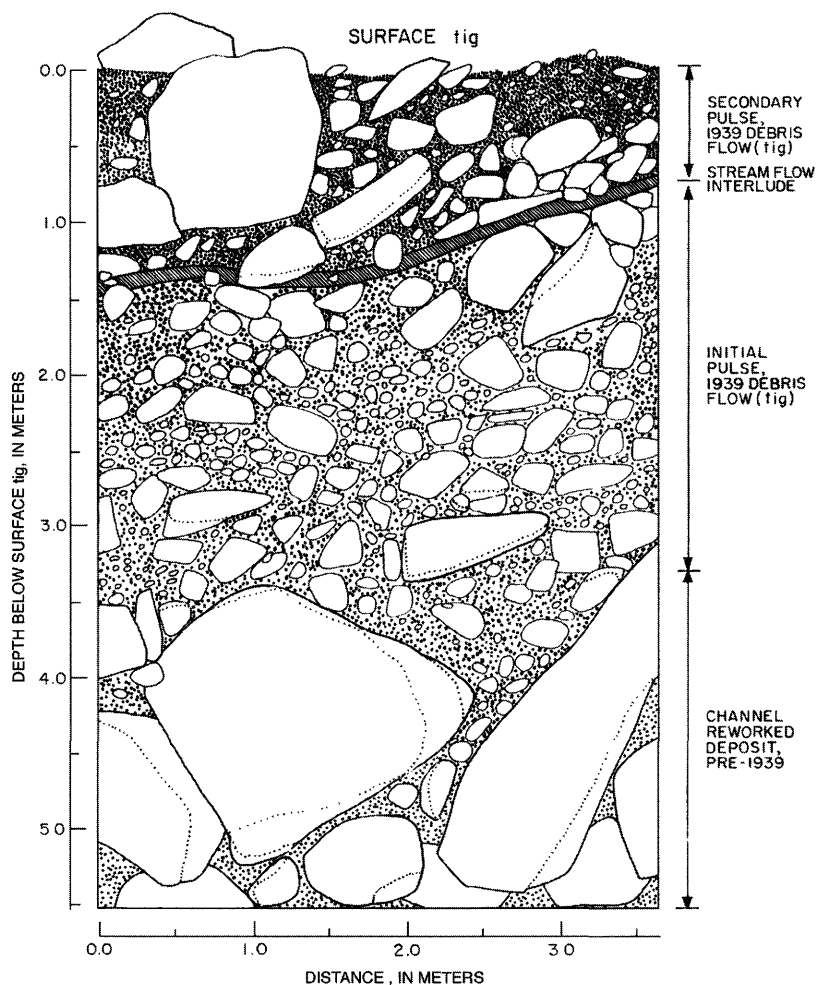


**Figure 9.** Stratigraphy of the 1939 debris-flow deposit (surface tig, pl. 1). A streamflow deposit of reddish silty sand (thin hatched band) is an intermediate phase of the event, separating the initial pulse (1.5-3.5 m) from a secondary pulse (0-1.2 m). The largest boulders at the bottom have b-axis diameters of 0.75-1.4 m.

0.74 ha above the 140 m<sup>3</sup>/s stage of the Colorado River along the edge of the debris fan. Ninety percent of the boulders are basalt, have  $D_{50} = 512$  mm, and b-axis diameters up to 3.0 m (Webb and others, 1996). Pockets of river sand occur between the boulders. The subaerial part of surface rwr adjacent to Lava Falls Rapid was covered by the 1995 debris flow, except for some isolated boulders at the downstream end of the rapid that are in the river but not submerged at a discharge of 280 m<sup>3</sup>/s.

#### rwc

Debris-flow deposits in the channel of Prospect Canyon are periodically reworked by tributary floods. Surface rwc has an area of 0.9 ha, and the underlying

deposit consists of poorly sorted sediment ranging from sand to extremely large boulders. Some of the boulders on surface rwc have b-axis diameters of 7 m (Webb and others, 1996). Boulders larger than 3 m in diameter either remained stationary or were rotated during the 1995 debris flow. In places, small flood deposits of well-sorted fine sand are present on the downstream side of obstructions such as large boulders. Deposition of these flood deposits occurred during the 1993 flood and during recessional flow following the 1995 debris flow.

#### rwd

Reworked debris-flow and streamflow deposits are present in internal drainage channels that dissect

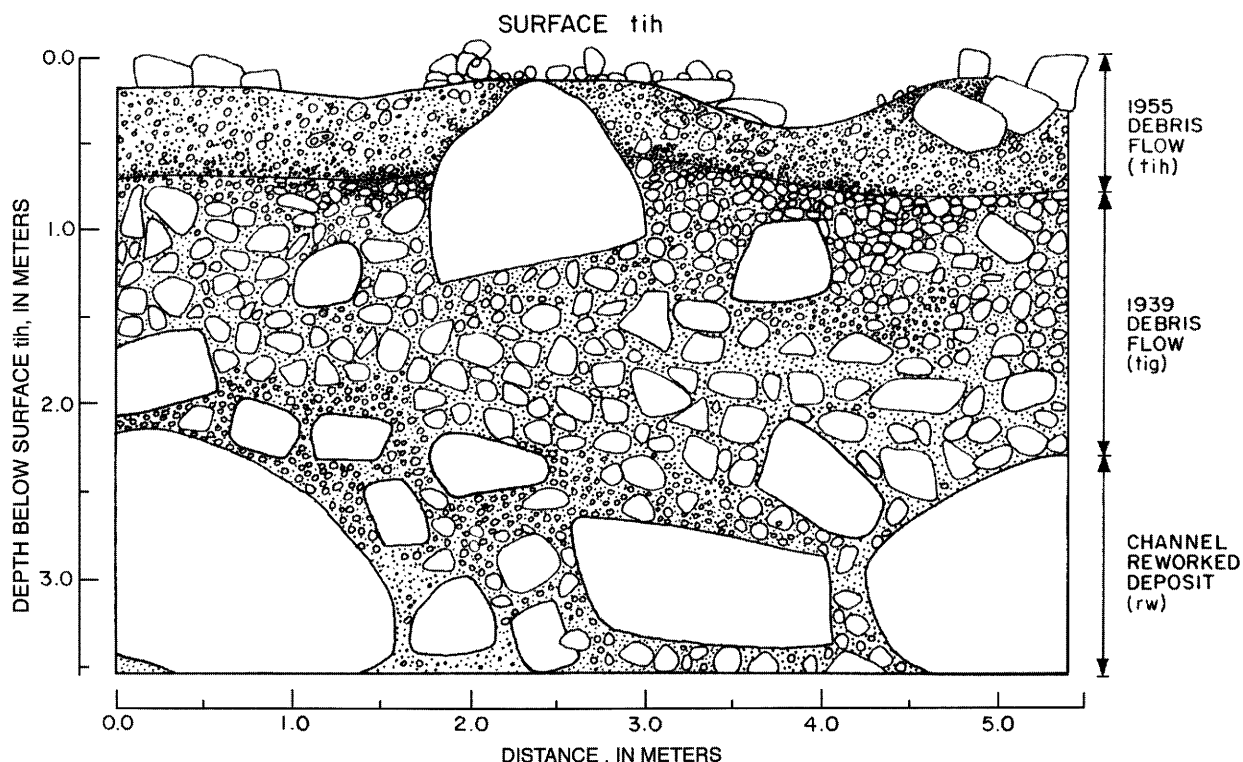


**Figure 10.** Stratigraphy of the 1955 debris-flow deposits (surface tih, pl. 1). The 1955 debris-flow deposit (0.6-1.0 m thick, tih) overlies the surface tig (1939; 0.3-2.0 m thick). Stratigraphic breaks are faint, particularly between the 1939 deposit (tig) and the underlying reworked channel deposits.

both the upper and inset debris-flow surfaces. The area of this surface is 0.32 ha (pl. 1). These channel deposits are associated with infrequent runoff generated within the Prospect Canyon debris fan. Most of the deposit underlying this surface is sand and gravel, but boulders are also present. Some of these channels could have developed during dewatering of the main debris-flow deposits and (or) recessional flow after a debris flow.

## HISTORICAL CHANGES IN LAVA FALLS RAPID

### Navigation of Lava Falls Rapid in 1994

Traditionally, river runners scout Lava Falls Rapid from the left bank for discharges greater than about 700 m<sup>3</sup>/s and from the right for lower-water routes. On the left side, the rapid is viewed from a point on surface tua called the Left Scout Point (fig. 11A). On the right side, the Scout Rock commands a full view of the rapid. The landmarks of Lava Falls Rapid have

names that are familiar to modern river guides. The most prominent features of the rapid are the Ledge Hole, the V Wave, the Big Wave, and the Black Rock (fig. 11A).

Hydraulic features in bedrock rivers have been classified by several researchers. Leopold (1969) described four types of waves according to water depth, cross-section changes, and obstacles on the bed. Kieffer (1985) described large waves as hydraulic jumps, or energy conversions from supercritical to subcritical flow. Kieffer (1987) established a lexicon for hydraulic features that we use to describe Lava Falls Rapid.

The Ledge Hole is in a class by itself as a navigational hazard. Its drop—the highest vertical fall in the rapid—is about 1.2 m. At typical water levels (150–600 m<sup>3</sup>/s), the Ledge Hole spans about a quarter of the entrance to the rapid, and water appears to pour over a fall into a recirculating hole. The linear shape of the Ledge Hole has led to speculation that a ledge or basalt dike underlies the hydraulic feature (Fradkin, 1984). At very low discharge (less than 100 m<sup>3</sup>/s), three large boulders forming the Ledge Hole are exposed. At



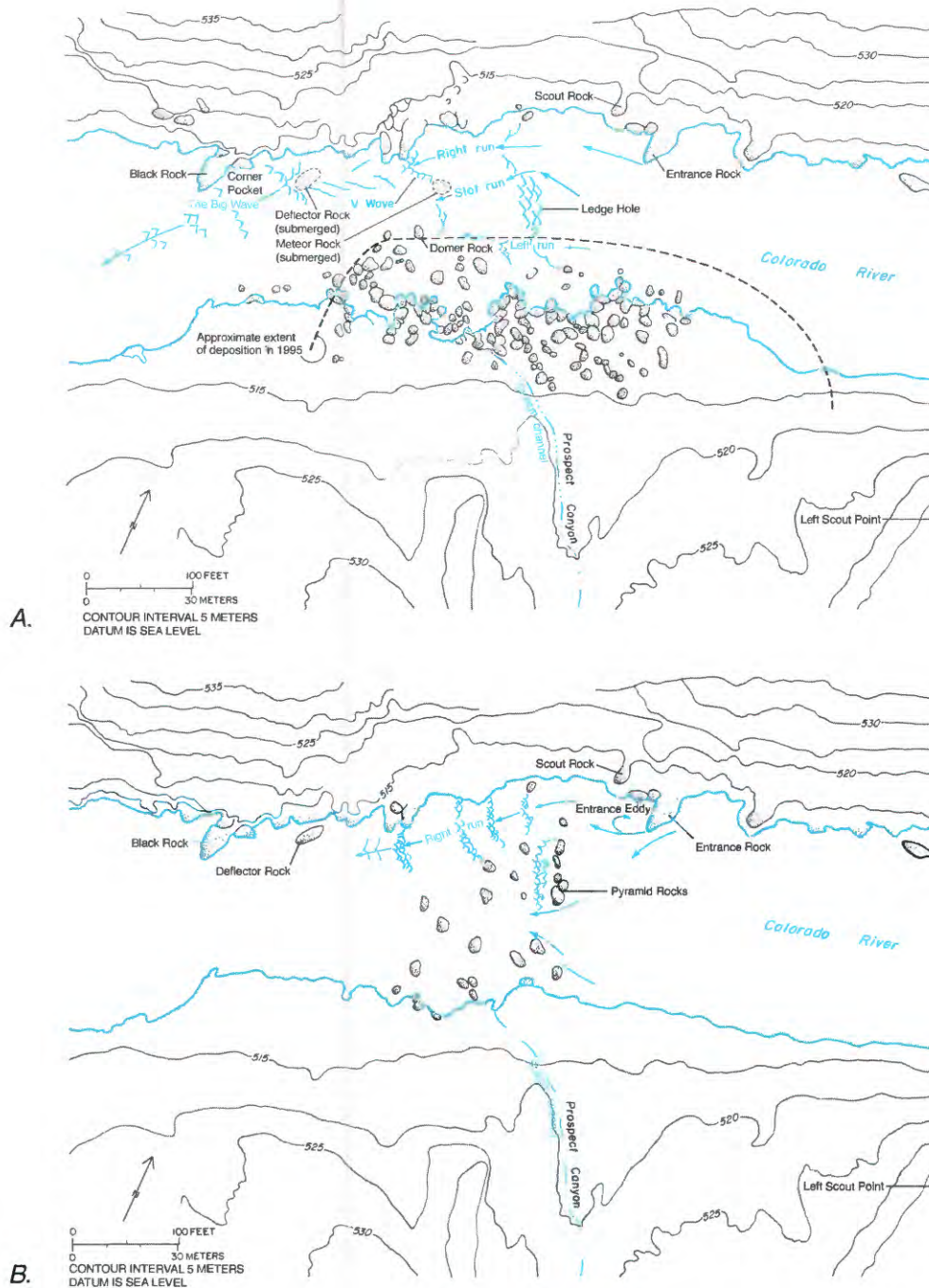


**Figure 11.** Lava Falls Rapid. *A*, Based on a 1994 aerial photograph taken at a discharge of  $234 \text{ m}^3/\text{s}$ , this map shows the modern configuration of Lava Falls Rapid, which was unchanged from 1973 to 1995. The Ledge Hole evolved during the 1950s as boulders accumulated in the center of the rapid. The V Wave is initiated by boulders near the right bank and the Meteor Rock, which probably was deposited in September 1939. The Big Wave forms by flow over the Deflector Rock, which was rotated and moved downstream during the 1939 debris flow. The Right Run, the most common route, is used at discharges less than  $850 \text{ m}^3/\text{s}$ . The Left Run is only feasible at a discharge greater than about  $600 \text{ m}^3/\text{s}$ , whereas the Slot Run is possible from about  $250\text{--}450 \text{ m}^3/\text{s}$ . The 1995 debris flow constricted the rapid by 62 percent, increased the velocity of the Right Run, made the Left Run feasible at lower discharges, and eliminated the Big Wave at most water levels. *B*, The configuration of the rapid from 1872 to 1939 was reconstructed using 37 historical photographs; the water level depicted is about  $280 \text{ m}^3/\text{s}$ . The Pyramid Rocks were prominent near the middle of what is now the entry to the Right Run and were exposed at discharges of less than about  $500 \text{ m}^3/\text{s}$ . The Deflector Rock dominated the right side of the rapid and forced flow to the left of the Black Rock. The left side of the rapid was a series of exposed or shallowly submerged boulders, although a second tongue was present on the left side of the Pyramid Rocks.



flood stage (greater than about 1,000 m<sup>3</sup>/s), the Ledge Hole becomes a massive wave.

Before the 1995 debris flow, river runners used three routes through Lava Falls (fig. 11A). Above about 600 m<sup>3</sup>/s, the Left Run opens adjacent to the left side of the Ledge Hole. At lower discharges, boulders—particularly the Domer Rock—make the left side hazardous. At intermediate discharges (300–600 m<sup>3</sup>/s), the Slot Run, on the right side of the Ledge Hole, is an option that requires a very precise entry. In the era of dam regulation, flows generally are low enough that the Ledge Hole can easily be avoided on the Right Run.

The Right Run at Lava Falls (fig. 11A) is used over most of the range of dam releases but it is by no means easy. This route requires entry close to the Entrance Rock, running a powerful lateral wave, and aligning the boat for the V Wave, a nearly symmetrical pair of reflex lateral waves that meet in the middle of the Right Run. The V Wave is generated from large boulders on the right shore and a large boulder in the rapid known as the Meteor Rock, which is submerged at most discharges and constricts the right side of the river. The pair of lateral waves that form the V Wave tend to alternately fold one over the other, adding an element of suspense as to which wave will crash on a boat first.

Once through the V Wave, boats pass through waves that are some of the biggest in Grand Canyon. On the downstream right side of the rapid (fig. 11A), the Black Rock, a large basalt boulder, diverts flow to the left. Just upstream from the Black Rock, a submerged boulder (see below) creates a large wave, appropriately called the Big Wave, which typically crashes upstream. Depending on the surges at this point, a boat can pass safely, be flipped by the Big Wave, be rafted onto the Black Rock, or be pushed into a very small, turbulent eddy called the Corner Pocket. Downstream, the tailwaves of Lava Falls Rapid dissipate into a pool.

Lower Lava Rapid is the next obstacle downstream from Lava Falls (fig. 2). This secondary rapid, formed from cobble and boulder outwash from Prospect Canyon debris fan, consists of a tight river bend against a vertical limestone cliff. Although Lower Lava Rapid is not noteworthy by itself, it forms a distinct hazard to passengers and crew when boats overturn in the main rapid upstream.

## The Wide, Stable Rapid (1872–1939)

Important factors to consider in analyzing early accounts of Lava Falls Rapid include the level of the expedition's whitewater expertise, the size and type of boats used, the context of the trip, and the discharge in the river. Advances in technique and equipment have revolutionized river running, and impressions of the severity of rapids such as Lava Falls have changed greatly during the last three decades. Three rapids—Lava Falls (mile 179.4), Separation (mile 239.5) and Lava Cliff (mile 246.0)—were serious challenges to early navigation in western Grand Canyon; explorers typically compared them (Marston, 1976). When Hoover Dam was completed in 1935 on the lower Colorado River, the rising waters of Lake Mead inundated Separation and Lava Cliff rapids.

John Wesley Powell, the first explorer of the Colorado River in 1869, was impressed with the lava flows over the rim and the severity of Lava Falls Rapid. Powell considered the rapid to be an artifact of the basalt dams that spanned the canyon. In his diary, he wrote:

Come to ... lava falls [the lava flows]. These falls must have been very great at one time. Lava comes down to high water mark — may be lower — and 1500 ft [500 m] high on either side. The cañon was filled... The falls [Lava Falls Rapid] now are among boulders some distance below the ancient fall (Cooley, 1988, p. 173).

Powell's crew thought Lava Falls Rapid was the closest thing to a waterfall that they had seen; they portaged it on the left. Powell later commented extensively on the difficulties his expedition encountered downstream at Separation Rapid (Powell, 1875), which led to the erroneous impression that Separation Rapid was a more formidable obstacle than Lava Falls (Marston, 1976). Powell's photographers travelled overland to make the first photographs of Lava Falls in April 1872 (figs. 12A and 15A; Fowler, 1972; Stephens and Shoemaker, 1987).

In the winter of 1889–90, Robert Brewster Stanton led the second complete expedition through Grand Canyon (Smith and Crampton, 1987). The goal of his expedition was to determine the feasibility of a water-level railroad from Grand Junction, Colorado, to Needles, California. He documented the route with systematic photography (Webb, 1996). On the afternoon of February 26, 1890, Stanton's expedition arrived "at the head of the great cataract formed by the lava dike" (Smith and Crampton, 1987, p. 225). The following day, the crew portaged the boats along the



left side while Stanton photographed the rapid (fig. 13A). In his diary, Stanton remarked that Lava Cliff Rapid was the most difficult whitewater he saw in Grand Canyon, as well as the most difficult place for constructing a railroad (Smith and Crampton, 1987).

Following Stanton in 1896, George Flavell, a skilled and confident outdoorsman, became the first person to navigate all three of the big rapids in western Grand Canyon (Carmony and Brown, 1987). Regarding his historic passage through Lava Falls Rapid, Flavell briefly wrote:

“A bad rapid [Lava Falls] was run which put about eight inches [200 mm] of water in the boat. It was pretty fresh, but we had to stand it” (Carmony and Brown, 1987, p. 69).

Although Lava Falls was not very challenging, Flavell was greatly impressed by Lava Cliff Rapid, which he stated “was as dangerous as any on the whole river” (Carmony and Brown, 1987, p. 70).

Two early 20th century expeditions yielded important photographs and notes on Lava Falls Rapid. In 1909, Julius Stone led a trip through Grand Canyon (Stone, 1932) with a photographer, Raymond Cogswell, who took the best set of photographs of the rapid made before the 1950’s (fig. 14). According to Cogswell’s diary,

It [Lava Falls Rapid] is impossible to run with safety, a sheer cascade of 8 feet [2.6 m]. One might scratch thru [sic]. We land stuff at head and portage down about 150 yards [146 m] to creek. Then one boat is lined and portaged down. Heavy work...The roar of the rapids and the menace of it, the spice of danger, and the thought of the comfort of a home fireside. We are jolly around the camp fire and enjoy it. This rapid full of rocks (R.A. Cogswell, unpublished diary, courtesy of the Huntington Library).

Cogswell’s photographs support his description of the length of the rapid, its fall, and the extraordinary number of exposed rocks that made navigation implausible.

Expeditions continued to photograph the rapid. The Kolb brothers, famed photographers of Grand Canyon, ran the river in the fall and winter of 1911–1912 (Kolb, 1914); they photographed Lava Falls after a portage in January 1912 (fig. 16). Other river runners photographed the rapid in 1927 and 1934 (fig. 17).

In 1923, the U.S. Geological Survey mapped potential dam sites along the Grand Canyon (Birdseye, 1924; Freeman, 1924). During the expedition, the water-surface fall of the Colorado River was measured

and “adjusted” in an undescribed manner to a uniform discharge of  $280 \text{ m}^3/\text{s}$ . Upon arrival at Lava Falls, they photographed the rapid at a discharge of  $260 \text{ m}^3/\text{s}$  but the surveying crew did not measure its fall. In the middle of the night, a flood of  $3,200 \text{ m}^3/\text{s}$  caused the river to rise 6.4 m in 24 hrs (Claude H. Birdseye, unpublished diary, 1923; Freeman, 1924), which delayed the surveying for several days. The expedition continued downstream on a discharge of about  $1,000 \text{ m}^3/\text{s}$ , and the surveyed fall of 12 m was measured over a 2.4-km distance that includes Lava Falls Rapid, Lower Lava Rapid, and several riffles downstream (Birdseye, 1924). The surveying problem generated by the 1923 survey caused the current misconception of a 12-m fall through Lava Falls (Webb, 1996).

Only five boatmen are known to have rowed boats through Lava Falls Rapid before 1940. In 1927, Clyde Eddy claimed the rapid had a sheer drop of “20 feet [6.1 m] or more” (Eddy, 1929). In December 1928, Jack Harbin, who was searching for two missing river runners, made the second successful boating run through the rapid (Cook, 1987, p. 109). According to an interview conducted by Otis “Dock” Marston in March 1948, Harbin attempted to enter the rapid on the right side but became snagged on a shallowly submerged rock. Eventually, his boat washed off of the rock but a wave in the rapid broke a board free from the boat, injuring his spine. The injury still caused Harbin problems in 1948.

The 1937 Carnegie-Cal Tech expedition chose to portage the rapid that geologist Robert P. Sharp described as “a short, nasty, rock rapids” (R.P. Sharp, unpublished diary entry for November 15, 1937; courtesy of Special Collections, Cline Library, Northern Arizona University). In July 1938, at a discharge of  $570 \text{ m}^3/\text{s}$ , Norman Nevills chose to line Lava Falls on the left, noting that the Right Run was possible but risky (Cook, 1987).

Buzz Holmstrom made the third successful passage in October 1938 (Lavender, 1985). In notes made after the trip, Holmstrom admitted to being scared, but nonetheless he began by circling in the Entrance Eddy (fig. 11B). After precisely positioning his boat, Holmstrom entered the upper hole, moved towards the left, and ducked behind what might have been the Meteor Rock (fig. 11A) to complete his run. In July 1939, Don Harris and Bert Loper also rowed down the right side at  $232 \text{ m}^3/\text{s}$  and “lightly touched a rock.”



**Figure 12.** Downstream view of Prospect Canyon and Lava Falls Rapid from Toroweap Overlook (Stake 967). A, (April 16, 1872; J.K. Hillers, courtesy of the National Archives). Lava Falls Rapid as viewed by the Powell Expedition was completely different from the rapid now familiar to thousands of whitewater enthusiasts. Using photogrammetric rectification, we found that the rapid began 85 m farther downstream on the left side, and the head of the rapid formed a line perpendicular to flow. A prominent tongue of water entered the left side of the rapid, and its tail waves at the bottom flowed directly downstream. At the discharge shown (approximately  $300 \text{ m}^3/\text{s}$ ), the area of the exposed debris fan is about 0.2 ha.



B, (June 10, 1979; R.M. Turner). After a series of debris flows from 1939 through 1966, Lava Falls Rapid changed substantially. At a discharge of about  $340 \text{ m}^3/\text{s}$  in 1979, the head of the rapid slanted downstream to the right side, and the main tongue was on the right side. The tail waves were much farther downstream and curved towards the left. Two distinct levees in the mouth of Prospect Canyon were deposited between 1872 and 1966; the largest levee was deposited by the 1939 debris flow, and the smaller, inset levee is remnant channel fill from the 1963 and 1966 debris flows. The debris-flow deposits in the mouth of Prospect Canyon are overgrown with dense riparian vegetation.

**Figure 12.** Continued.



C, (May 16, 1995; R.M. Turner). The debris flow of March 6, 1995, initially constricted the Colorado River by 62 percent, but reworking quickly widened the river and reduced the constriction, as shown here, to about 50 percent. The constriction increased the drop through Lava Falls Rapid, accentuating its hydraulics, but some formerly prominent waves, such as the Big Wave, were not present. The 1963 and 1966 debris-flow deposits were completely eroded from the margins of Prospect Canyon. At this discharge of about  $260 \text{ m}^3/\text{s}$ , the exposed area of the new debris fan is 0.62 ha.

**Figure 12.** Continued.



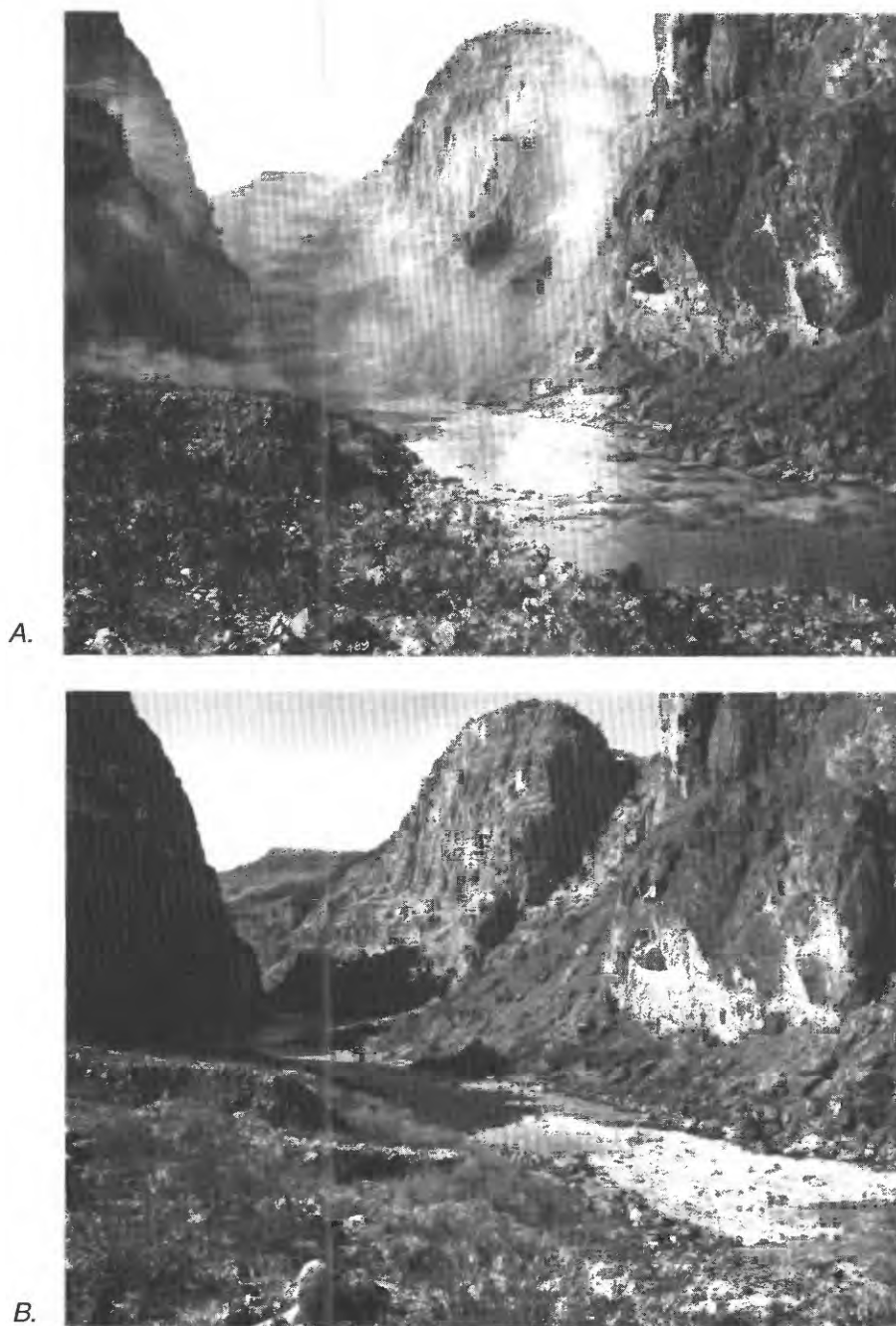


**Figure 13.** Downstream view of Lava Falls Rapid from the high surface on the left side (Stake 1510b). The channel of Prospect Canyon, which enters the Colorado River from the left, appears in the center of the view. A, (February 27, 1890; R. B. Stanton, courtesy of the National Archives). The last vestiges of smoke from a large fire set by the Stanton expedition are shown at left center. The left side of the rapid has flat, relatively slow-moving water adjacent to the mouth of Prospect Canyon. The Deflector Rock is visible on the right side approximately 15 m upstream from the Black Rock. Tail waves from the rapid are deflected away from the Black Rock and the main flow is down the center of the rapid. The water level is 280-400 m<sup>3</sup>/s. B, (February 11, 1990; R. M. Turner). Debris flows from Prospect Canyon changed the rapid substantially in the 20th century. The rapid now begins farther upstream. The 1939 debris flow deposited the prominent low surface at left center. Deposition during the 1939 event forced flow through the rapid to the right; the Deflector Rock moved downstream and was submerged at most water levels. The Black Rock deflects typical dam releases to the left. Debris flows in 1954, 1955, 1963, and 1966 deposited sediment along the left side of the rapid, changing a relatively quiescent area to whitewater choked with boulders.



**Figure 14.** Upstream view of Lava Falls Rapid from the left side (November 10, 1909; R. Cogswell, courtesy of the Bancroft Library, University of California at Berkeley). Boulders that appear on the debris fan and in the river in this view also appear in views taken by Hillers (1872) and Kolb (1912). Photographs taken in 1923 and 1927 show the same boulders, which demonstrates the stability of the rapid in floods of at least  $6,200 \text{ m}^3/\text{s}$ .

Movie footage indicates their runs were similar to Holmstrom's. Afterwards, Loper wrote:

...although it was a BAD rapid we did not find it as bad as Hance Rapid ... Hance has a fall of 27 feet [8.8 m] and Lava has 23 feet [7.5 m] fall ... in a little more than 1/2 of the distance (Bert Loper, unpublished diary, courtesy of the Huntington Library).

For early explorers, the decision whether to portage or run the rapid was influenced largely by water level. Lava Falls Rapid at that time was short, in accord with the descriptions of "falls" and "cascade." The total fall was variously described as between 3 and 7 m; photographs suggest the fall was closer to 3 m. Large boulders, which typically were exposed or shallowly submerged, created serious hazards for wooden boats. At low water, no specific tongue was present; instead, a line of drops perpendicular to the channel occurred across the top of the rapid. Potential routes appear in

photographs on the right and left sides, but the only documented routes were on the right. Before 1939, tail waves in the rapid appeared to follow a straight path to the bottom of the rapid at all water levels. At discharges below about  $300 \text{ m}^3/\text{s}$ , the rapid ended upstream from the Black Rock (fig. 11B).

Lava Falls Rapid had three significant features that stand out in the pre-1939 photographs and movies (fig. 11B). In similar views of the rapid taken from Toroweap Overlook in 1872 and from an aircraft in 1936, the rapid is wide and the lip of the rapid slants downstream toward the left side. At discharges less than about  $500 \text{ m}^3/\text{s}$ , a prominent pile of boulders at the top left of the rapid marked the beginning of the cascade. These boulders, which collectively take on the appearance of a pyramid from a distance, are referred to here as the Pyramid Rocks. The boulders are not present in any photographs taken after 1939 and are not the boulders that form the current Ledge Hole. No



boulders are exposed at dam releases above  $85 \text{ m}^3/\text{s}$  at the former position of the Pyramid Rocks.

The wide, rocky rapid began farther downstream on the left and was characterized by relatively slow velocities before 1939. By rectifying the 1872 photograph from Toroweap Overlook (fig. 12A), we determined that the point on the left side where whitewater began was about 85 m downstream from the same point in 1994. Using the movie shot during the Harris-Loper trip of 1939, at a discharge of  $220 \text{ m}^3/\text{s}$ , we estimated that the boats, which were not rowed downstream, had a velocity of about 2 m/s through the Right Run. Kieffer (1988) estimated an average surface velocity of about 5 m/s for the Right Run in 1985.

Another significant feature of the pre-1939 rapid is a large basalt boulder located just upstream from the Black Rock (fig. 11B). This boulder, which is rectangular with exposed dimensions of 4 and 8 m, can be distinguished in photographs taken from Toroweap Overlook; it was submerged above a discharge of  $850 \text{ m}^3/\text{s}$ . We named this boulder the Deflector Rock because it forced water away from the Black Rock and deflected the tail waves of the rapid down the center of the channel at all water levels. Flow immediately upstream from the Black Rock was relatively calm because of the presence of the Deflector Rock. Movies taken in 1938 and 1939 clearly show a mildly turbulent eddy upstream from the Black Rock that contained driftwood. Now, spectacular boat upsets occasionally occur near the former position of the now-submerged Deflector Rock, and the Corner Pocket upstream from the Black Rock occasionally traps boats.

A third significant feature present before 1939 was an accumulation of large boulders that dominated the surface of the debris fan, particularly the part that was just above water at  $280 \text{ m}^3/\text{s}$ . Several of these distinctive boulders, with diameters of 3–4 m, are in the same place in photographs taken in 1872 (fig. 15A), 1890 (fig. 13A), 1909 (fig. 14), 1912 (fig. 16A), and 1934 (fig. 17). In addition to the lack of change in the largest boulders between 1872 and 1934, no smaller boulders were added to the debris fan and a mature riparian thicket appears in the mouth of Prospect Canyon. Several 1872 views by William Bell of the Wheeler Expedition and J.K. Hillers (not shown) depict a small channel in Prospect Canyon where a broad debris-flow conduit was present in 1995. A similar view, taken in 1936, shows the same conditions in Prospect Canyon as in 1872. The lack of change shown in photographs of the debris fan indicates that

no debris flows occurred from 1872 through 1939. The small, inactive channel in the 1872 view suggests that no debris flows had occurred for a minimum of several decades before 1872.

### The Period of Frequent Debris Flows (1939–1966)

A major debris flow in a Grand Canyon tributary appears to increase the probability that more will occur shortly thereafter (Webb, 1996). Debris flows commonly destabilize sediment on colluvial wedges and in channels that easily can be mobilized by later floods. Terraces of poorly consolidated debris-flow deposits are undercut, providing an additional source for easily mobilized sediments. Despite the fact that severe storms required for initiation are controlled by atmospheric processes beyond the canyon rim, the presence of readily mobilized sediment in the drainage basin allows for frequent debris flows. For these reasons, after a long hiatus, Prospect Canyon had a succession of debris flows that altered the shape and flow patterns of Lava Falls Rapid.

The first and largest historic debris flow in Prospect Canyon occurred between July 15, 1939, and August 17, 1940, as documented by a 1939 amateur movie and 1940 photographs (table 7). A 1941 photograph by McKee, from a similar vantage point as Bell's 1872 view of Prospect Canyon, shows a widened channel full of boulders at the head of the debris fan. The 1939 debris flow and subsequent river reworking changed most of the features of Lava Falls Rapid. The Pyramid and Deflector rocks were moved from their previous positions, the pattern of flow through the rapid was significantly altered, the debris fan was covered with at least 4 m of poorly sorted sediment, and surface till was deposited on the left side of Prospect Canyon (figs. 6, 13). Using historical photographs, we identified the 10 largest boulders that were deposited by the 1939 debris flow; they are still present. The boulders, all of which are basalt, weigh between 3 and 22 Mg (Webb and others, 1996).

In August 1940, Norm Nevills again scouted Lava Falls Rapid and Barry Goldwater photographed it from the aggraded debris fan. Where Goldwater stood was 4 m above water in 1993. His photographs show a debris fan with a near vertical and slightly reworked distal margin. He wrote:

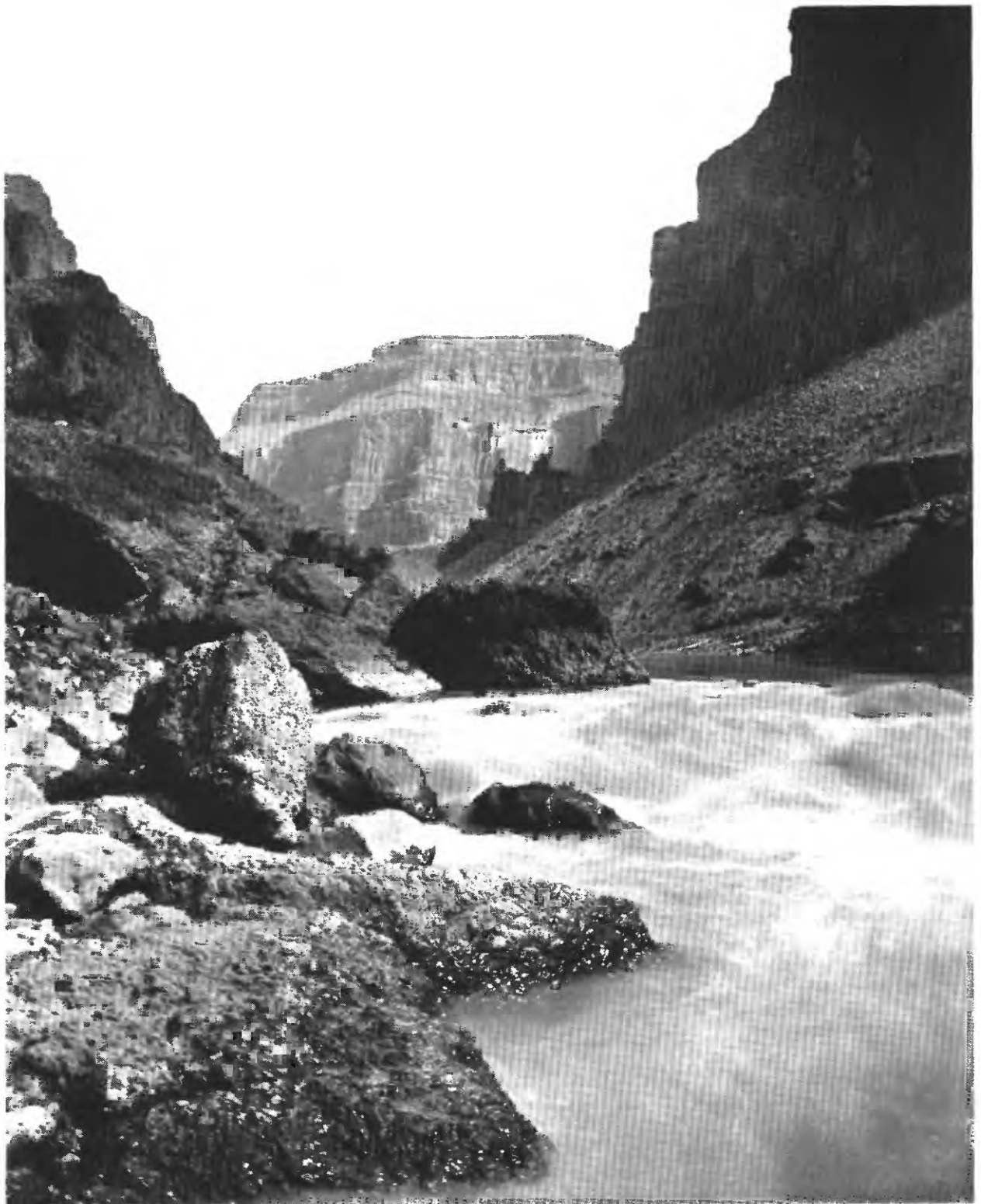
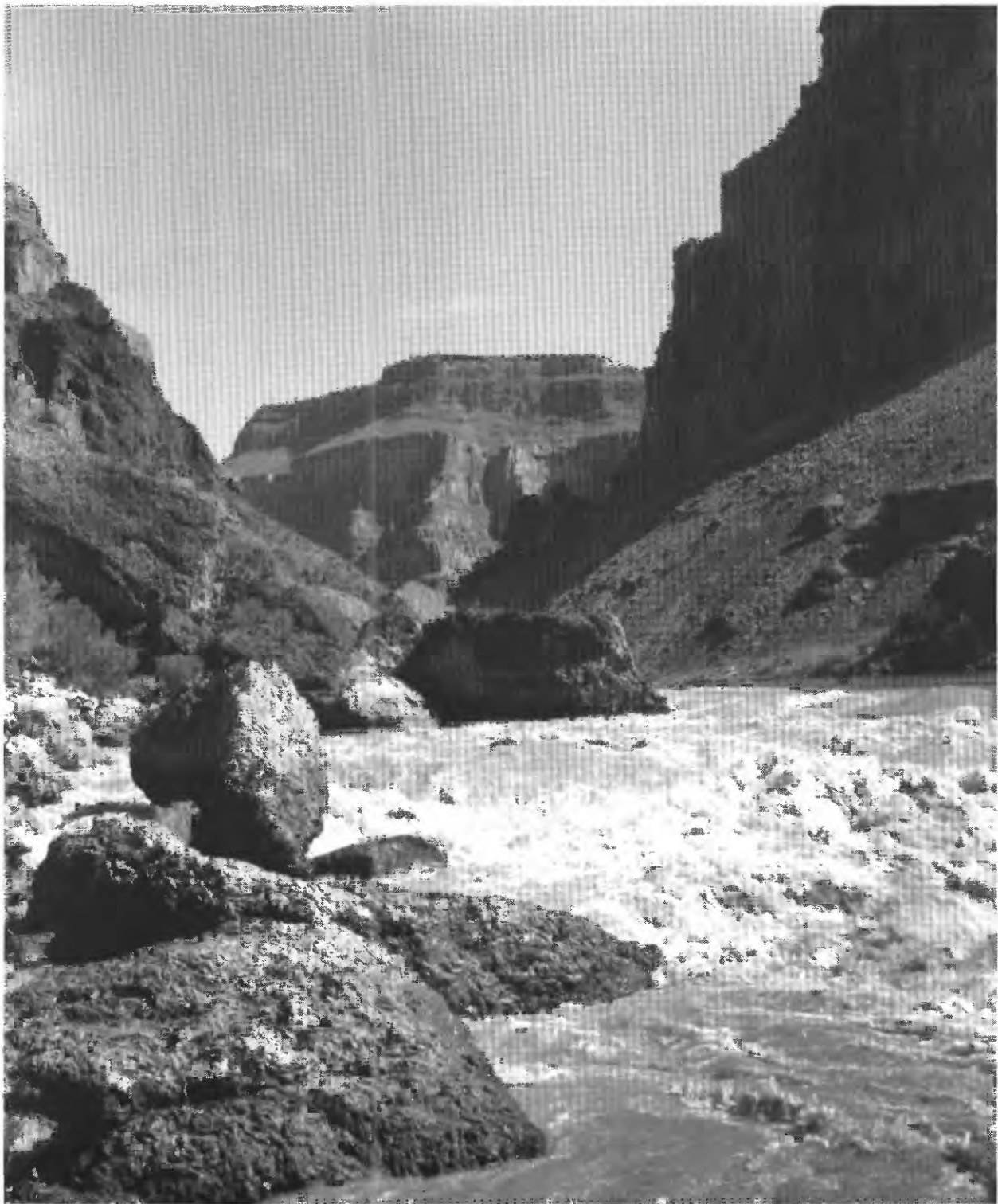


**Figure 15.** Upstream views of the head of Lava Falls Rapid from the right side (Stakes 2598 and 2662). A, (April 19, 1872; J.K. Hillers, courtesy of the National Archives). At a discharge of about  $280 \text{ m}^3/\text{s}$ , the Entrance Rock appears in the center; the Entrance Eddy is behind this rock, and the first hole that Buzz Holmstrom, Don Harris, and Bert Loper had to run in 1938 and 1939 appears at lower right. Many rocks and small pourovers are visible in the center of the photograph. This photograph is also shown in Graf (1979).



*B*, (March 8, 1993; L. Hymans). Even though flow in the Colorado River ( $310\text{--}340\text{ m}^3/\text{s}$ ) is only slightly higher, the stage appears much higher than in 1890. A turbulent eddy forms behind the Entrance Rock. Now, rocks or pourovers are not visible above  $140\text{ m}^3/\text{s}$ . Also, water flows around the right side of the large basalt boulder in the center of the view.

**Figure 15.** Continued.

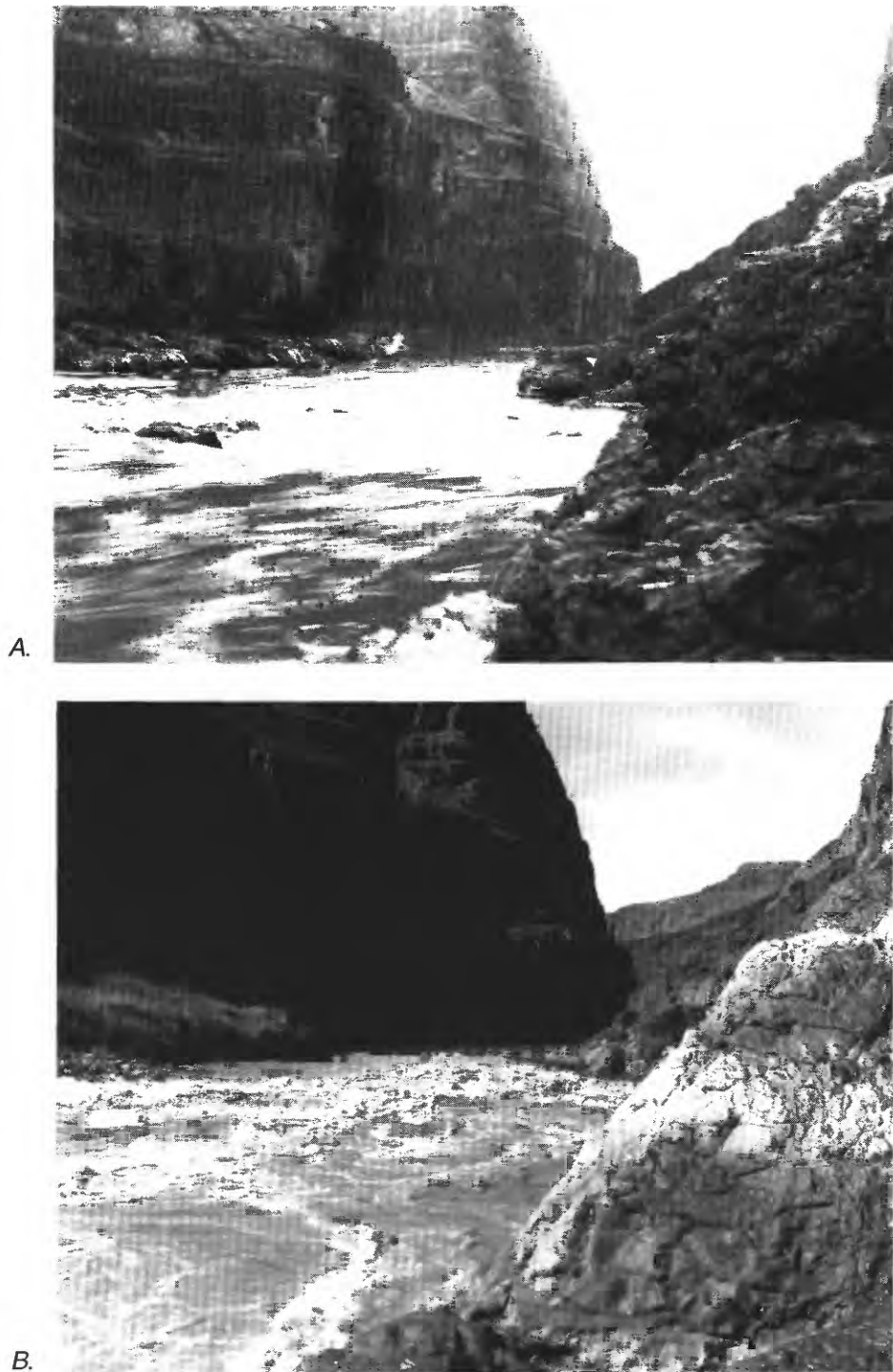


**Figure 16.** Downstream view of the right side of Lava Falls Rapid (Stake 2599). *A*, (January 1, 1912; E. Kolb, courtesy of Northern Arizona University Special Collections). The discharge is 28–85 m<sup>3</sup>/s, and the Deflector Rock, near the right shore, obstructs the view of the Black Rock. The sand bar at the left and rocks that are exposed in the center of the rapid were typically covered at discharges greater than 280 m<sup>3</sup>/s. Several expeditions, including the Kolb brothers, camped on the sand bar after portaging the rapid. *B*, (March 9, 1993; L. Hymans). At a discharge of 310 m<sup>3</sup>/s, no rocks are exposed in the center of the rapid. The Deflector Rock was rotated and moved downstream toward the center of the channel and usually is submerged. The Big Wave, to the left of the Black Rock, forms from flow over the submerged boulder. A large part of the basalt boulder in the right foreground has been eroded.



**Table 7.** Dates and photographic evidence for debris flows and other floods in Prospect Canyon.

Year	Type of event	CONSTRAINING DATES OF PHOTOGRAPHIC EVIDENCE		Known date <sup>1</sup> of event	Probable date <sup>2</sup> of event
		Before event	After event		
1939	Debris flow	July 15, 1939	August 17, 1940	n.d.	September 6, 1939
1954	Debris flow	June 14, 1954	August 29, 1954	July 24, 1954	
1955	Debris flow	July 20, 1955	October 1955	n.d.	July 24, 1955
1956	Flood	April 16, 1956	September 29, 1956	n.d.	July 31, 1956
1963	Debris flow	August 24, 1963	September 25, 1963	n.d.	September 18, 1963
1966	Debris flow	July 1966	April 30, 1967	December 6, 1966	
1993	Flood	August 18, 1992	March 9, 1993	February 8, 1993	
1995	Debris flow	March 5, 1995	March 6, 1995	March 6, 1995	

Notes: n.d., no data.

<sup>1</sup>Known data are from eyewitness accounts or written reports.

<sup>2</sup>Probable dates of debris flows are based on rainfall records (Webb and others, 1996).

At Lava Falls most of the water flows over to the right bank where it plunges over a fall that seems to be twelve or fifteen feet [3.7–4.6 m] high. That of course left only the left side to consider as a possibility of running, and, if that possibility didn't show itself, we faced a portage (Goldwater, 1940, p. 93–94).

Nevills ran the rapid, but his diary does not indicate whether he went right or left. When Nevills returned in 1941, he decided that lining was the “obvious” way to run the rapid (Heald, 1948). From his reaction, it is not obvious if the 1939 debris flow changed the navigational severity of Lava Falls Rapid—Nevills portaged before and after the 1939 debris flow.

All sediment and boulders smaller than 1 m in diameter deposited by the 1939 debris flow were reworked by the Colorado River in 1941. The net effect of the 1939 debris flow and subsequent reworking is evident in photographs taken in 1941 and 1942 (figs. 18A and 19A). The upper left side of the rapid, which had quiet water before 1939, became choked with boulders. The V Wave formed (fig. 20), suggesting the 1939 debris flow deposited the Meteor Rock in the rapid. The Deflector Rock moved about 10 m downstream (fig. 11) and is visible in aerial photographs taken at a discharge of 79 m<sup>3</sup>/s in the 1950s (fig. 21C). The Big Wave formed as water flowed over the submerged Deflector Rock. The tail waves, which previously flowed straight at the bottom of the rapid, curved to the left after 1939. Because of the increased constriction, flow shifted toward the right side of the rapid and impinged directly on the Black Rock. There were fewer exposed boulders in the center of the rapid for river runners to avoid, but the

constriction created more powerful waves. With only a few exceptions, rocks on the right exposed at discharges greater than 280 m<sup>3</sup>/s were unchanged, and no new boulders were added to the right side.

We could not document the occurrence of any debris flows in the 15-yr period from 1939 to 1954. Available photographs of Lava Falls during that period show no changes and levees deposited in 1939 remained prominent and unchanged.

A small debris flow occurred in Prospect Canyon in 1954. Photographs constrain the date between June 14 and August 29, 1954 (table 7). Georgie White, a long-time river guide (also known as Georgie Clark; Clark and Newcomb, 1977), arrived at Lava Falls on July 24 and saw Prospect Canyon running at “full force.” Large boulders were entering the river in a manner White likened to a “big black lava flow” (Georgie White, unpublished diary of 1954 river trip, Otis Marston Collection, Huntington Library). White's observations are only the second eyewitness account of a Grand Canyon debris flow, after Robert Brewster Stanton's account of a debris flow in South Canyon (Stanton, 1965; Smith and Crampton, 1987; Webb, 1996). Péwé (1968) reports a 1967 debris flow near Lees Ferry, just upstream from the start of Marble Canyon.

In low-level aerial photographs, the 1954 debris flow appears to have aggraded the channel of Prospect Canyon by about 1.5 m. Like the 1939 debris flow, this debris flow filled in the previously open left side of the rapid with boulders, which forced the main flow down the right side and constricted the Colorado River to less than half its average width. The tail waves curved farther to the left at the bottom of the rapid. Of more



**Figure 17.** View of Lava Falls Rapid from the left side (July 31, 1934; B. Fahrni, courtesy of the Utah State Historical Society. All rights reserved. Used by permission.). The crew of the 1934 Frazier-Hatch expedition are lining boats to the head of the rapid to begin a portage. The discharge was 60 m<sup>3</sup>/s, one of the lowest summer levels recorded in the 20th century, and the boulders that form the rapid protrude from the water. The Pyramid Rocks are visible at the upper right of the view. Many of the boulders shown in this view were dislodged or buried by the 1939 debris flow. After 1957, the Ledge Hole formed downstream from the boulders visible in this 1934 view.

significance to navigation of the rapid, the Ledge Hole began to form. Despite this, the 1954 debris flow decreased the overall severity of Lava Falls (P.T. Reilly, oral commun., 1991). Previous spaces between the large boulders were filled in with new sediment and the flow became less turbulent with fewer holes scattered around the rapid. The volume of sediment deposited by the 1954 event was the smallest of the six historic debris flows in Prospect Canyon. Because of subsequent erosion, no depositional evidence remains of this debris flow on the Prospect Canyon debris fan.

Another debris flow, the second largest of this century, occurred in 1955. Its date is constrained by photographs taken on July 20 and in October 1955 (table 7). The 1955 debris flow removed or buried all the 1954 deposits and constricted the Colorado River by two-thirds; the rapid was only 20 m wide in aerial

photographs taken during low water on March 25, 1956 (fig. 21B). The deposits from this debris flow, which form surface tih, constricted the channel of Prospect Canyon, also by about two-thirds, and partly overtopped the 1939 debris levee (fig. 6). Many large boulders were deposited in the rapid; some of these now form the Ledge Hole.

The mid-1950s were low-water years on the Colorado River. Several years of winter drought affected much of the United States, particularly in New Mexico, Colorado, and Texas (Thomas, 1962). Discharges in the Colorado River were low and most of the 1955 debris-flow deposit remained on the left side of Lava Falls (fig. 21B). Aerial photographs (fig. 21C) reveal that a flash flood occurred in Prospect Canyon between April 16 and September 29, 1956. The small volume of sediment deposited by the 1956 flood had little effect on Lava Falls Rapid.



A.



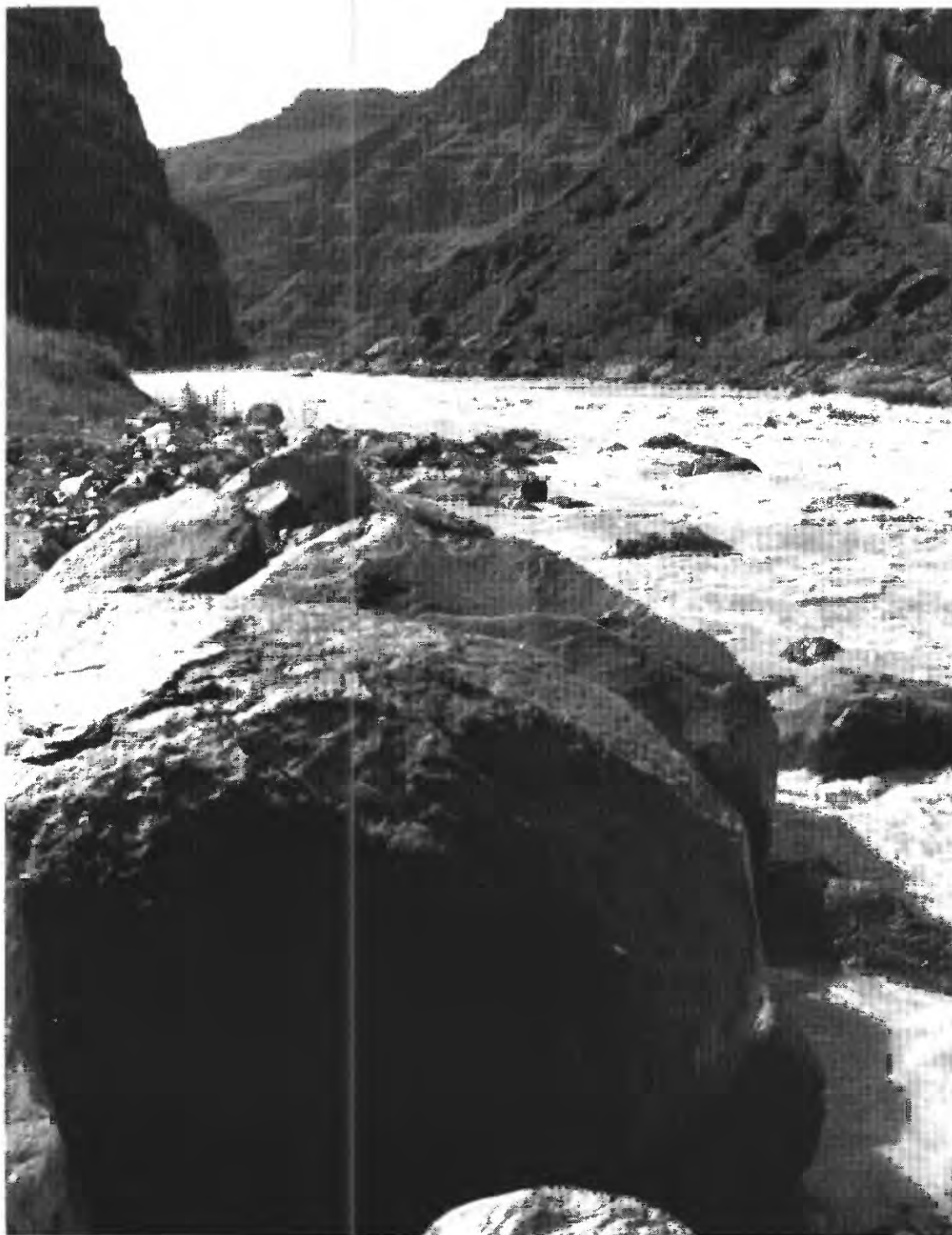
B.

**Figure 18.** Views of Lava Falls Rapid from the left side (Stake 2660a). *A*, (July 26, 1942; N. Wilson, courtesy of the University of Utah Marriott Library). In this upstream view, the crew of the Nevills expedition is lining boats along the left side of the rapid. The 1939 debris flow completely changed the flow pattern in the rapid. The Pyramid Rocks were removed from the center of the rapid, and large holes punctuated the left side. The photographer stood on a debris fan that was 3–4 m higher than the fan in 1993; the deposits of the 1939 debris flow were subsequently reworked by Colorado River floods or Prospect Canyon debris flows. *B*, (March 10, 1993; S. Tharnstrom). At a discharge of 310–340 m<sup>3</sup>/s, the apparent stage is about 0.5 m lower than in 1942. Debris flows after 1942 deposited rocks in the center of the rapid that form the Ledge Hole, which does not appear in the 1942 view. Riparian vegetation has colonized much of the debris fan.





**Figure 19.** Downstream view of Lava Falls Rapid from the left side (Stake 2741). A, (July 27, 1941; W. Heald, courtesy of the University of Utah Marriott Library). A crew member of the 1941 Nevills expedition rests on a rock during a portage down the left shore. At a discharge of about  $570 \text{ m}^3/\text{s}$ , water is piling up against the Black Rock, shown in the upper right of the view. The pattern of the tail waves, which has changed in comparison to pre-1939 views, is the result of increased constriction of the Colorado River and displacement of the Deflector Rock during the 1939 debris flow. All foreground rocks in this photograph were deposited in 1939.



*B*, (March 10, 1993; S. Tharnstrom). Flow in the Colorado River is about 230–280 m<sup>3</sup>/s. Although many boulders have been transported in and out of the field of view by debris flows after 1941, several boulders in the midground remain. The boulder that the Nevills' crew member is resting on in 1941, as well as the boulders immediately upstream, are in the same place. The foreground boulder, which has a b-axis diameter of 1.85 m, was probably deposited during the 1955 debris flow. The pattern of waves at the bottom of Lava Falls Rapid is similar in 1941 and 1993.

**Figure 19.** Continued.

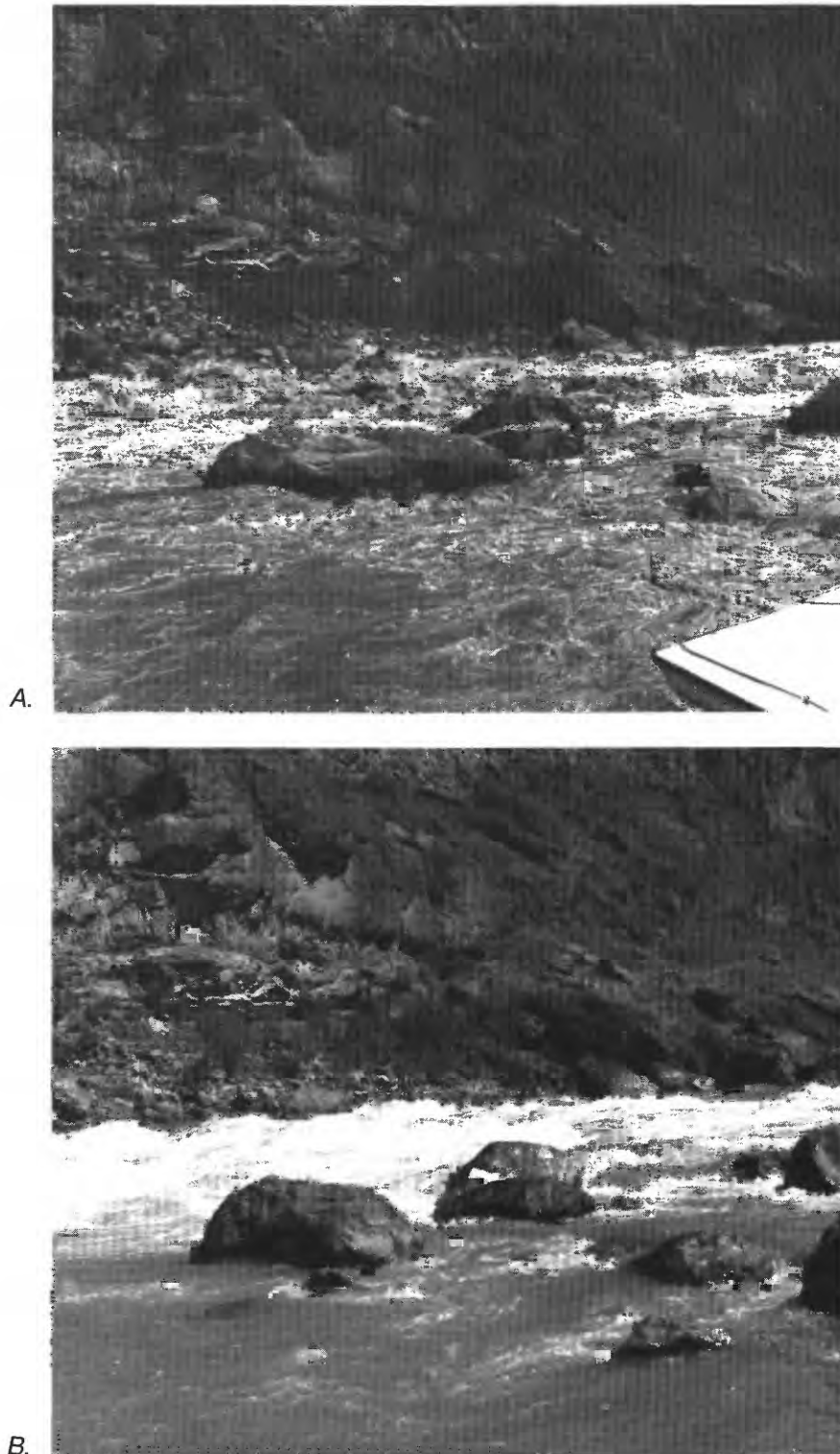


**Figure 20.** Upstream view of Lava Falls Rapid from the left side (Stake 2046). *A*, (July 7, 1950; P. T. Reilly). A motor boat passes through the V Wave, which appear in the left center of this upstream view. The large boulder at bottom center is approximately 1.5 m in diameter. The discharge is 470 m<sup>3</sup>/s. *B*, (August 16, 1991; R.H. Webb). The discharge is slightly lower than in the 1950 photograph. Several boulders in the foreground were not dislodged by debris flow and Colorado River floods after 1950. However, one foreground boulder has been transported out of the field of view. A boulder of approximately the same dimensions was also transported into the field of view (lower right). Both boulders probably were deposited by the 1955 debris flow.

The drought ended in the winter of 1956–1957. The 1957 Colorado River flood peaked at  $3,540 \text{ m}^3/\text{s}$  on June 13. All evidence of the 1954 debris fan and the 1956 flood deposit, as well as most of the 1955 debris fan, was removed (figs. 21A, 21E, and 21F). The flood entrained boulders and other particles smaller than about 1.5 m in diameter from the Prospect Canyon debris fan and transported them downstream. When the flood receded, only the largest boulders persisted on the left side of the rapid (fig. 22A). The debris fan, which withstood 2 years of smaller floods during the drought years, reverted to a configuration similar to what was present before the 1954 debris flow. The large boulders in the middle of the rapid were rearranged to form the Ledge Hole (fig. 11A).

After the 1954 and 1955 debris flows, there were no debris flows in Prospect Canyon for 9 years. With closure of Glen Canyon Dam in March 1963, spring floods in the Colorado River were mostly eliminated and peak discharges were reduced.

However, debris flows continued to occur in Prospect Canyon, the next one between August 24 and September 25, 1963 (table 7). The 1963 debris flow constricted the Colorado River by about two thirds (fig. 23A) and had the finest-grained surface deposit of any historic debris flow from Prospect Canyon. Despite the presence of relatively mobile material adjacent to the rapid, most of the deposit was unchanged by small dam releases from 1963 to February 1965 (figs. 23B, 24). The 1963 debris fan persisted until a large dam release in May–June 1965. The reworked debris fan that appears in the late-May 1965 aerial photographs is not substantively different from the debris fan shown in photographs taken just before 1963, suggesting that few new boulders were added to the rapid by the 1963 debris flow.

Photographs taken in July 1966 and April 1967 document the occurrence of a small debris flow in Prospect Canyon (table 7; figs. 25A). The deposition was first observed in March 1967 by the first river runner that year (John Cross II, written commun., 1967) and is best shown in a photograph from August 1967 (fig. 26A). An unusually intense winter storm in December 1966, which caused debris flows in Crystal Creek (mile 98.3), Lava Canyon (mile 65.5; Cooley and others, 1977; Webb and others, 1989) and elsewhere along the river, is the likely cause for this debris flow at Prospect Canyon. An August 1967 photograph (fig. 26A) shows the extent of the aggraded debris fan. Poorly sorted sediment was deposited on the

debris fan and small boulders were deposited on the left side of Lava Falls Rapid, reportedly closing off a previously used route (John Cross II, written commun., 1967). Most of the 1966 debris fan was removed by the cumulative effects of relatively small dam releases in 1972 and a small flood in the Little Colorado River in 1973.

## Quiescence (1966–1995)

Only a few small streamflow floods occurred in Prospect Canyon between 1966 and 1995, the period when the largest number of river runners navigated Lava Falls. During February 1993, a streamflow flood in Prospect Canyon deposited a small volume of cobbles on the debris fan. Although some scouring occurred in the bed of Prospect Canyon, Lava Falls Rapid was unchanged.

## The 1995 Debris Flow

Lava Falls Rapid changed dramatically in the early morning hours of March 6, 1995, when a debris flow initiated in Prospect Canyon aggraded the debris fan and constricted the rapid (Webb and Melis, 1995). Most of the authors were camped at the rapid during the debris flow and observed some of its effects immediately afterward. The storm also caused flooding in eastern Grand Canyon (Rihs, 1995), as did the December 1966 storm (Cooley and others, 1977). Of the six historic debris flows in Prospect Canyon, the 1995 debris flow was unique because it entered the Colorado River at a higher river discharge ( $490 \text{ m}^3/\text{s}$ ) than the previous five debris flows.

Steady rainfall began at midnight on March 5 and continued through the day. The storm culminated in steady heavy rainfall that began about 1800 hrs on March 5 and continued until after midnight on March 6. Although daily precipitation was not excessive at Peach Springs and Seligman, precipitation was heavy at Grand Canyon and Bright Angel Ranger Station, and a total of 43 mm fell during the early morning hours of March 6 at Tuweep Ranger Station. Between 0100 and 0130 hrs, we heard a roaring sound of 3–5 minute duration from Prospect Canyon. Part of the noise sounded like a rockfall.

Throughout the following morning, a 325-m waterfall with two distinct vertical sections discharged



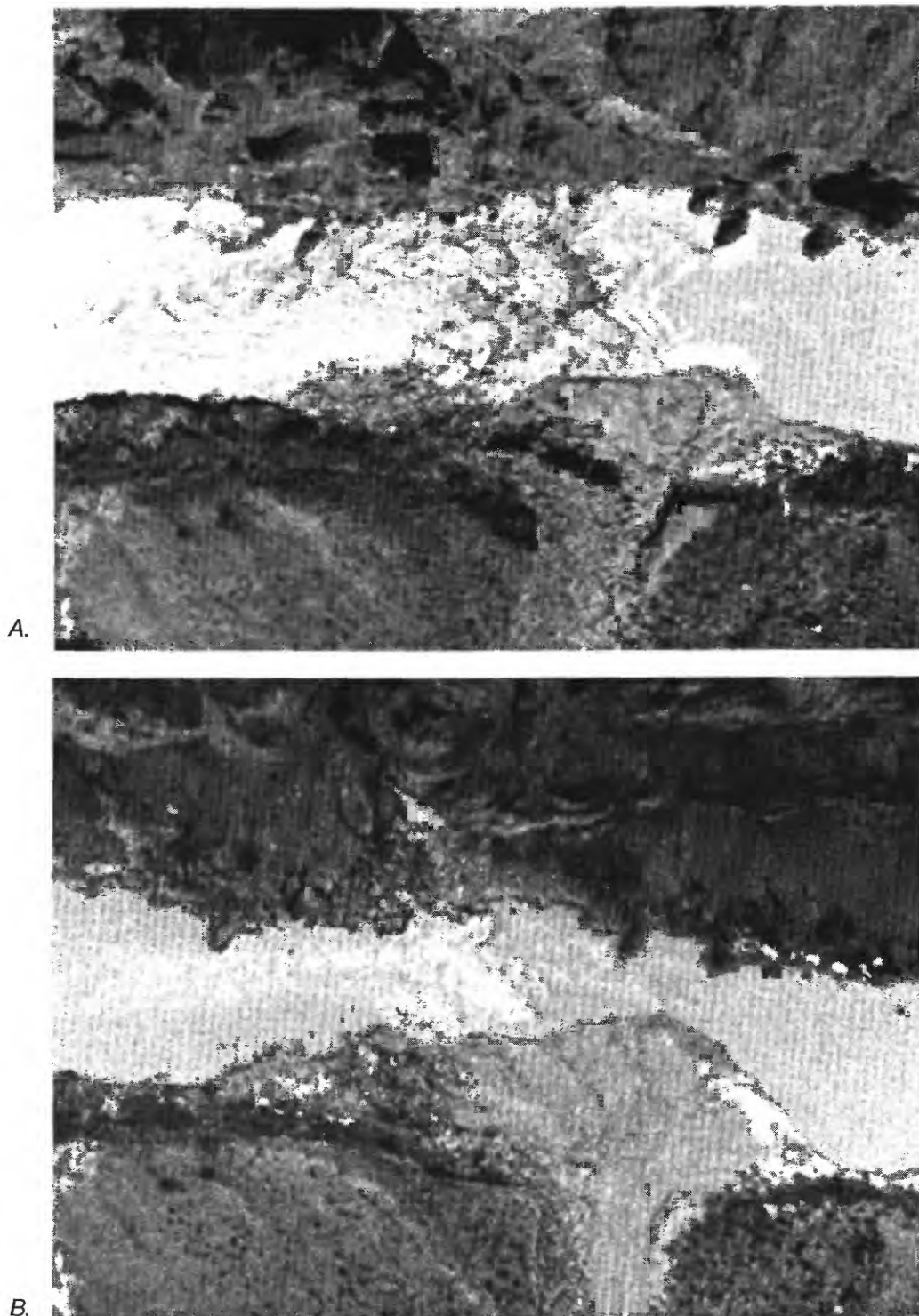
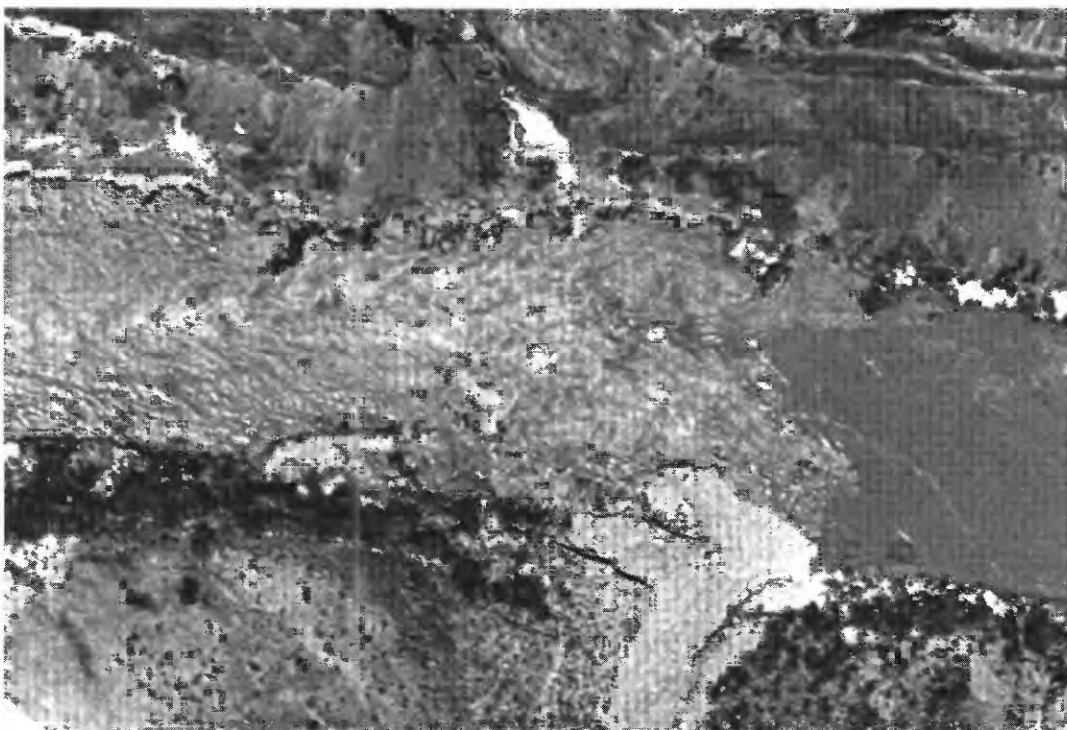


**Figure 21.** Oblique aerial views of Lava Falls Rapid and Prospect Canyon (photographs by P. T. Reilly). *A*, (March 21, 1955). Although the discharge is  $400 \text{ m}^3/\text{s}$ , the 1954 debris fan (at center) constricts the Colorado River by about 30 percent. The channel of Prospect Canyon (upstream on the left) is a meandering band of fresh debris-flow and fluvial deposits. The tongue at the head of the rapid is on the right side, and the tail waves curve toward the left side at the base of the rapid. *B*, (March 25, 1956). The 1955 debris flow, which formed a smaller debris fan than the 1939 debris flow, overtopped the 1939 levee on the left side of Prospect Canyon in several places (fig. 6, pl. 1) but did not destroy vegetation. The river was at  $180 \text{ m}^3/\text{s}$  and rising when the photograph was taken; originally, the fan extended farther into the river.



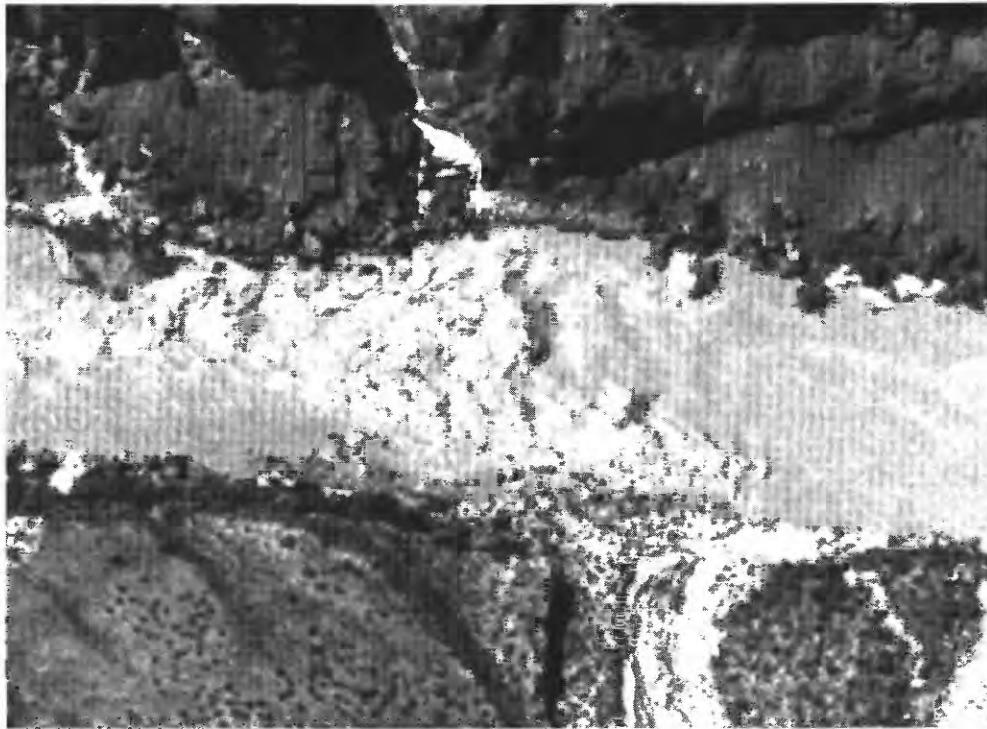
C.



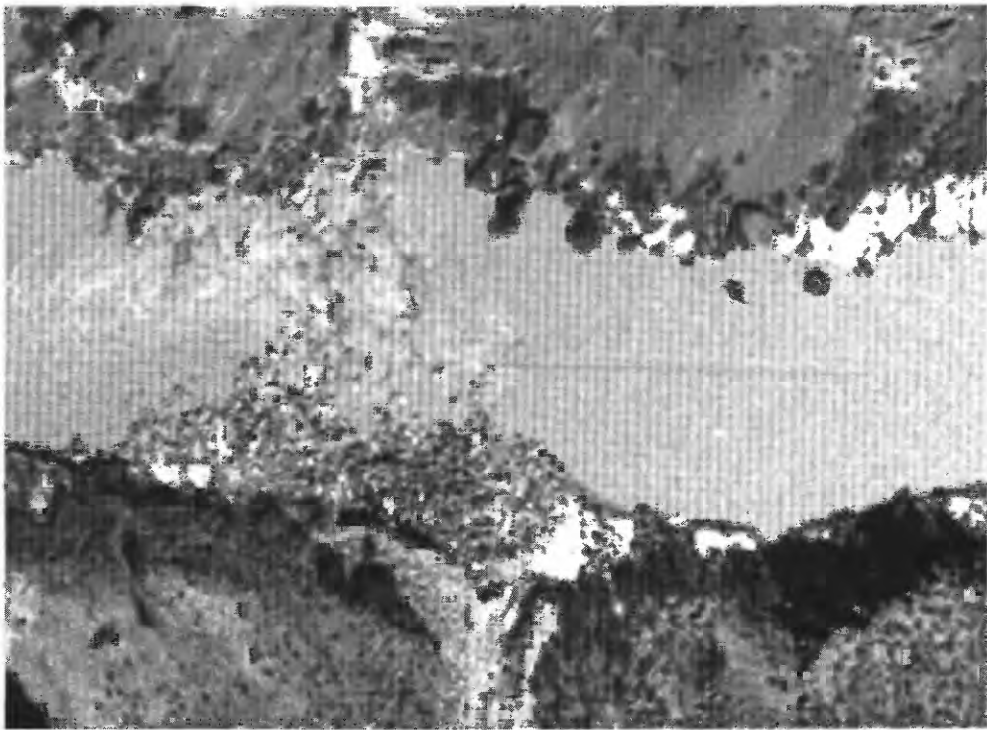
D.

C, (September 29, 1956). The 1956 Prospect Canyon flood deposit is the fresh-looking material in the center of the debris fan. At a discharge of  $80 \text{ m}^3/\text{s}$ , the displaced Deflector Rock is visible upstream from the Black Rock. The view documents the extent of reworking of the 1955 debris flow by the 1956 flood in the Colorado River, which peaked at  $1,890 \text{ m}^3/\text{s}$ . The reworked zone appears as a coarsening of particle size on the distal end of the debris fan. D, (May 4, 1957). Remnants of the 1955 debris-flow and 1956 flood deposits were eroding under the rising waters of the Colorado River ( $520 \text{ m}^3/\text{s}$ ). The contact of the 1956 deposits and the 1955 debris-flow deposits form a dark band penetrating the center of the fan.

**Figure 21.** Continued.



E.



F.

E, (April 20, 1958). The Colorado River peaked at  $3,540 \text{ m}^3/\text{s}$  in 1957, and the flood removed most of the 1955 and 1956 debris-fan deposits. Small pockets of 1955 levee deposits were still present in April 1958. The Ledge Hole, which formed after the 1957 flood reworked the 1955 deposit, appears in the center of the rapid, which had a discharge of  $1,870 \text{ m}^3/\text{s}$ . F, (October 4, 1958). The Colorado River peaked at  $3,030 \text{ m}^3/\text{s}$  in 1958, but flow was only  $190 \text{ m}^3/\text{s}$  when Reilly took his photograph. Only the largest boulders deposited in 1939 and 1955 remained on the debris fan. The Ledge Hole is distinct at the top center of the rapid, and the Big Wave is present in front of the Black Rock. The horizontal line is a scratch on the negative.

**Figure 21.** Continued.

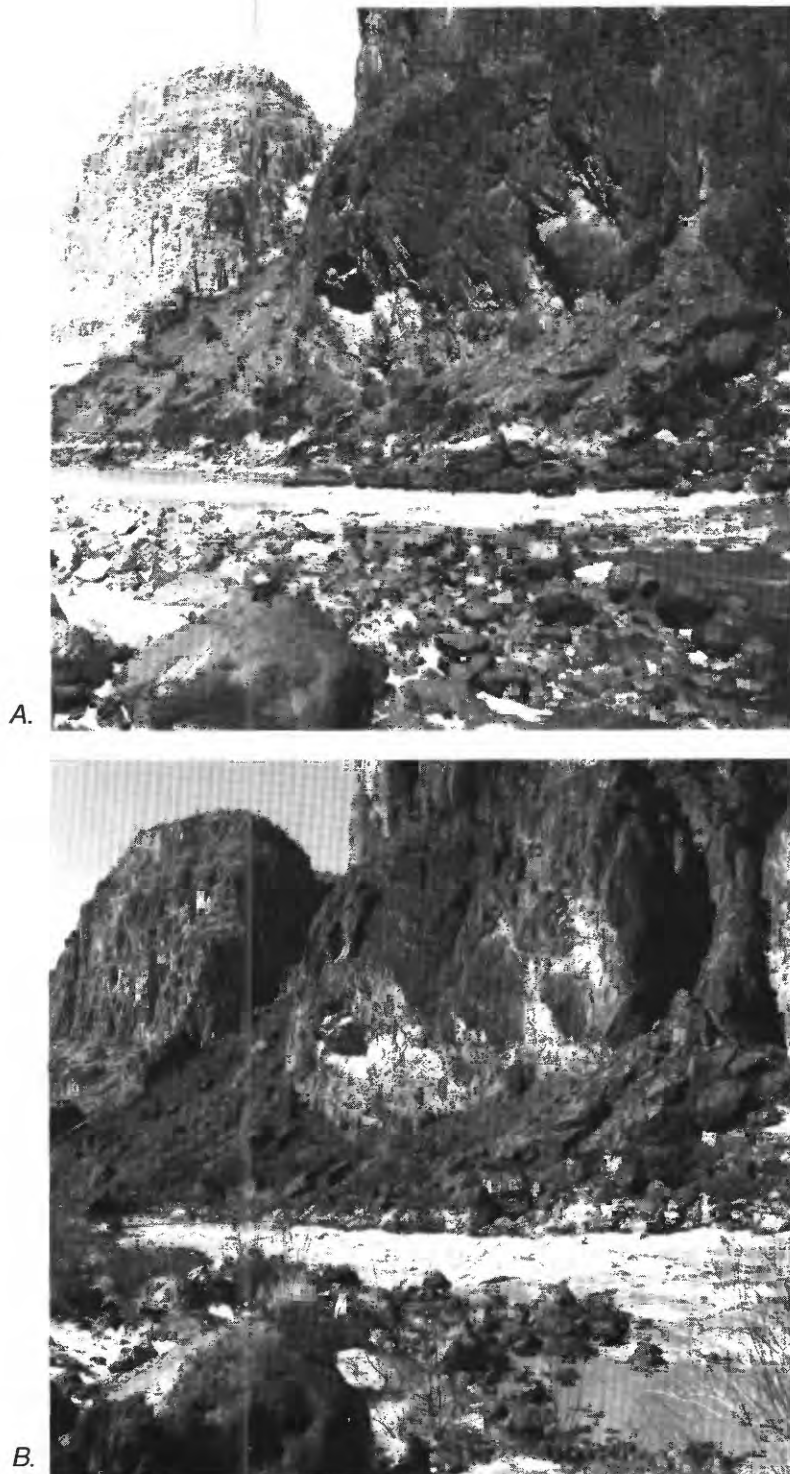


**Figure 22.** Downstream view of Prospect Canyon debris fan and the tailwaves of Lava Falls Rapid (Stake 2002). *A.* (July 20, 1958; G. Staveley, courtesy of the Huntington Library). The discharge is  $220 \text{ m}^3/\text{s}$ , and the boulders on the debris fan are the net result of the 1939, 1954, and 1955 debris flows and subsequent reworking by the Colorado River. The 1957 flood in the Colorado River reworked the deposits of the 1954 and 1955 debris flows. *B.* (February 20, 1991; D. Edwards). Although the stage was about 0.5 m higher than in the 1958 view, 6–10 boulders with diameters of 1 m or larger remain. Most of the foreground debris fan was buried by debris flows in 1963 and 1966 and was subsequently re-exposed. The debris fan decreased in size slightly between 1958 and 1991 although the size of boulders in the reworked zone appears unchanged.





A.



B.



**Figure 23.** Upstream view of Lava Falls Rapid from the right side (Stakes 2005 and 3050). *A.* (September 25, 1963; photographer unknown, courtesy of the Huntington Library). This photograph was taken a short time after the September 1963 debris flow and shows its maximum constriction at a discharge of about  $56 \text{ m}^3/\text{s}$ . The boulders on the distal margin of the debris fan and in the center of the view were deposited by debris flows between 1939 and 1955; these boulders create the Ledge Hole at higher discharges. The Meteor Rock, which creates the V Wave, appears on the right side of the view. The view shows the relatively fine grained particle size that is characteristic of the 1963 deposits. *B.* (February 21, 1965; J. Visbak, courtesy of the Huntington Library). This view, which is not a match of *A.*, shows Lava Falls at a discharge of about  $198 \text{ m}^3/\text{s}$ . Dam releases up to  $550 \text{ m}^3/\text{s}$  eroded the distal edge of the debris-flow deposit from 1963 through early 1965. Unlike the 1939 and 1955 debris flows, photographic evidence suggests that few boulders greater than 1 m in diameter were transported in the 1963 debris flow. As a result, most boulders in the 1963 debris flow fan were entrained during high dam releases in May–June 1965. *C.* (March 10, 1993; L. Hymans). The discharge was about  $350 \text{ m}^3/\text{s}$  in this match of the 1965 view. Reworking of the 1963 and 1966 debris-flow deposits was complete by that time, leaving little evidence of the former constriction. The boulders forming the Ledge Hole are submerged in this view but their hydraulic effect is clearly visible in the center of the view. The Meteor Rock was also covered, but the noteworthy hole that forms downstream of the Meteor Rock is visible.



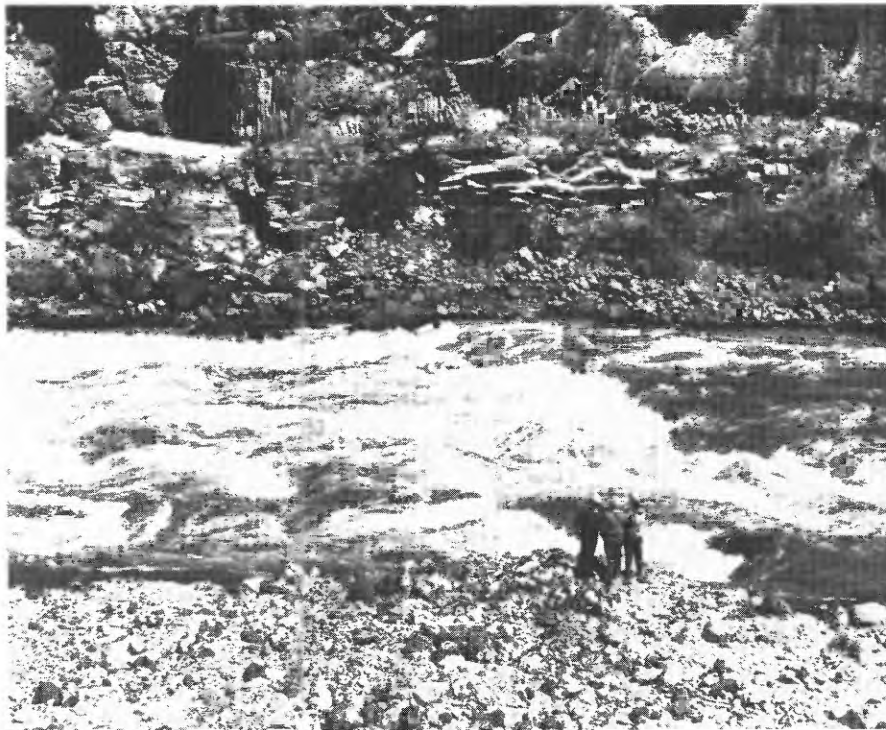
**Figure 24.** Oblique aerial view of Lava Falls Rapid and Prospect Canyon (May 20, 1964; P. T. Reilly). At a discharge of  $37 \text{ m}^3/\text{s}$ , the 1963 debris-flow deposit constricts the river by about 60 percent; the debris fan initially extended nearly to the middle of the Ledge Hole. This view shows the reworking by a peak discharge of  $540 \text{ m}^3/\text{s}$ . The Meteor Rock is visible in the center of the rapid, and the usually submerged Deflector Rock divides the tail waves.

what we estimated to be  $10\text{--}30 \text{ m}^3/\text{s}$  of sediment-laden streamflow into the upper part of Prospect Canyon (fig. 27). A later inspection of the channel above the waterfall suggested that gravel and small cobbles were the largest particles transported over the waterfall. Runoff from Prospect Canyon lasted 18–20 hrs and stopped after dark on March 6. As described above for surface tij, the debris flow consisted of several pulses. Using the classification of Melis and others (1997), the 1995 debris flow was a type II event.

At 0600 hrs on March 6, the new debris fan at Lava Falls Rapid extended 32–50 m into the Colorado River, which had a discharge of  $540 \text{ m}^3/\text{s}$ . Deposition reached the left edge of the Ledge Hole, and the debris fan covered about 200 m of the left side the rapid (fig. 11A). The fan sloped continuously into the river with no cutbank on its distal margin or a break in slope. As the morning progressed, the distal margin of the debris fan was eroded laterally by 7–8 m, leaving a 2.6 m high cutbank on the left side of the rapid.

Throughout the morning, large sections of the new fan were undercut and fell into the rapid. Recessional flow in Prospect Canyon cut two channels through the debris fan, further reducing its volume. Tributary floodwater entering on the left side of the rapid contributed to the failures of the distal margin. By about 1300 hrs on March 6, the configuration of the debris fan had stabilized (fig. 28B).

Flow in the river was confined to a channel about 50 percent of its previous width, which caused distinct changes to the hydraulics of Lava Falls Rapid. The water-surface profile (fig. 29A) initially was greatly influenced by large waves on the right side and the stage-discharge relation at the head of the rapid had increased by more than 1 m. Flow velocity through the rapid, particularly in the Right Run (fig. 11A), had increased. At a discharge of  $312 \text{ m}^3/\text{s}$ , we measured an average surface velocity of 4.3 m/s on the left side, whereas Kieffer (1988) reported velocities of 3.3 m/s at a similar discharge on the left side. The Ledge Hole,



A.



B.

**Figure 25.** View from the left side across the top of Lava Falls Rapid (Stake 2739). *A.* (April 30, 1967; D. Harris). The crew of this 1967 trip stands on the 1966 debris-flow deposit while scouting routes through the rapid, which had a discharge of about  $280 \text{ m}^3/\text{s}$ . The largest visible boulder in the 1966 deposit is less than 1 m in diameter. *B.* (March 8, 1993; R.H. Webb). The discharge was slightly lower than that in 1967. Most of the 1966 debris-flow deposit was removed in April 1973; the 1983 flood ( $2,720 \text{ m}^3/\text{s}$ ) caused few changes in Lava Falls Rapid. The largest boulders, which controlled the major waves and holes in the rapid, were unchanged.





A.



B.

**Figure 26.** Downstream view of Lava Falls Rapid from the high surface on the left side (Stake 2964b). A, (August 1967; G. Luepke). At a discharge of about  $340 \text{ m}^3/\text{s}$ , the 1966 debris flow constricts the Colorado River by about 36 percent. According to the first river runner to view the rapid, the only effect of this debris flow was to eliminate the Left Run. A typical dam release and a small flood in the Little Colorado River on April 19, 1973, combined to form a peak discharge of  $1,080 \text{ m}^3/\text{s}$ , which removed the 1966 deposit. B, (March 6, 1995; Webb). The deposit of the March 1995 debris flow was much larger than that of the 1966 event, but its shape is similar. The amount of sediment deposited in 1995 is about half the amount deposited during the 1955 debris flow.



**Figure 27.** (March 6, 1995; S. Tharnstrom). The firehose effect created by streamflow falling over a 325-m fall at the head of Prospect Canyon on March 6, 1995.

which had a new rock lodged on its left edge, had a different shape, a sharper drop, and a stronger wave than before. The right lateral of the V Wave was much stronger than the left lateral. The Big Wave initially was very large but disappeared by the end of the day. A large, continuously breaking wave rolled off of the Black Rock, and large whirlpools formed to the right of and behind the Black Rock. Cobbles and boulders were heard rolling along the river bed above the sound of the rapid.

Downstream from Lava Falls Rapid, eddies on both sides of the river were replaced by fast-moving water over a long and narrow debris bar (fig. 28B). The tail waves, which had previously veered to the left, now moved straight downstream (fig. 28). A secondary riffle temporarily formed adjacent to Warm Springs (figs. 2, 3), but its 1-m waves subsided to about 0.25 m as the day progressed. We interpreted the secondary riffle as flow around and over a new debris bar where the pool used to be; the size of the riffle diminished as a gravel/cobble bar migrated downstream into Lower Lava Rapid.

The rapid changed slowly after noon on March 6. By midafternoon, a navigation route developed just to the left of the Ledge Hole. By March 8, the configuration of the rapid and its water-surface profile stabilized (fig. 29A). At a discharge of 400 m<sup>3</sup>/s, the constriction from the new debris fan caused the stage in the rapid to appear as if the discharge was 170 m<sup>3</sup>/s higher. The drop at the head of the rapid increased by 0.9 m from the 1994 water-surface profile for a roughly equivalent discharge (fig. 29B); in other words, the total drop through the main part of the rapid increased from 3.1 m in 1994 to 4.0 m in 1995.

## INITIATION OF DEBRIS FLOWS IN PROSPECT CANYON

Debris flows in Prospect Canyon are initiated under very specific conditions. Runoff generated in Prospect Valley must flow over the waterfall at the head of Prospect Canyon in sufficient quantity to erode and mobilize the colluvial wedges, channel deposits, and debris-flow deposits below. In addition, a sufficient volume of colluvium and (or) alluvium must have accumulated below the waterfall. Although most Grand Canyon tributaries are small, and debris flows typically are initiated during intense summer thunderstorms,

runoff in Prospect Valley can be generated by the broad array of hydroclimatic conditions that affect other watercourses in the southwestern United States.

## Hydroclimatology

Three general storm types are capable of causing debris flows in Grand Canyon (Melis and others, 1994). During Arizona's summer monsoon, which usually occurs between June and September (Hirschboeck, 1985), intense rainfall from convective thunderstorms can initiate debris flows. Dissipating tropical cyclones, which can cause intense and sustained precipitation in the southwestern United States between July and October (Hansen and Shwarz, 1981; Smith, 1986), have caused some of the most severe flooding in the region (Roeske and others, 1978; Aldridge and Eychaner, 1984; Roeske and others, 1989; Webb and Betancourt, 1992). Unusually warm winter storms, possibly combined with rainfall on existing snowpacks, also can cause debris flows in Grand Canyon (Cooley and others, 1977).

Monsoonal conditions result from moist air entering the southwestern United States from Mexico and (or) the eastern North Pacific Ocean (Hansen and Shwarz, 1981). The interannual variability of monsoonal precipitation is weakly related to variability in global-circulation patterns (Webb and Betancourt, 1992) and affects how many storms have the potential to initiate debris flows in the canyon. For the southern Colorado Plateau, Hereford and Webb (1992) documented a decline in warm-season rainfall, which they defined as occurring from June through October, after about 1941. For eastern Grand Canyon, Hereford and others (1993) reported that the wettest period in the post-dam period (1963–1990 in their case) was 1978–1984.

Among the 600 tributaries of Grand Canyon, dissipating tropical cyclones are known to have initiated debris flows in Prospect Canyon only in 1939 and 1963. Most tropical cyclones form in the eastern North Pacific Ocean and travel northwestward along the coast of Mexico before dissipating over the ocean. The residual moisture from these storms is typically transported into Arizona with cutoff low-pressure and frontal systems entering Arizona from the west and northwest (Smith, 1986).

Warm winter storms initiated debris flows in Grand Canyon in 1966 and 1995. These storms, which occur from November through March, cause heavy

rain and snow that mostly affect large drainage basins like Prospect Valley. These long-duration storms affect large areas and may trigger multiple hillslope failures, leading to high-volume debris flows and sustained runoff such as the Crystal Creek debris flow of December 1966 (Cooley and others, 1977; Webb and others, 1989; Melis and others, 1994). Winter rainfall in Grand Canyon has increased, particularly since the mid-1970s (fig. 30B).

The occurrence of debris flows in Prospect Canyon is only weakly related to regional storms. With the exception of the 1939 event, point rainfall records at several stations near Prospect Canyon do not consistently show unusually high rainfall on the dates of debris flows, although for each date, one station may have recorded a relatively long recurrence-interval daily or storm total (Webb and others, 1996). For example, the 1955 debris flow appears to have been initiated when Mount Trumbull had the largest storm in its record, but rainfall was not unusual in other parts of the region. Most of the rainfall stations are at least 40 km from the Prospect Valley drainage basin (table 4), and rainfall recorded at these stations may not be representative of the storm conditions in the Prospect Valley drainage basin.

Debris-flow initiation in Prospect Canyon is not related to the amount of seasonal precipitation. Although monthly precipitation was high when most of the debris flows occurred (fig. 31), seasonal precipitation was not consistently high. For example, the 1966 and 1995 debris flows occurred during the 24th and 18th wettest winters (November–March), respectively, in the 92-year record (fig. 30B). The 1939, 1954, 1955, and 1963 debris flows occurred during the 1st, 75th, 35th, and 13th wettest summers (July–September), respectively (fig. 30A). Debris flows in Prospect Canyon may not require season-long buildup of antecedent soil moisture; however, above-average rainfall in the preceding month may be a contributing factor.

The areal extent of storm cells that cause intense precipitation may be too small to affect both the Prospect Valley drainage basin and surrounding rainfall stations. At Tuweep Ranger Station, 40 km from Prospect Canyon, the storm that caused the September 1963 debris flow was relatively brief with a maximum hourly intensity of 4.5 mm/hr (fig. 32A; U.S. Department of Commerce, 1963). During the debris flow of December 6, 1966, radar maps of cloud cover do not show unusually large storm cells in western

Grand Canyon (Butler and Mundorff, 1970). Steady, gentle rain fell at Tuweep Ranger Station, followed by 3 hours of rainfall with intensities of 10–11 mm/hr (U.S. Department of Commerce, 1966; fig. 32B). Radar maps (not shown) at the time of the 1995 debris flow also did not show unusually large storm cells despite significant rainfall intensities of up to 11 mm/hr (fig. 32D).

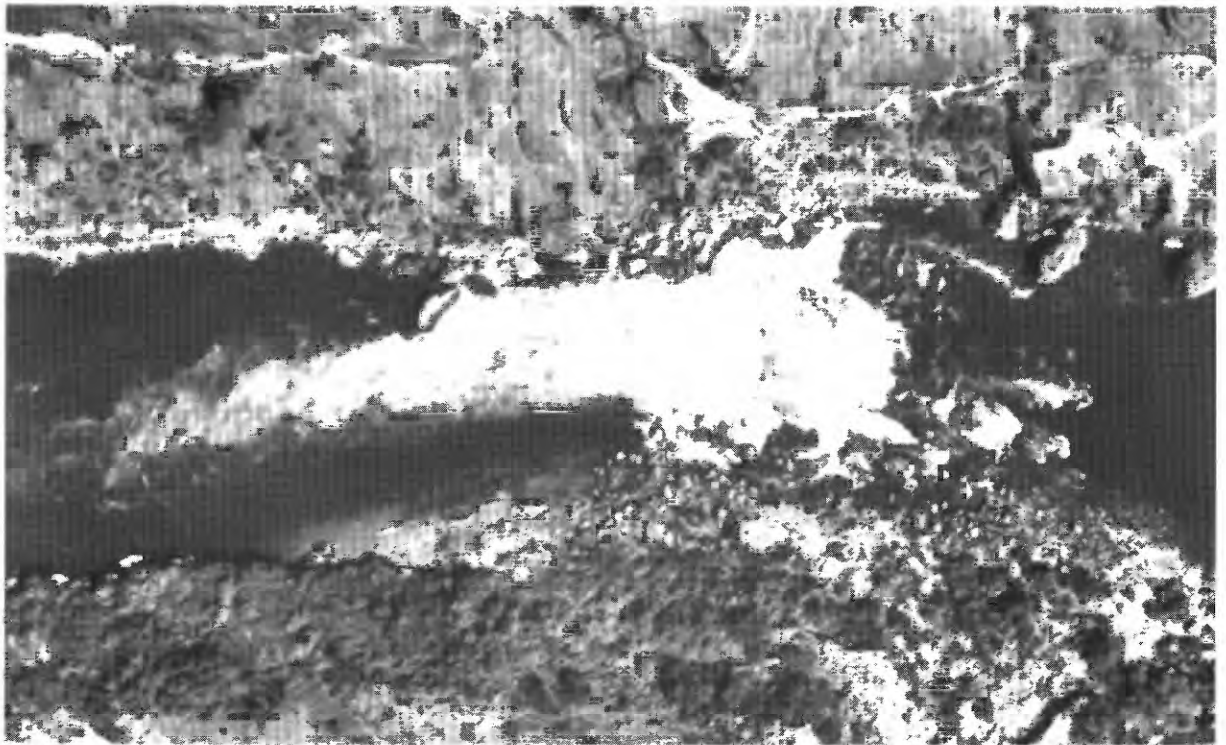
Storms that initiate debris flows are different in an important way from storms that cause streamflow floods, particularly during winter. Both the December 1966 and March 1995 storms ended with notably high-intensity rainfall (fig. 32B and 32D). The runoff that initiated both the 1966 and 1995 debris flows likely came from microbursts of precipitation from clouds centered over the watershed. In contrast, the rainfall that caused the February 1993 streamflow flood in Prospect Canyon had sustained but light intensities (fig. 32C). Bursts of rainfall at the end of a storm appear to be a requirement for debris-flow initiation.

## The Firehose Effect

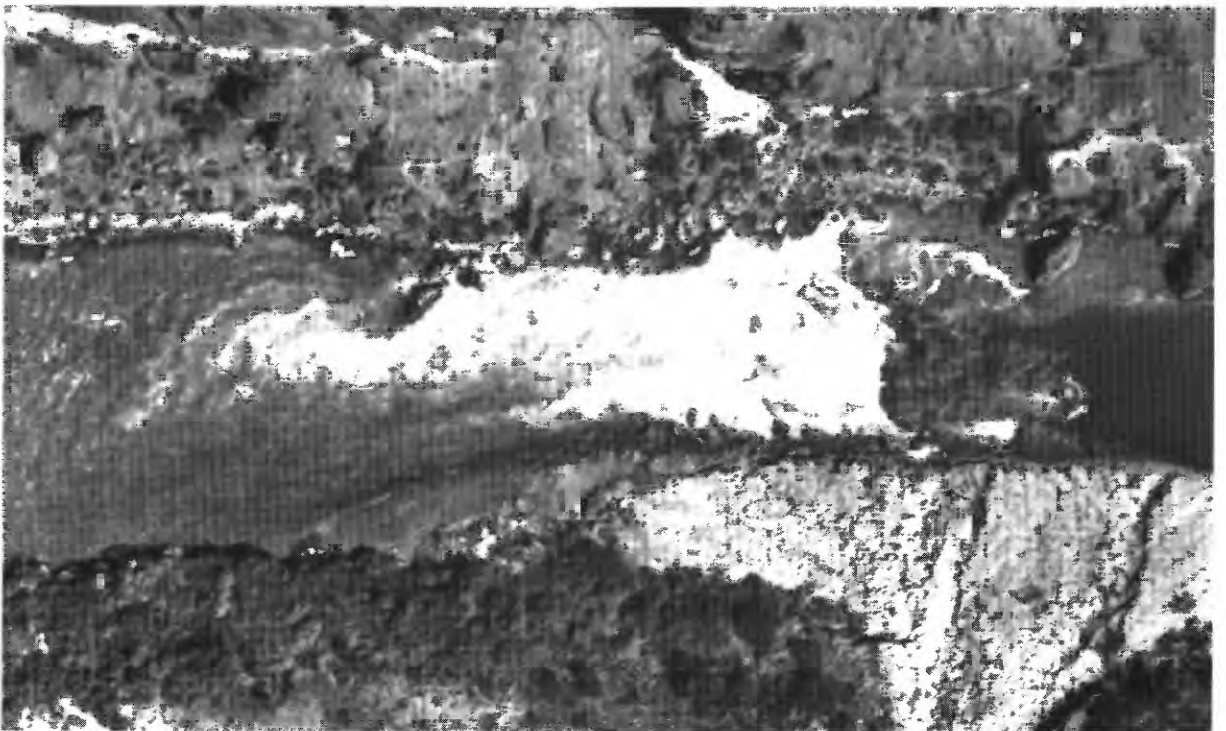
Because of the waterfall separating Prospect Valley and Prospect Canyon (fig. 3), the firehose effect is the primary process of debris-flow initiation in Prospect Canyon. This process involves the impact of a concentrated stream of water falling on unconsolidated colluvial wedges. The power generated by falling water in Prospect Canyon is extremely large; for example, a clear-water discharge of 100 m<sup>3</sup>/s, a 10-year flood in Prospect Valley, develops a terminal velocity of about 80 m/s under the 325-m waterfall (assuming an uninterrupted fall and negligible friction losses). This falling water has an impact power of approximately 80 Mw, which is more than sufficient to erode colluvial wedges and bedrock.

During the 1995 debris flow, streamflow poured over the waterfall, hitting high-angle colluvial wedges (shown in the center of fig. 27) and the channel of Prospect Canyon. The falling water eroded an 8-m deep, 20-m wide, and 15-m high cylindrical section of the colluvial wedge and a crater 13 m in diameter and 6 m deep in the bottom of Prospect Canyon. In addition, sediment was scoured to a depth of about 4 m from a 200-m reach of the channel immediately downstream from the crater. The total volume removed from the impact areas and channel bed was 6,000 m<sup>3</sup>,

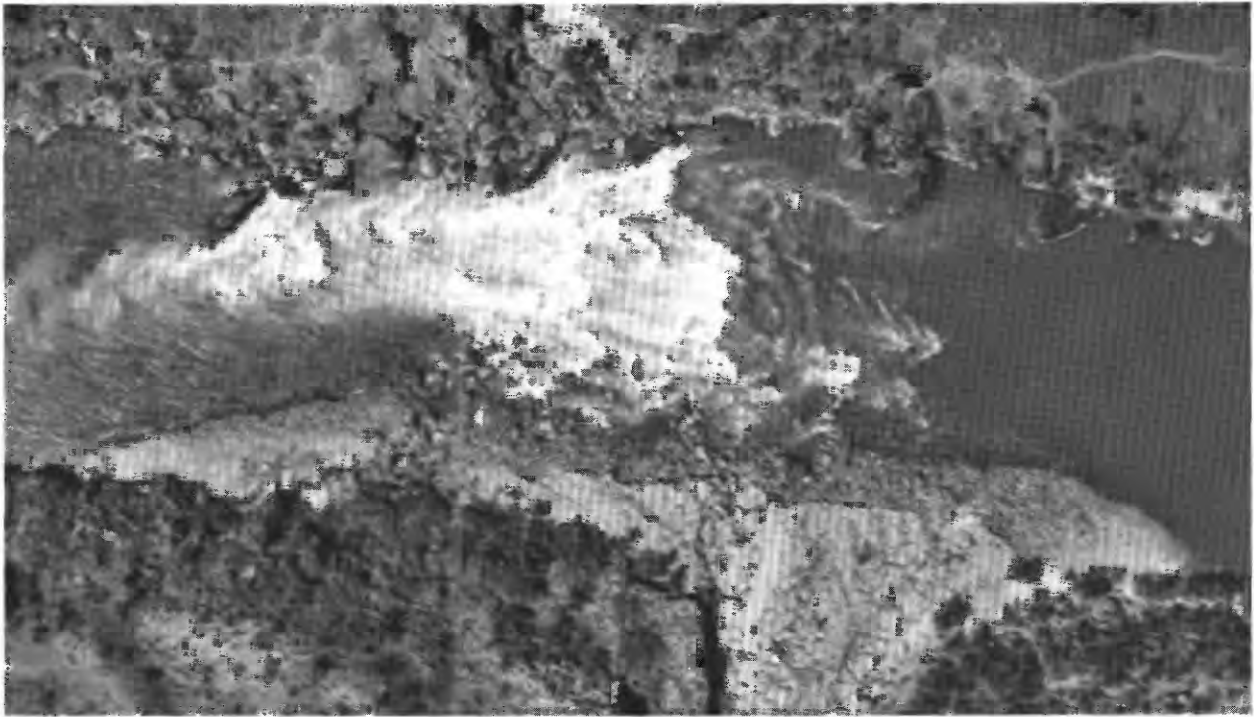




A.



B.



C.

**Figure 28.** Vertical aerial photographs of Lava Falls Rapid. *A*, (June 1, 1994). Before the 1995 debris flow, the rapid had a constriction of 28 percent at a discharge of  $230 \text{ m}^3/\text{s}$ . *B*, (May 30, 1995). After the 1995 debris flow, Lava Falls Rapid had a 50 percent constriction at a discharge of  $260 \text{ m}^3/\text{s}$ . The debris fan did not change significantly between March 8 and May 30. *C*, (April 9, 1996). Reworking during the rising limb of the 1996 controlled flood removed  $5,900 \text{ m}^3$  of the edge of the 1995 debris fan, increasing the width of the rapid by an average of 6 m and decreased the constriction to 30 percent. The discharge is about  $256 \text{ m}^3/\text{s}$ .

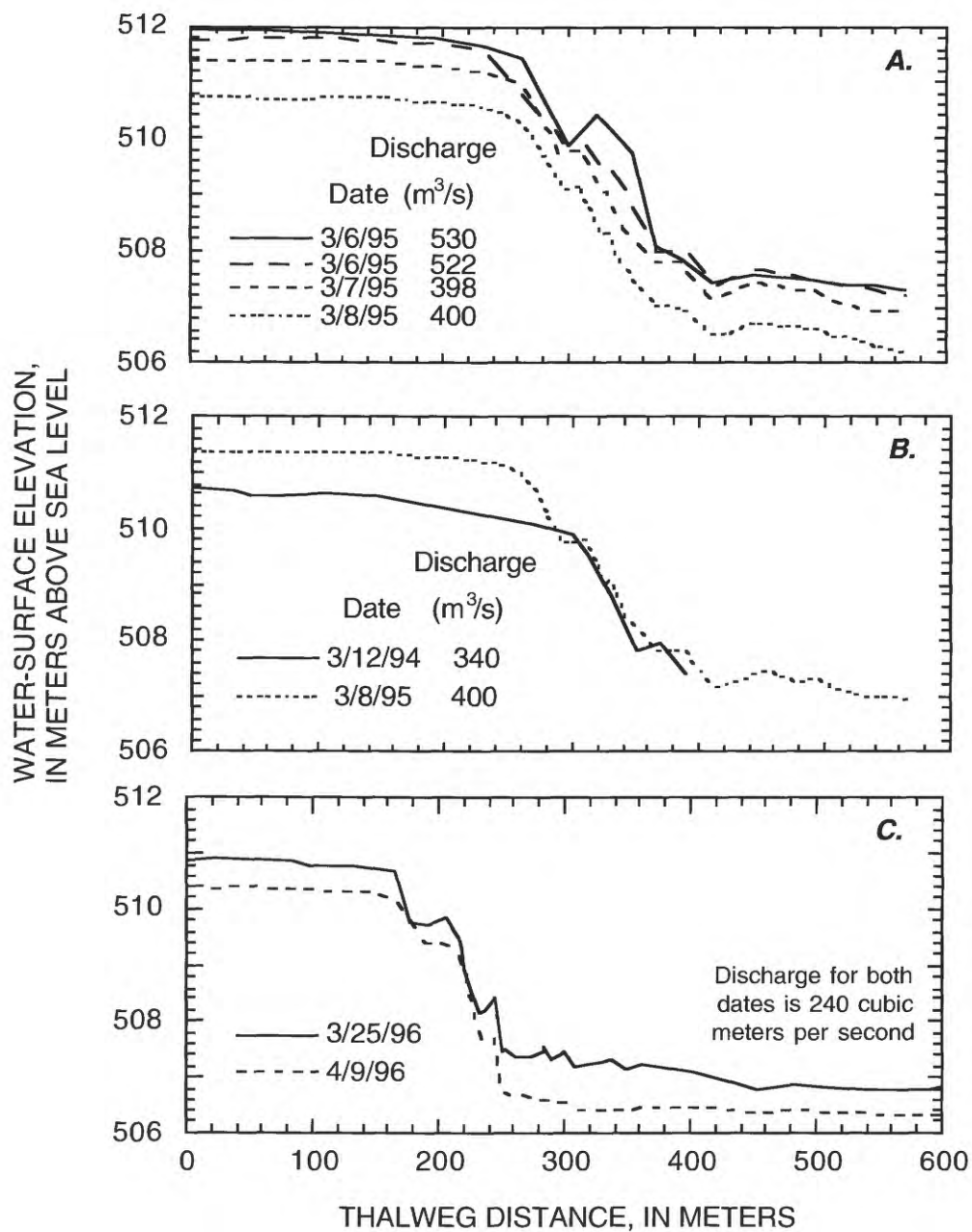


**Figure 29.** Longitudinal profile of the water-surface fall on the right side of Lava Falls Rapid. *A*, Changes in water-surface profile after the 1995 debris flow. *B*, Comparison of water-surface profiles in March 1994 and March 1995. *C*, Comparison of water-surface profile as a result of the 1996 controlled flood.

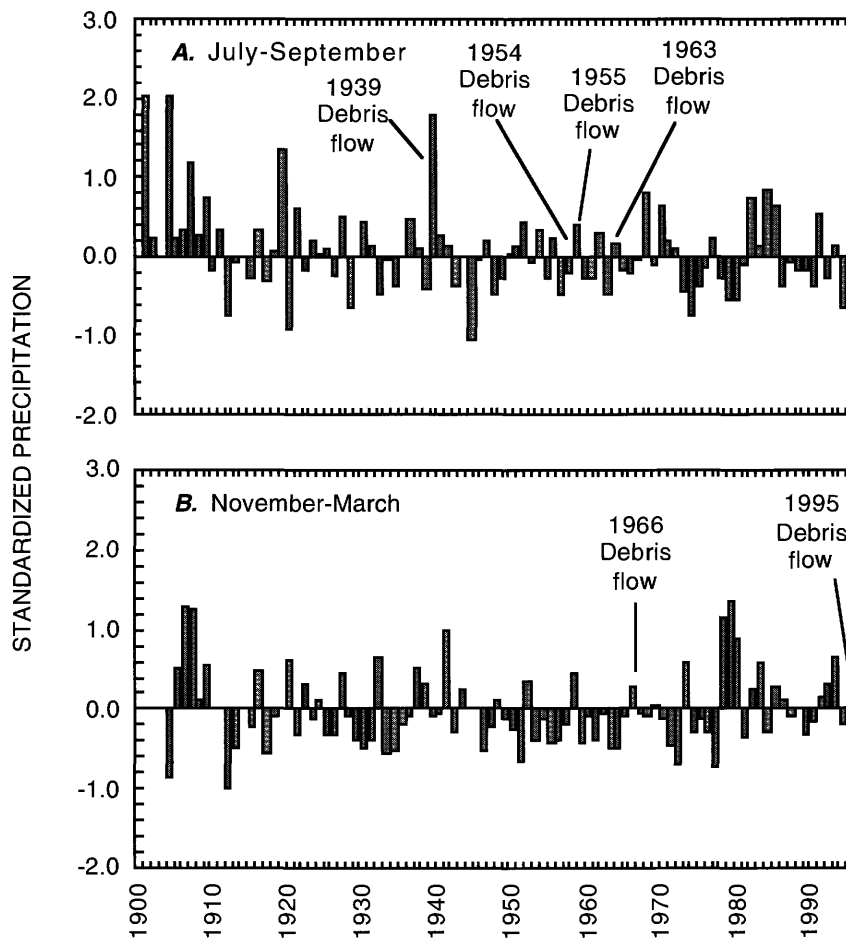


**Figure 30.** Standardized seasonal precipitation for eight stations in the vicinity of western Grand Canyon (table 4). Seasonal precipitation is converted to a time series with mean = 0 and variance = 1; positive values represent above average precipitation. Negative values represent below-average precipitation. A, Summer (July-September) precipitation. B, Winter (November-March) precipitation.

or about 64 percent of the volume of sediment deposited on the debris fan.

The amount of sediment transported by the 1995 debris flow increased with distance downstream in Prospect Canyon because alluvial deposits, particularly channel banks, were undercut and eroded. This “bulking-up” occurred when channel banks collapsed during passage of the debris flow initiated under the waterfall. We assumed the unit weight of flow,  $\gamma = 22,000 \text{ N/m}^3$  for a debris flow with a discharge of  $500 \text{ m}^3/\text{s}$  ( $100 \text{ m}^3/\text{s}$  of streamflow mobilized into a debris flow). Using an energy slope equal to the bed slope of 0.315 in Prospect Canyon and a channel-width range of 15–20 m, the range in unit stream power was

$170\text{--}230 \cdot 10^3 \text{ W/m}^2$ . This value of stream power is more than an order of magnitude greater than the stream power reported for large streamflow floods (Costa and O’Connor, 1995) because our calculation is for a debris flow on a steep slope. However, the duration of debris flows is short (1–5 min.) and the total energy expended is relatively small.

Although other studies have suggested streamflow can bulk-up into a debris flow by failure of channel banks alone (Johnson and Rodine, 1984), there is no evidence of a debris flow in Grand Canyon that was initiated solely by streamflow undercutting channel banks (Melis and others, 1994). Debris flows initiated below the waterfall at the head of Prospect



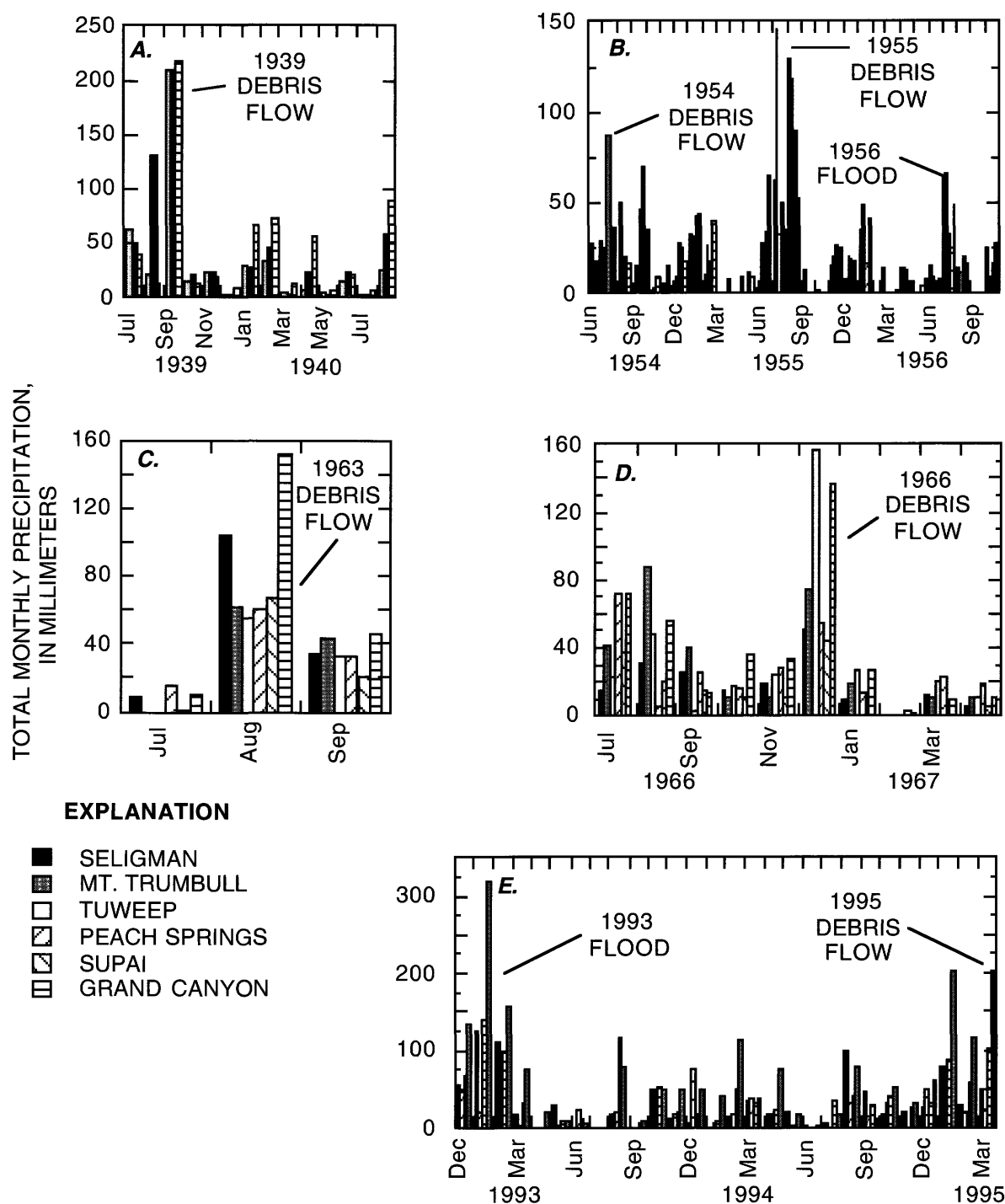


**Figure 31.** Monthly precipitation near the Prospect Valley drainage basin associated with Prospect Canyon debris flows and floods. *A.* July 1939 to August 1940. *B.* June 1954 to October 1956. *C.* July to September 1963. *D.* July 1966 to April 1967. *E.* December 1992 to March 1995.

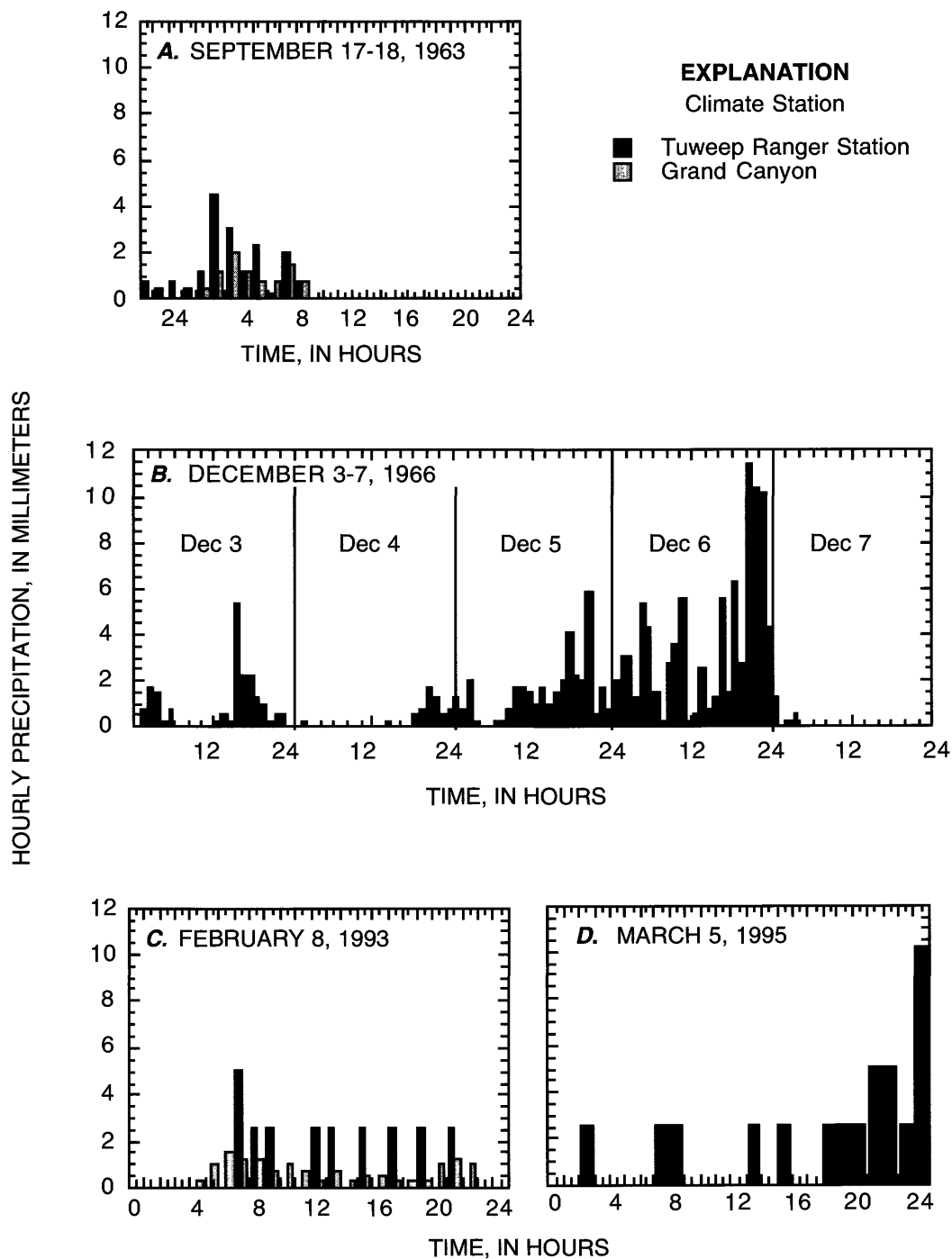


**Figure 32.** Hourly precipitation at Tuweep Ranger Station and Grand Canyon during three historical debris flows and one flood in Prospect Canyon. *A*, September 1963. *B*, December 1966. *C*, February 1993 (streamflow flood). *D*, March 1995.

**Table 8.** Peak discharge estimates from superelevation evidence for the debris flows of 1939, 1955, and 1963 in Prospect Canyon at cross section A - A'.

Year of flow	R <sub>c</sub> (m)	ΔH <sub>r</sub> (m)	T <sub>c</sub> (m)	Velocity (m/s)	Area (m <sup>2</sup> )	Discharge (m <sup>3</sup> /s)
1939	50	3.0	40	6.1	170	1,000
1955	50	0.7	20	4.1	70	290
1963	50	1.5	20	6.1	60	370

Canyon entrain considerable amounts of additional sediment through erosion of colluvial wedges, channel banks, and bed sediments between the waterfall and the Colorado River. After the March 6, 1995, debris flow, the only sediment exposed in the channel that was not moved were boulders greater than 2–3 m in diameter.

## MAGNITUDE AND FREQUENCY OF DEBRIS FLOWS

### Discharge Estimates

We identified superelevated debris-flow deposits for the 1939, 1955, and 1963 events near section A - A' on the Prospect Canyon debris fan (pl. 1). With the exception of the 1939 debris flow, we found only depositional evidence to constrain the cross-sectional area at the point of maximum superelevation. The site on the Prospect Canyon debris fan was a poor one for estimating discharge of debris flows. In the right-hand bend just upstream from cross section A - A', a continuous line of boulders, combined with photographic evidence, provided the elevations of the flow surface on the inside and outside of the bend. No bedrock is exposed in the alluvial channel, which has changed in cross section (fig. 6) despite the presence of large boulders that were not moved by recent debris flows, particularly the 1995 event. The channel slope through the bend is 0.093.

Using the depositional evidence and surveyed cross sections, we estimated discharges for three debris flows (table 8). The 1939 debris flow had a discharge of about 1,000 m<sup>3</sup>/s, a discharge larger than the 1966 debris flow in Crystal Creek (280 m<sup>3</sup>/s; Webb and others, 1989), which previously was considered the largest historic debris flow in Grand Canyon. The 1955 and 1963 debris flows were of a similar discharge, about 300–400 m<sup>3</sup>/s. No depositional evidence remains

of the 1954 and 1966 debris flows, and we could not estimate a peak discharge for the 1995 debris flow because it did not overtop channel banks to leave depositional evidence. Recessive streamflow after the 1995 debris flow obliterated any mudlines that might have been deposited during the peak discharge of the debris flow.

To provide another perspective on magnitude and frequency, we determined the approximate water content of the sediment fraction less than 16 mm in diameter to be 7–14 percent. Because this size fraction is about 25 percent of the total particle-size distribution (fig. 4A), the actual water content may have been less than 5 percent for the snout of the debris flow. As stated in the "Methods" section, the estimated 100-year streamflow flood in Prospect Valley is 800 m<sup>3</sup>/s. Assuming this flood would produce a debris flow in Prospect Canyon with no attenuation of flow and assuming that flood water constitutes 5 percent of the debris-flow volume, the 100-year debris-flow discharge could be as large as 16,000 m<sup>3</sup>/s. Because the largest Prospect Canyon debris flow in 120 years is 1,000 m<sup>3</sup>/s, this number appears to be unrealistically high. We conclude that the regression equations of Thomas and others (1994) for estimating flood frequency may be inappropriate for the Prospect Valley drainage basin.

### Debris-fan Volumes

The entire Prospect Canyon debris fan above the 140 m<sup>3</sup>/s stage of the Colorado River has a total volume of  $1.9 \cdot 10^6$  m<sup>3</sup>. To estimate the uneroded volume of surface tua (1050 BC), the highest surface on the Prospect Canyon debris fan (pl. 1), we added the volume of the entrenched channel and the volume of the projected debris fan surface across the Colorado River. The reconstructed debris fan from surface tua had an area of 15.9 ha and a volume of  $3.5 \cdot 10^6$  m<sup>3</sup> (table 9, fig. 33), assuming that the entire debris fan

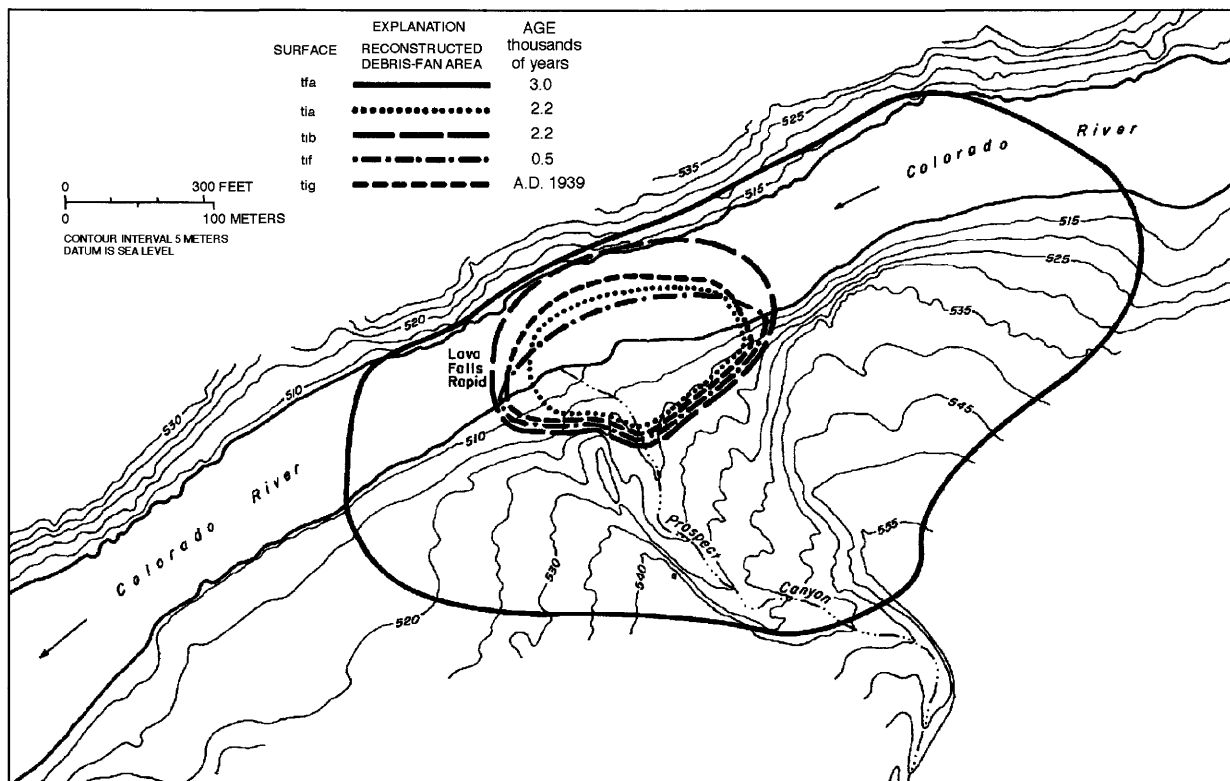


**Figure 33.** The spatial extent of five debris fans deposited by Holocene debris flows from Prospect Canyon. The location of the edge and the thickness of the debris fan were determined by projection into the river from remnant deposits (table 9).

was created by one debris flow. If more than one event created surface tua, as suggested in figure 8, then the uppermost debris flow has a volume of about  $0.8\text{--}0.95 \times 10^6 \text{ m}^3$ . The projected slope of surface tua indicates that the debris flow crossed the Colorado River. The height above the center of the river at a stage of  $140 \text{ m}^3/\text{s}$  was 19.3 m (point V), 16.9 m (point U), and 15.0 m (point T, pl. 1). On the basis of Kieffer's (1988) reported depths of the Colorado River at these points, the maximum thickness of the deposit above the bed of the Colorado River was 30.3 m (point V), 27.7 m (point U), and 24.2 m (point T).

Kieffer (1988) attributes the large basalt boulders on the right side of Lava Falls Rapid—for example, the Black Rock, the Entrance Rock, and the Scout Rock (fig. 11)—to rockfall from the basalt cliffs above the rapid. This accumulation of boulders is unusual for the reach of channel above and below the rapid where relatively few large basalt boulders appear under similar cliffs (see Kieffer, 1988). An alternative explanation is that these boulders were deposited by a debris flow (or debris flows) that dammed the Colorado River, such as the 1050 BC event that formed surface

tua. The projected area of the reconstructed tua surface covers most of the large boulders, including the Black Rock by 1–2 m and the Entrance Rock by 5 m, and is at about the same elevation as the Scout Rock. Similar-sized boulders remain in the channel of Prospect Canyon (Webb and others, 1996), supporting the possibility of Prospect Canyon as the source for some of the boulders on the right side of the rapid.

Other Holocene and historic debris flows may not have been large enough to cross the Colorado River at the mouth of Prospect Canyon. The other surfaces have a relatively steep slope, and projection into the river results in only a moderate-size debris fan (fig. 33). The 1939 debris flow (surface tig), the largest historic event, deposited a debris fan of 1.25 ha and had a volume of  $44,000\text{--}63,000 \text{ m}^3$  (table 9); in comparison, the uneroded fan of the 1966 Crystal Creek debris flow had a volume of about  $58,000 \text{ m}^3$  before reworking (Melis and others, 1994). The 1965 debris fan at Warm Springs Rapid on the Yampa River in Colorado had a volume of  $40,000 \text{ m}^3$  (Hammack, 1994), or slightly smaller than the largest historic Prospect Canyon debris fans. Other Prospect Canyon debris flows



**Table 9.** Characteristics of late Holocene debris fans deposited at the mouth of Prospect Canyon.

Surface	Year of flood (type) <sup>1</sup>	Method <sup>2</sup> of dating	Maximum debris-fan area (ha)	Maximum <sup>3</sup> debris-fan thickness (m)	Minimum <sup>3</sup> debris-fan thickness (m)	Range in debris-fan volume (10 <sup>3</sup> m <sup>3</sup> )	Recurrence interval of volumes (yrs)	Maximum <sup>4</sup> constriction (%)
tua	1050 BC (DF)	<sup>3</sup> He	15.9 <sup>5</sup> 15.9 <sup>5</sup>	22 6 <sup>9</sup>	22 5 <sup>9</sup>	3,500 800-950	n.c.	100
tia	250 BC (DF)	<sup>3</sup> He	1.19 <sup>5</sup>	12	10	119-131	600	50
tib	250 BC (DF)	<sup>3</sup> He	2.23 <sup>5</sup>	20	15	335-446	2,000	100
tic-tie	n.d. (DF)	n.d.	n.c.	n.c.	n.c.	100-400 <sup>6</sup>	1,500	n.c.
tif	AD 1434 (DF)	<sup>14</sup> C	1.07 <sup>5</sup>	5.0	4.0	43-54	200	45
tig	1939 (DF)	<sup>3</sup> He, <sup>14</sup> C, P	1.25 <sup>5</sup>	5.0	3.5	44-63	200	80
n.s.	1954 (DF)	W	0.42 <sup>7</sup>	2.0	1.6	3.2-8.4	15	40
tih	1955 (DF)	<sup>14</sup> C, P	0.73 <sup>7</sup>	2.9	2.1	15-21	60	70
n.s.	1956 (F)	P	0.24 <sup>7</sup>	0.8	0.5	1.2-1.9	n.a.	n.a.
tii	1963 (DF)	<sup>14</sup> C, P	0.73 <sup>7</sup>	1.9	1.7	12-14	40	60
tii	1966 (DF)	<sup>14</sup> C, P	0.38 <sup>8</sup>	1.6	1.0	3.8-6.1	15	35
tij	1995 (DF)	W	0.56 <sup>7</sup>	1.7	1.7	9.4	30	60

*Notes:* All areas and volumes are for sediments exposed above a discharge of 140 m<sup>3</sup>/s. n.d., no data, n.a., not applicable, n.c., not calculated, n.s., no surface associated with this event.

<sup>1</sup> F, streamflow flood, DF, debris flow.

<sup>2</sup> <sup>3</sup>He, cosmogenic <sup>3</sup>He; <sup>14</sup>C, radiocarbon dating; P, historical photography combined with rainfall records and <sup>137</sup>Cs; W, witnessed.

<sup>3</sup> Maximum thickness was estimated during field surveys of noneroded debris-flow deposits; minimum thickness is the thickness of debris-flow deposit that would cover immobile boulders at mouth of Prospect Creek.

<sup>4</sup> The maximum constriction is the percent reduction in river width, compared with an average of upstream and downstream widths, at the narrowest part of the rapid.

<sup>5</sup> Areas, volumes, and constriction ratios were determined by projection of the slopes of remnant deposits (pl. 1) into the Colorado River.

<sup>6</sup> Estimated by comparison with other debris fans.

<sup>7</sup> Areas, volumes, and constriction ratios were determined by rectification of aerial photography (figs. 21, 24) using image-processing software.

<sup>8</sup> Areas, volumes, and constriction ratios were determined by rectification of oblique ground photography (fig. 12) using image processing software.

<sup>9</sup> Determined from approximate thickness shown in figure 8.

deposited 1,200–21,000 m<sup>3</sup> of sediment on the debris fan (table 9). The depositional volumes of debris flows from Prospect Canyon are comparable to the volumes of debris flows from other tributaries in Grand Canyon. The range in volumes of Prospect Canyon debris flows is large, probably because the Prospect Valley drainage basin is the largest tributary for which the volume of debris flows has been estimated (fig. 34).

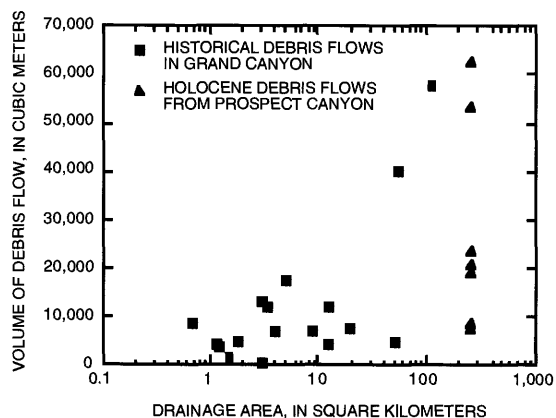


**Figure 34.** The volume of sediments deposited on debris fans by historical debris flows in Grand Canyon (modified from Melis and others, 1994) and by Holocene debris flows from Prospect Canyon.

## Constrictions of the Colorado River

Holocene debris flows from Prospect Canyon deposited debris fans with  $C_w$  that range from 30–100 percent and the maximum  $C_w$  from 35–100 percent (fig. 33, table 9). In 1872, the average  $C_w$  (at 280 m<sup>3</sup>/s, reconstructed by rectifying fig. 12A) was 5 percent, and  $C_w$  in 1994 at 230 m<sup>3</sup>/s (fig. 28A) was 30 percent (table 10). Therefore, historic debris flows decreased the width of Lava Falls Rapid by about 25 percent before the 1995 debris flow.

Values of  $C_w$  for Holocene debris flows at Lava Falls Rapid span most of the range of  $C_w$  in Grand Canyon (fig. 35). In her discussion of constriction ratios, Kieffer (1985, 1987) noted that Crystal Rapid likely had a maximum constriction of about 75 percent before reworking, or less than the 80 percent constriction caused by the 1939 debris flow from Prospect Canyon (table 10). The 1939 debris flow from Prospect Canyon apparently had a greater effect on the Colorado River than the 1996 Crystal Creek debris flow.

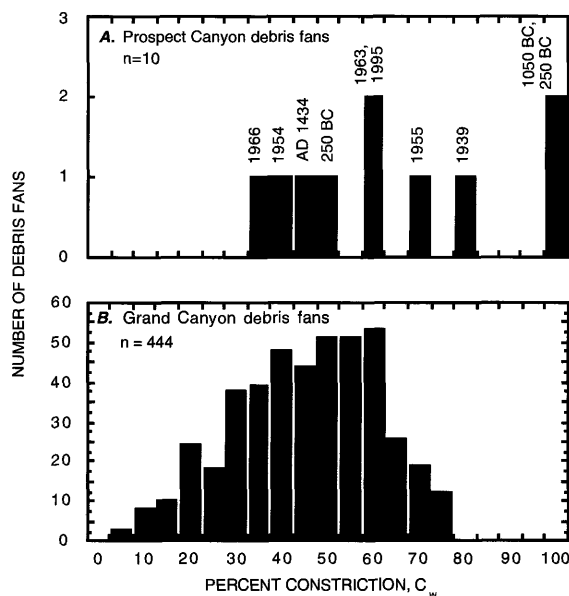


**Figure 35.** Constrictions of debris fans. A, Maximum extent of Prospect Canyon debris fans aggraded by Holocene debris flows and reworked by the Colorado River (table 10). B, Debris fans in Grand Canyon (Melis, 1997).

## Debris-fan Frequency

The evidence of Holocene debris flows is sufficient to estimate recurrence intervals for this type of flash flood in Prospect Canyon. Throughout Grand Canyon, debris flows have an average recurrence interval of one debris flow every 20–50 yrs (Melis and others, 1994). In the photographic history spanning 123 yrs, Prospect Canyon has had six debris flows (table 7); if these were considered independent of one another, the historical frequency of debris flows is one every 20 yrs. Debris flows from Prospect Canyon are clustered in time—most occurred during the middle part of the 20th century when five debris flows occurred in a 27-year period (a recurrence interval of every 5 yrs). Alternatively, six debris flows occurred from 1939 through 1995 for a recurrence interval of about 10 yrs. Regardless of the estimation period, the frequency of historic debris flows from Prospect Canyon (one every 5–20 yrs) is greater than the frequency of debris flows in other Colorado River tributaries (Melis and others, 1994).

We combined the age-dating information with the volume data to estimate the frequency of debris flows from Prospect Canyon. We established a type I censored-data model with three censoring thresholds of debris-flow volume to reflect the known depositional

**Table 10.** Constrictions of historic aggraded and reworked debris fans at the mouth of Prospect Canyon.

Year	Date of photograph or survey	River discharge on date (m <sup>3</sup> /s)	Maximum river discharge between dates (m <sup>3</sup> /s)	Constriction C <sub>w</sub> (%)	Method	Comments
1872	April 16	280	n.a.	5	<sup>1</sup>	Fully reworked debris fan
1939	September 6	150	8,500	80	<sup>2</sup>	Newly aggraded debris fan
1954	July 24	250	3,460	40	<sup>3</sup>	Mostly reworked 1939 debris fan
1955	March 19	540	530	30	<sup>3</sup>	Partially reworked 1954 debris fan
1955	March 21	400	540	30	<sup>3</sup>	Partially reworked 1954 debris fan
1956	March 25	180	1,140	70	<sup>3</sup>	Partially reworked 1955 debris fan
1956	April 16	300	520	60	<sup>3</sup>	Partially reworked 1955 debris fan
1956	August 29	80	1,900	70	<sup>3</sup>	Partially reworked 1955 debris fan and 1956 flood
1957	May 4	520	680	35	<sup>3</sup>	Rising discharge, partially reworked debris fan
1958	April 20	710	3,540	15	<sup>3</sup>	Mostly reworked debris fan
1958	June 1	3,000	3,000	15	<sup>3</sup>	Mostly reworked debris fan
1958	October 4	190	3,050	30	<sup>3</sup>	Mostly reworked debris fan
1960	October 2	130	1,310	40	<sup>3</sup>	Mostly reworked debris fan
1962	November 3	230	2,420	30	<sup>3</sup>	Mostly reworked debris fan
1963	August 22	60	230	30	<sup>3</sup>	Mostly reworked debris fan
1964	April 20	40	550	60	<sup>3</sup>	Partially reworked 1963 debris fan
1965	May 18	790	1,290	30	<sup>3</sup>	Mostly reworked debris fan
1966	May 19	500	1,650	30	<sup>2</sup>	Mostly reworked debris fan
1967	August	340	520	35	<sup>2</sup>	Partially reworked 1966 debris fan
1973	June 19	390	1,080	20	<sup>3</sup>	Mostly reworked debris fan
1989	October 8	160	2,720	30	<sup>3</sup>	Mostly reworked debris fan
1994	June 1	240	970	30	<sup>3</sup>	Mostly reworked debris fan
1995	March 6	530	620	60	<sup>4</sup>	Newly aggraded debris fan
1995	May 30	260	530	50	<sup>3</sup>	Partially reworked 1995 debris fan
1996	March 23	250	720	40	<sup>3</sup>	Partially reworked 1995 debris fan
1996	April 6	250	1,270	30	<sup>3</sup>	Mostly reworked 1995 debris fan

Notes: The method for calculating constrictions is described in the notes for table 8 and in the text. Values of C<sub>w</sub> are rounded to the nearest 5 percent. n.a., not applicable.

<sup>1</sup>Constrictions were determined by rectification of oblique ground photography (fig. 12) using image-processing software.

<sup>2</sup>Constrictions were determined by projection of the slopes of remnant deposits (pl.1) into the Colorado River.

<sup>3</sup>Constrictions were determined by rectification of aerial photography (fig. 21) using image-processing software.

<sup>4</sup>Constrictions were determined by field-survey data.

and temporal data. The first threshold, at  $3 \cdot 10^6 \text{ m}^3$ , is the total volume of surface tua, which was the largest debris flow in the last 3 ka. We changed this threshold to  $0.8 \cdot 10^6 \text{ m}^3$  to test the effect of our assumption that surface tua is one debris flow versus several. The second threshold, at  $0.1 \cdot 10^6 \text{ m}^3$ , reflects the prehistoric inset surfaces, including surface tia through surface tif (table 9, pl. 1) and had a time range of 2.2 ka. The final depositional threshold had a magnitude of  $3 \cdot 10^3 \text{ m}^3$ , a duration of 123 yrs, and represented the six historical events. The latter threshold effectively reduces the problem of obliterative overlap of very small events and eliminates the problem of years with zero depositional volume.

The recurrence intervals for the debris fans (table 9) provide a magnitude-frequency relation for historical debris flows from Prospect Canyon. The small historic debris flows, such as the 1995 event, have recurrence intervals of 15-60 yrs. The AD 1434 and 1939 debris flows are 200-year events. Surface tia (250 BC), the oldest of the inset surfaces, has a recurrence interval of 600 yrs, and surfaces tib and tic-tie have recurrence intervals of 2,000 and 1,500 yrs, respectively (table 9). Change in the volume of surface tua altered the recurrence intervals for the largest debris flows; for example, the recurrence intervals for surfaces tib and tic-tie increased to 3,000 and 2,500 yrs, respectively.

Surface tua, which is an order of magnitude larger than the second largest debris flow, had a recurrence interval on the order of 10,000 yrs, on the basis of either the assumption that the entire debris fan is one event or that just the upper 5–6 m is one debris flow. The standard error of the volume for recurrence intervals of 100-1,000 yrs is 25–30 percent. To understand the effect of dating uncertainty, we varied the length of the first threshold between 3.0 ka and 3.6 ka, and we found that the volumes calculated for the 10-, 100-, and 1,000-year recurrence intervals were nearly identical.

## REWORKING OF DEBRIS FANS BY THE COLORADO RIVER

Reworking of rapids by river floods was initially described by Graf (1979, 1980) and Howard and Dolan (1981). Kieffer (1985, 1987, 1990) presented a conceptual model for reworking of debris fans in Grand Canyon, incorporating elements from the

previous studies. This model, based on alteration of Crystal Rapid during the large releases from Glen Canyon Dam in 1983 (Kieffer, 1985), consists of the stages of (1) damming of the river by a debris flow, (2) the river overtopping the debris fan, forming a “waterfall” on the downstream side, and (3) headcut progression from downstream to upstream across the debris fan, depending on discharges in the river. The history of reworking of the Prospect Canyon debris fan shows the instability of rapids controlled by debris flows, and suggests a modification of Kieffer’s conceptual model.

The effectiveness of unregulated flood and dam releases in alleviating constrictions is extremely important. Before regulation in 1963 by Glen Canyon Dam, the 2-year flood on the Colorado River was approximately  $2,140 \text{ m}^3/\text{s}$ ; the 100-year flood was  $5,650 \text{ m}^3/\text{s}$  (fig. 36).

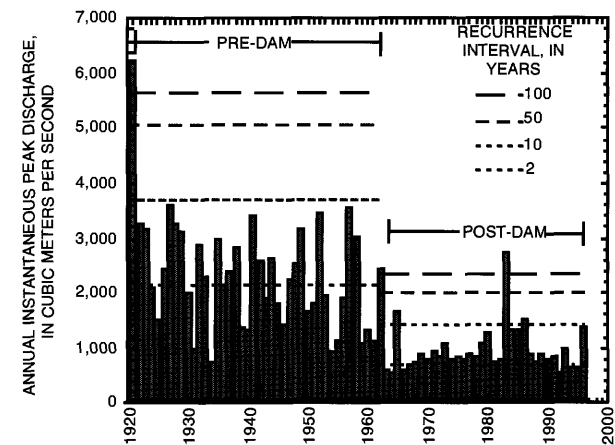


**Figure 36.** Annual series of instantaneous peak discharges for the Colorado River near Grand Canyon, Arizona. Recurrence intervals were calculated using a log-Pearson type III distribution for pre-dam (1921–1963) and post-dam (1963–1995) discharges.

The largest historical flood was  $8,500 \text{ m}^3/\text{s}$  in 1884; several prehistoric Holocene floods exceeded  $8,500 \text{ m}^3/\text{s}$  and one may have been as large as  $11,000 \text{ m}^3/\text{s}$  (Hereford and others 1993, 1996; O’Connor and others, 1994). Regulation by Glen Canyon Dam reduced the apparent 2-year flood to about  $890 \text{ m}^3/\text{s}$ . Floods on the unregulated Colorado River were larger and of longer duration than dam releases (figs. 37, 38).

## Reworking of Historical Debris Fans

At the time of the Powell Expedition (figs. 11B, 12A), Lava Falls Rapid was wide with an average constriction of 5 percent (table 10). That the rapid did



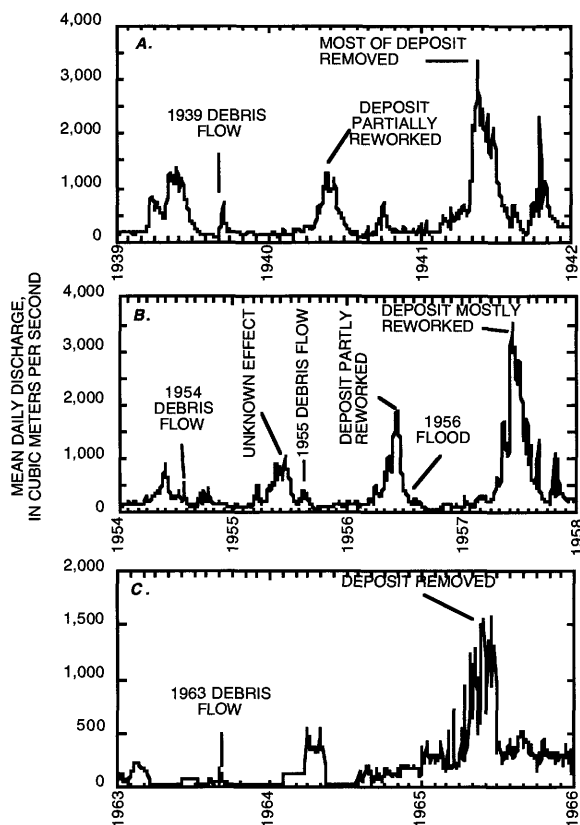


**Figure 37.** Hydrographs of the Colorado River showing the timing of tributary floods and debris flows and reworking by river discharges. A, 1939 to 1942. B, 1954 to 1958. C, 1963 to 1966.

not change between 1872 and 1939 is significant because several large floods occurred in the Colorado River between 1921 and 1939 (fig. 36). The Pyramid and Deflector rocks, and many boulders on the debris fan, were unaffected by floods in excess of  $5,660 \text{ m}^3/\text{s}$  that occurred in 1884 and 1921; equivalent-sized floods also may have occurred in 1891, 1905, and 1916. Photographs taken in 1909 and 1934 at low water (figs. 14, 17) show boulders in excess of 3 m in diameter on the bed in Lava Falls Rapid. The boulders were wedged together in groups; water flowing over them formed large waves and holes that compelled most expeditions to portage around the rapid.

The 1939 debris flow initially constricted the Colorado River by 80 percent. If the top of the 1939 levee is projected over to the right bank of the Colorado River, the resulting width of the Colorado River would have been only 5.2 m. The debris fan aggraded in 1939 (table 9) and subsequently the rapid was widened to an unknown extent by the 1941 flood (peak discharge of  $3,400 \text{ m}^3/\text{s}$ ), but no “rock garden” (partially submerged debris fan) formed below the rapid, as suggested by Kieffer’s model. Photographs from the 1940s

(figs. 18 and 19) show a slightly wider rapid than in the early 1990s, which suggests the constriction in the 1940s may have been less than 25 percent.

Two debris flows in the 1950s again constricted Lava Falls Rapid (tables 8 and 9). The 1954 debris flow increased the constriction to 40 percent, but Colorado River discharges up to  $540 \text{ m}^3/\text{s}$  reduced the constriction to about 30 percent by the following spring. The 1955 debris flow increased the constriction to 70 percent, which formed a stable configuration for nearly 2 yrs despite discharges up to  $1,900 \text{ m}^3/\text{s}$  (table 10). Aerial photographs from 1956 and 1957 (figs. 21C and 21D) show no evidence—neither erosional nor depositional—that the debris fan was overtopped; the surface appears to be a pristine debris-flow deposit that has been eroded along the river margin. Instead, the river eroded the margin of the debris fan and then transported boulders when river stage created sufficient stream power. The first photographs after the 1957 and 1958 floods, taken at low discharge in October 1958, showed a constriction of 30 percent (table 10).

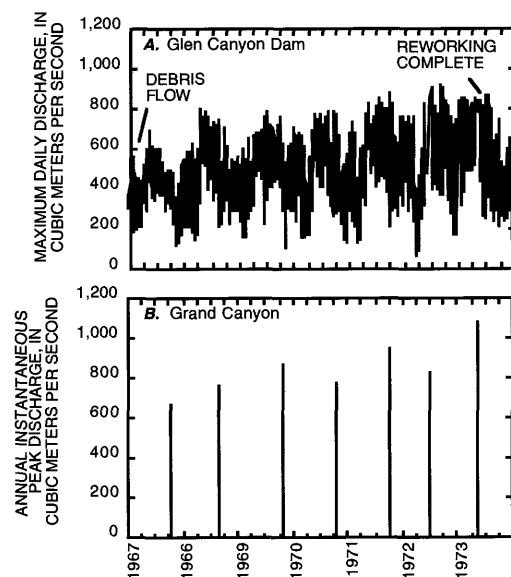


**Figure 38.** Hydrographs of the Colorado River from December 1966 to 1974 showing the timing of the 1966 debris flow and releases from Glen Canyon Dam. A, Maximum daily discharge. B, Annual peak discharge.

The two debris flows in the 1960’s, which occurred during the first 4 years of operation of Glen Canyon Dam, were reworked by an unusually large dam release and a combination of dam release and tributary floods (figs. 37, 38). The 1963 debris flow

caused a 60-percent constriction; the 1965 releases from Glen Canyon Dam, which peaked at  $1,650 \text{ m}^3/\text{s}$ , reduced the constriction to 30 percent. The 1966 debris flow created a 35-percent constriction (table 10). A powerplant release of  $840 \text{ m}^3/\text{s}$  on May 26, 1972 partially reworked the debris fan, and the combination of low dam releases and a small flood in the Little Colorado River on April 17, 1973, created a peak discharge of  $1,080 \text{ m}^3/\text{s}$ , which eroded most of the aggraded debris fan and reduced  $C_w$  to 20 percent (table 10). Additional changes in Lava Falls Rapid occurred during the  $2,720 \text{ m}^3/\text{s}$  flood of 1983, but these were relatively minor, and the constriction in 1994 was 30 percent. The amount of elapsed time from deposition to reworking increased from 1–2 yrs to 3–7 yrs because of a decrease in the frequency of floods caused by the operation of Glen Canyon Dam (fig. 36).

Not including the 1995 deposit, the total volume of sediment deposited by historical debris flows at Lava Falls Rapid was about  $110,000 \text{ m}^3$ . Most of this sediment was reworked by the Colorado River, leaving a net residual deposit of  $2,000 \text{ m}^3$  that increased the river's constriction from about 5 percent in 1872 to 30 percent in 1994. Including the  $4,800 \text{ m}^3$  eroded from the 1995 debris fan, a total of  $115,000 \text{ m}^3$  of sediment was eroded from the debris fan and transported downstream between 1939 and 1995. Using the sediment-budget approach described by Melis and Webb (1993), approximately 70 percent of this volume ( $86,000 \text{ m}^3$ ) was boulders (greater than 256 mm, fig. 39A) that were transported to Lower Lava Rapid or downstream. This prodigious supply of boulders from Prospect Canyon is the reason the total drop from the top of Lava Falls Rapid to the bottom of the lowermost secondary riffle is 12 m. The five alternating debris bars that control the secondary riffles are spread over a distance of 2 km downstream from Lava Falls (Stevens, 1990).

## Reworking of the 1995 Debris Fan

The 1995 debris flow from Prospect Canyon initially constricted the Colorado River by about 60 percent (table 9; Webb and Melis, 1995). The reworking that followed provides a good example of the interactions between the Colorado River and newly aggraded debris fans. Reworking began immediately after cessation of the debris flow and lasted 12 hrs without overtopping of the debris fan by the Colorado River. Within that half day, 45 percent ( $4,200 \text{ m}^3$ ) of the

volume of the new debris fan was removed by the Colorado River; an additional  $660 \text{ m}^3$  was eroded by recessional flow in Prospect Canyon. Twelve hours

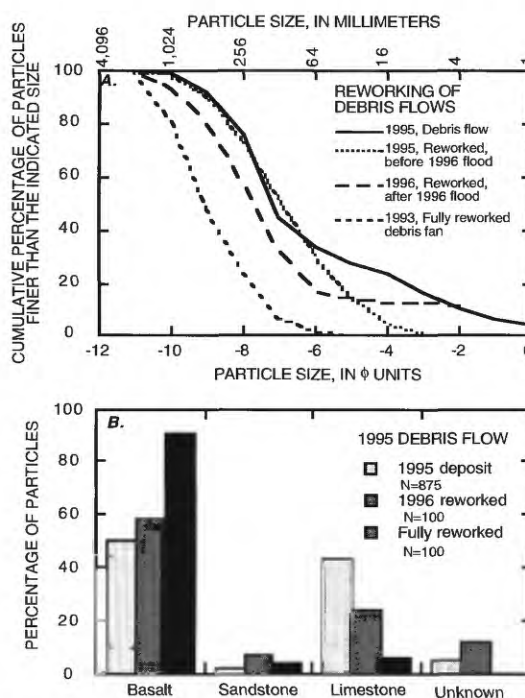


**Figure 39.** Effects of river reworking on sediment particle size and lithology on the Prospect Canyon debris fan. *A*, Comparison of the particle-size distribution on the intact and reworked margins of the debris-flow deposit. *B*, Comparison of rock types transported in the main lobe of the 1995 debris flow with the lithologies of sediments on the reworked debris fan.

after the deposition, 52 percent of the deposit was removed.

Reworking increased the median particle size ( $D_{50}$ ) of the 1995 deposit from 350 mm to 512 mm (fig. 39A) on the distal margin of the aggraded fan adjacent to Lava Falls Rapid. Reworking preferentially removed limestone, which constituted 43 percent of the 1995 deposit and only 24 percent of the reworked deposit. In contrast, the percentage of basalt clasts increased from 50 percent before the flood to 58 percent afterward (fig. 39B). Before the 1995 debris flow, the debris fan contained 90-percent basalt and 5-percent limestone.

We observed similarities and differences between reworking at Lava Falls Rapid and Kieffer's (1985, 1987, 1990) conceptual model of debris-fan reworking. The larger reworked particles were deposited in the pool downstream from the Black Rock in an elongated debris bar that is submerged by shallow water at  $263 \text{ m}^3/\text{s}$  (fig. 28B). The elongated debris bar

corresponds in position to Kieffer's (1990) "rock garden." During the initial reworking of March 6, 1995, existing waves in Lava Falls Rapid increased in size, but a hydraulic jump did not form either in response to or because of reworking, as Kieffer (1985, 1990) suggests would occur. Instead, the configuration of waves in Lava Falls Rapid could be related to specific boulder accumulations, and their presence is relatively independent of discharge within the normal range of dam releases.

During the 1996 controlled flood, we observed and measured debris-fan reworking at Lava Falls Rapid (Webb and others, 1997). We noted the relation between the period of active erosion and the hydrograph at Lava Falls Rapid (fig. 40). As the discharge increased on the morning of March 27, the stage increased accordingly until a discharge of about  $1,000 \text{ m}^3/\text{s}$  (about 1130 hrs). The stage was approximately 0.2 to 0.5 m below the top of the aggraded debris fan, and we observed the beginning of bank collapse by slab failures of debris-flow deposit at 1120 hrs. Bank collapse began on the downstream side of the debris fan. By 1200 hrs, the cutbank of the aggraded debris fan was collapsing frequently, and the stage above the rapid became nearly constant with time despite an increasing discharge (fig. 40). For about an hour, boulders could be heard rolling along the bed of the river. Bank collapse greatly decreased in frequency by 1300 hrs, and boulders were heard rolling only occasionally by 1400 hrs. Between 1400 and 1500 hrs, the stage rose again, becoming constant after 1500 hrs despite the slow rise in discharge (fig. 40).

The 1996 controlled flood removed  $5,900 \text{ m}^3$  of the 1995 deposits, compared with  $4,860 \text{ m}^3$  removed by the initial reworking in 1995.  $D_{50}$  on the Prospect Canyon debris fan increased from 210 to 530 mm during the controlled flood;  $D_{85}$  increased from 0.65 to 1.2 m (Webb and others, 1987). As a result of reworking, the particles on the distal margin of the debris fan were larger and better sorted because finer particles were preferentially removed (fig. 39A). Reworking during the 1996 controlled flood preferentially removed limestones, leaving a deposit composed of 90-percent basalt particles (fig. 39B). Removal of limestones is partially explained by a lower particle density and because limestone clasts generally are smaller than basalt clasts on the Prospect Canyon debris fan. These results are in agreement with Melis and Webb (1993) who report similar preferential

lithologic removal during reworking at other debris fans.

At Lava Falls Rapid, velocities on the left and right sides decreased by about half (Webb and others, 1997). This velocity decrease is consistent with the sizeable decrease in channel constriction (table 10). At the top of the rapid, the water-surface elevation at  $250 \text{ m}^3/\text{s}$  decreased by 0.2 m. The total fall through the rapid increased by 0.3 m because partial removal of a small, submerged debris bar that had formed downstream from the rapid after the 1995 debris flow lowered the water-surface elevation in the pool (fig. 29C).

At Lava Falls Rapid, the 10 radio-tagged particles were entrained at discharges between 470 and  $1,020 \text{ m}^3/\text{s}$  (table 11) on the rising limb of the flood hydrograph (fig. 40). We relocated 8 of the 10 particles downstream from Lava Falls Rapid after the flood (fig. 41). The smallest particle (number 3, a cobble) travelled 420 m to another debris bar that forms the secondary rapid (Lower Lava). The six remaining relocated particles were deposited in the pool immediately downstream from the main rapid. The average travel distance for the eight relocated particles was 230 m (table 11).

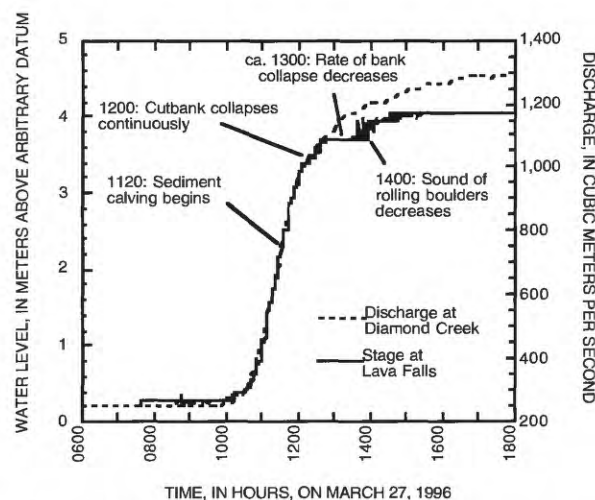


**Figure 40.** The relation between stage, discharge, and reworking of the debris fan at Lava Falls Rapid during the 1996 controlled flood. The stage record at Lava Falls Rapid is for March 27, 1996, and the hydrograph for the Colorado River above Diamond Creek gaging station is adjusted for a discharge-independent travel time of 7.46 hrs.

Because of reworking by the 1996 controlled flood, navigation of Lava Falls Rapid is essentially the same as it was before the 1995 debris flow. Velocities at about  $250 \text{ m}^3/\text{s}$  on the left and right sides of the

**Table 11.** Characteristics of radio-tagged particles at Lava Falls Rapid transported during the 1996 controlled flood in Grand Canyon (from Webb and others, 1997).

Particle number	Lithology	Size	B-axis diameter (m)	Volume (m <sup>3</sup> )	Weight (Mg)	Entrainment time	Approximate discharge (m <sup>3</sup> /s)	Travel distance (m)
3	Basalt	Cobble	0.21	0.003	0.009	1141	830	420
1	Sandstone	Cobble	.22	.006	.017	1102	470	n.d.
4	Sandstone	Boulder	.34	.007	.018	1143	860	230
7	Basalt	Boulder	.28	.011	.029	1202	940	310
2	Sandstone	Cobble	.23	.015	.040	1112	560	110
6	Sandstone	Boulder	.31	.021	.055	1214	1,020	50
8	Sandstone	Boulder	.38	.061	.16	1145	870	250
5	Basalt	Boulder	.49	.065	.18	1136	780	n.d.
10	Sandstone	Boulder	.70	.17	.45	1212	1,010	240
9	Sandstone	Boulder	.66	.23	.61	1207	1,000	220

Notes: n.d., no data.

rapids decreased by half—3.1 to 1.7 m/s on the left and 4.6 to 2.3 m/s on the right—as a result of the controlled flood (Webb and others, 1997). Although the total water-surface fall through Lava Falls Rapid increased by 0.3 m, the stage-discharge relation at the top of the rapid decreased by 0.4 m, causing exposure of several large boulders on the left side at low discharges. The low-water control added by the 1995 debris flow—new boulders that affect flow through the rapid at small discharges—was almost completely removed, and only one boulder remains.

## DISCUSSION AND CONCLUSIONS

Lava Falls Rapid is a formidable reach of whitewater and an example of how debris-flow processes in relatively small bedrock tributaries can control the grade and hydraulics of a major river. Lava Falls Rapid previously was assumed to be an unchanging rapid controlled by the remnants of Pleistocene basalt dams (Fradkin, 1984; Nash 1989). Instead, we have shown that Lava Falls, the most unstable rapid in Grand Canyon, is created, maintained, and periodically modified by frequent debris flows from Prospect Canyon. The highest deposits on the debris fan, deposited about 1050 BC, indicate predominant late Holocene aggradation of one of the largest debris fans in Grand Canyon. Moreover, the 1050 BC debris flow raised the base level of the Colorado River by 30 m before the deposit was

reworked. At Granite Park, 50 river kilometers downstream, Lucchitta and others, U.S. Geological Survey (written commun., 1995), indicate the Colorado River has downcut 10 m in the last 11 ka. This downcutting indicates that the local effects of debris flows on the river corridor may be of the same magnitude as the long-term downcutting of Grand Canyon in the Holocene.

## Age Dating and Frequency of Debris Flows

Using cosmogenic <sup>3</sup>He<sub>c</sub> and conventional <sup>14</sup>C dating, combined with repeat photography, we determined absolute ages for late Holocene debris-flow surfaces on the Prospect Canyon debris fan in Grand Canyon. We then calculated recurrence intervals for debris-flow volume using the age-dating data to constrain the temporal range of deposition. These recurrence intervals indicate that small debris flows, such as the 1995 event, occur relatively frequently in Prospect Canyon. The largest volume debris flows recur at a frequency of several hundred to several thousand years. The uncertainty in age-dating techniques adds only slightly to the uncertainty in recurrence intervals, suggesting that a robust magnitude-frequency model for late Holocene debris flows can be based on a combination of dating techniques.

The <sup>3</sup>He<sub>c</sub> dating technique appears to work for debris flows carrying olivine-laden basalts as young as a few thousand years, but there is a yet unsolved



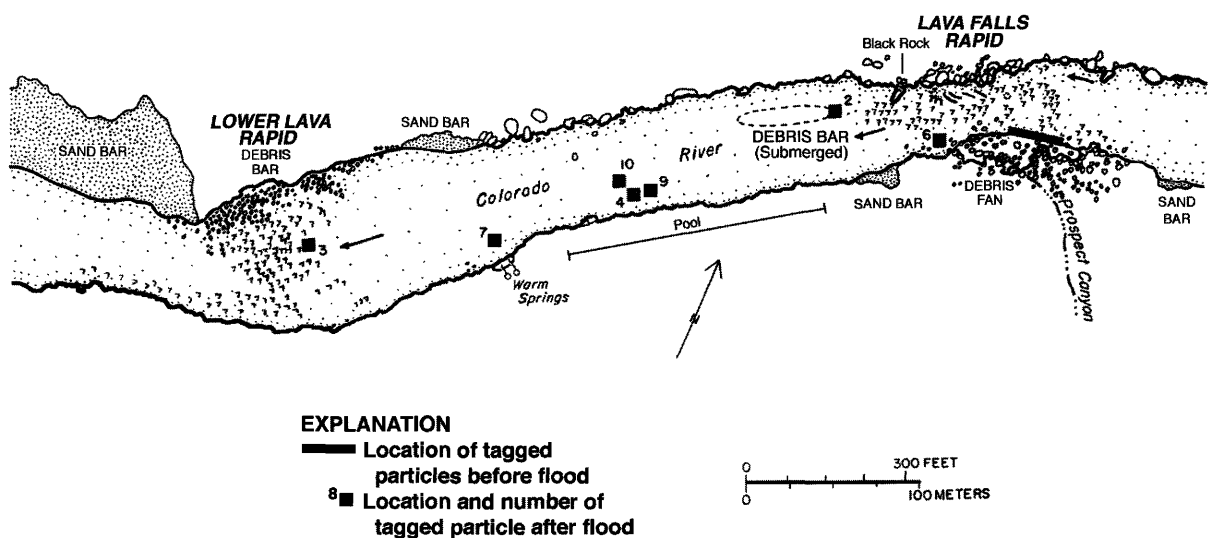


**Figure 41.** Depositional sites of eight radio-tagged cobbles and boulders transported downstream from Lava Falls Rapids during the 1996 controlled flood (see table 11).

uncertainty about corrections for previous cosmic-ray exposure history and a small amount of inherited radiogenic  $^4\text{He}$ . Damon and others (1967) reported excess  $^{40}\text{Ar}$  in basalts near Lava Falls Rapid, and although Wenrich and others (1995) note that basalts in the Uinkaret Volcanic Field contain evidence of mantle contamination, they indicated it was greatest in the oldest lava flows. Laughlin and others (1994) suggest young  $^3\text{He}$  dates should be corrected on the basis of  $^{40}\text{Ar}$  analyses. Because of these uncertainties, a brute force approach might be used in which many different samples are analyzed instead of one or two samples, as is typically collected from older exposure surfaces and those with “single-event” histories.

Despite these problems, we conclude that the three major debris fan surfaces in the Prospect Canyon debris complex—tua, tia, and tib—have integrated exposure ages of about  $3.0 \pm 0.6$ ,  $2.2 \pm 0.4$ , and  $2.2 \pm 0.6$  ka, respectively. These integrated exposure ages are maximum ages because of the problem of previous exposure, and the true age of emplacement may be a few hundred years younger than those given but probably within the stated uncertainty.

The  $^{14}\text{C}$  analyses suggest that woody detritus is infrequently purged from Prospect Canyon. The 1939 and 1955 debris flows transported wood that was significantly older than the known date of these debris flows; which was expected: Ferguson (1971) found persistence of driftwood for as long as 1,000 yrs along the mainstem Colorado River, and Webb (1996) documented dead trees in Grand Canyon that remained standing for 400–500 yrs. Carbon-14 ages on prehistoric debris flows may be as much as 600 yrs older than the flow. Although post-bomb radiocarbon dating has been reportedly reliable in past flood studies (Baker and others, 1985), our results confirm the unreliability of some types of organic debris in post-bomb  $^{14}\text{C}$  analyses (Ely and others, 1992). Because  $^{14}\text{C}$  dates on recent debris flows are close to the known age of the deposit, we speculate that several debris flows may be required to flush most of the organic debris from the drainage. Moreover, in Prospect Canyon, the lag in association of the  $^{14}\text{C}$  age of organic material appear to be the same order of magnitude—500 to 1,000 yrs—as the uncertainty in  $^3\text{He}_c$  age owing to prior exposure history.

The  $^{137}\text{Cs}$ -dating technique did not perform well for the problem of distinguishing historical debris-flow deposits. Six of 17 samples that should have contained significant activities of  $^{137}\text{Cs}$  had no detectable activity; whereas two subsurface samples of pre-1952 deposits had detectable  $^{137}\text{Cs}$ . Despite previous success in Grand Canyon (Melis and others, 1994),  $^{137}\text{Cs}$  analyses yielded results that indicate the technique does not reliably differentiate the age of pre-1952 versus post-1952 deposition of debris-flow sediments in Prospect Canyon. We attribute the detectable  $^{137}\text{Cs}$  in pre-1952 deposits to atmospheric fallout and unexpectedly deep leaching of the isotope before sorption and (or) illuviation of clay particles with  $^{137}\text{Cs}$  ions already attached. Because  $^{137}\text{Cs}$  sorption is related to the amount of clay in the deposit (Ely and others, 1992), lack of  $^{137}\text{Cs}$  in post-bomb deposits may be explained by the coarse nature of Prospect Canyon debris flows.

The largest debris flow, which corresponds to surface tua, has an uncertain but very high recurrence interval (on the order of 10,000 yrs). The Toroweap Fault, reportedly the most active in Arizona, had a large earthquake about 3,000 yrs ago with a magnitude of 7.1 to 7.2 on the Richter scale (Jackson, 1990b). Such an earthquake would produce abundant talus in Prospect Canyon that could be mobilized into an unusually large debris flow, if sufficient runoff occurred. Other studies suggest possible unusually large winter storms in discrete periods of the late Holocene. In a study of ephemeral lakes in the Mojave Desert west of Prospect Canyon, Enzel (1992) and Enzel and others (1989) found deposits indicative of a persistent lake. One  $^{14}\text{C}$  date indicates the lake formed about 3,600 yrs ago under persistent atmospheric-circulation patterns that would spawn unusually large, winter floods. Given the lag between  $^{14}\text{C}$  age and the transporting event, the same storms causing persistent lakes in the Mojave Desert may possibly have initiated large debris flows in Prospect Canyon. Either the paleoearthquake or the unusually large winter floods, or both, could have indirectly produced surface tua.

Prospect Canyon has produced the highest frequency of debris flows of any tributary in Grand Canyon (Melis and others, 1994). Depending on the interval chosen, the frequency of debris flows ranges from one every 5 yrs to one every 20 yrs. Debris flows were not random in the historical period—from April 1872 to July 1939 there were no debris flows in Prospect Canyon, whereas five debris flows occurred in

a 27-year period between 1939 and 1966. Because most historical debris flows do not appear to be related to regional hydroclimatic patterns in the Grand Canyon region, we attribute the nonstationarity in debris-flow occurrence to local destabilization of colluvial wedges and channel deposits in Prospect Canyon. If the sediment sources diminish or stabilize, the frequency of debris flows would be expected to decline. Movement on the Toroweap Fault, which has been inactive for at least 3,000 yrs (Jackson, 1990a), may help supply colluvium for future debris flows.

Debris flows occur more frequently in Prospect Canyon owing to several significant differences from other debris-flow producing tributaries in Grand Canyon. Because of its large drainage area, the Prospect Valley drainage basin produces runoff in response to regional storms as well as summer thunderstorms, which have caused most of the historic debris flows in other Grand Canyon tributaries. Debris flows are produced in Prospect Canyon predominantly by the firehose effect from a channel draining a large area and falling onto colluvium below a precipice. Mass failure of bedrock units as well as colluvium initiated the largest debris flows from other Grand Canyon tributaries (Melis and others, 1994). The basalt plug that creates the 325-m waterfall at the head of Prospect Canyon is a lithologic control on the height and location of the firehose-effect process in Prospect Canyon.

Trends in the regional precipitation patterns strongly influence debris-flow initiation in Prospect Canyon. The results of Hereford and Webb (1992) and Hereford and others (1993) are verified in our analysis of precipitation anomalies in western Grand Canyon, which shows a general decline in summer precipitation, particularly after 1970 (fig. 30A). This is significant because August and September precipitation has produced more than 90 percent of debris flows since 1939 (Melis and others, 1994). Hereford and Webb (1992) showed that precipitation from dissipating tropical cyclones has declined on the Colorado Plateau except for the years 1972 and 1983, when precipitation from this source was well above normal. Although summer precipitation has declined, winter precipitation has increased (fig. 30B) and the last two debris flows from Prospect Canyon have occurred during regional winter storms.

## Conceptual Model of Debris-fan Reworking

The instability of Lava Falls Rapid is best illustrated by the historical alteration of primary hydraulic features and constrictions. Debris flows in 1939, 1954, 1955, 1963, and 1966 changed the pattern of flow through Lava Falls Rapid experienced by the first explorers, and created the hydraulic features that are well known to contemporary river runners (fig. 11A). Before 1939, the constriction at Lava Falls was only 5 percent (table 10). In 1939, the rapid was constricted by 80 percent, which is the largest historic constriction known in Grand Canyon. The interaction of Prospect Canyon debris flows and reworking by the Colorado River increased the average constriction from 5 percent in 1872 to 30 percent in 1994. A debris flow in March 1995 increased the constriction from 30 to 60 percent; however, half a day of Colorado River flow reduced the 1995 constriction to 50 percent. Sandstone and limestone particles, which generally are smaller and have a lower density, were preferentially removed, leaving a lag deposit dominated by basalt (fig. 39B).

Lava Falls Rapid illustrates the long-term interaction of frequent debris-flow deposition and mainstem reworking. Between 1872 and 1939, the configuration of Lava Falls Rapid did not change despite large Colorado River floods in 1884 and 1921. Smaller, unregulated river floods that occurred after the 1939, 1954, and 1955 debris flows reworked most of the deposits within 2 yrs. The 1963 and 1966 debris-fan deposits were removed in 3–7 yrs by even smaller releases from Glen Canyon Dam. Rapids may be stable for long periods between debris flows despite the occurrence of long recurrence-interval floods, particularly after debris-flow matrix has been winnowed from the deposits and when suturing of boulders has occurred on the bed of the rapid (Webb, 1996).

Two previous estimates of flood magnitude necessary to rework debris fans are considerably higher than the discharges that historically have reworked the Prospect Canyon debris fan. Kieffer (1985) concluded that a Colorado River flood of  $11,300 \text{ m}^3/\text{s}$  is necessary to widen a severely constricted rapid, such as Crystal Rapid, to the average constriction of 50 percent (fig. 35). At Warm Springs Rapid on the Yampa River in Utah, Hammack (1994) estimated that a discharge of  $2,750 \text{ m}^3/\text{s}$  (a 500 to 1,000-year flood) would be required to remove most of the debris fan aggraded in 1965. As the history of Lava Falls Rapid shows, historical floods of only  $3,400 \text{ m}^3/\text{s}$  were sufficient to

widen the more severely constricted channel at Lava Falls Rapid to a 30-percent constriction between 1939 and 1995. Kieffer's (1985) argument was based on the decrease in mean velocity through the rapid as the constriction is removed and the critical velocity required to initiate boulder transport. Our findings indicate that the initial mechanism that widens rapids is lateral channel erosion of the debris fan owing to bank collapse of unconsolidated, matrix-supported sediments, not entrainment of individual boulders from the top of the debris fan. Boulders enclosed in a poorly sorted matrix that are dislodged by lateral erosion have initial motion, which allows for transport by lower discharges than theoretically predicted.

During the 1996 controlled flood, we observed significant reworking as discharges increased from 1,000 to  $1,200 \text{ m}^3/\text{s}$ . We observed two types of reworking: (1) failure of unconsolidated debris-flow deposits by lateral erosion and (2) the entrainment of individual particles from the bed of the river. Most of the reworking of the 1995 debris fan, which had not been subjected to river discharges greater than  $670 \text{ m}^3/\text{s}$  before the 1996 controlled flood, resulted from slab failures of unconsolidated debris-flow deposits that were laterally eroded. These slab failures provided initial motion for large particles at discharges less than what would normally be required to entrain these particle sizes from a previously reworked debris fan. Other cobbles and boulders, particularly the ones embedded with radio transmitters, were entrained from the bed as individual particles. As demonstrated with the radio-tagged particles at Lava Falls Rapid, most of the particles were deposited in the pool downstream from the rapid and not on the alternating debris bars farther downstream (fig. 41). The average travel distance of 230 m demonstrates the effectiveness of discharges as small as  $1,300 \text{ m}^3/\text{s}$  in rearranging boulders on some debris fans in the Colorado River.

Reworking of the Prospect Canyon debris fan ended after approximately 4 hrs when large boulders armored the remaining unconsolidated bank, preventing further bank failures. In this case, duration of the flood appeared to be unimportant to reworking, contrary to the observations of Hammack and Wohl (1996) at Warm Springs Rapid. The two mechanisms of coarse-particle entrainment documented in this study have important implications for understanding the mobility and evolution of channel features, such as islands and channel bars downstream from large fans

and rapids, during both regulated and unregulated flows in the Colorado River.

The history of aggraded debris fans and reworking by the Colorado River at Lava Falls Rapid provides the basis for a general model of debris fan evolution in Grand Canyon (fig. 42). Kieffer's (1985, 1987) model does not completely apply to reworking of debris fans at Lava Falls Rapid because historical debris flows from Prospect Canyon and other tributaries in Grand Canyon (including Crystal Creek) have not crossed and dammed the Colorado River (Webb, 1996). Consequently, the "waterfall" that Kieffer hypothesized to occur on the downstream side of the newly aggraded debris fan is actually water flowing through the steepened, constricted rapid and around the distal margin of the debris fan. In our conceptual model of Lava Falls Rapid, the initial  $C_w$  of a recently aggraded debris fan ranges from 60–80 percent (fig. 42B). Relatively small river discharges (less than about 1,500 m<sup>3</sup>/s) cause minor reworking of the debris fan (figs. 21C, 42C), whereas large Colorado River floods (greater than about 2,000 m<sup>3</sup>/s) remove most of the debris-fan constriction and form secondary riffles downstream (fig. 42D). Because dam releases are typically much smaller than floods in the unregulated Colorado River (fig. 36), reworking of debris fans that formed in the last 30 yrs have mostly followed the model shown in figure 42C, which is similar to Kieffer's model.

## Rapids and Management of Glen Canyon Dam

The history of Lava Falls Rapid illustrates that most rapids in canyon rivers are not an equilibrium fluvial form unless viewed strictly in the short intervals between debris flows. We concur with Howard and Dolan (1981), who concluded that the position of rapids in Grand Canyon is not controlled by equilibrium river processes as previously reported (Leopold, 1969). The location of primary rapids in Grand Canyon is controlled by point sediment sources, typically tributaries, and regional structural control, such as active faults. Secondary riffles and rapids—such as Lower Lava Rapid—are indirectly controlled by tributaries. Reworking of aggraded debris fans at tributary junctures provides the boulders and cobbles that compose the controlling debris bars at secondary riffles or rapids downstream. Lava Falls Rapid also shows that rapids are not necessarily controlled by events that occurred in a different

climatic regime (Graf, 1979). Although the late Holocene debris flow that dammed the Colorado River about 1050 BC may have occurred during a period of unusually frequent winter storms, it did not occur in a climate that was significantly different from the 20th century (Webb, 1996). Rapids that appear stable and of great antiquity may be so only until the next debris flow triggers changes by constricting the river or adding boulders to the rapid.

Rapids in bedrock canyons controlled by tributary alluvium are aggradational features whose morphology and particle size reflect the net effect of tributary-mainstem interactions (Graf, 1979). The boulders that form the core of rapids in Grand Canyon are essentially immobile by both dam releases and by unregulated Colorado River floods, although recently deposited boulders with b-axis diameters as large as 4 m have been dislodged and moved short distances. The presence and changing configurations of rapids such as Lava Falls indicate that the river's erosional energy is presently expended in abrading and removing boulders to widen the channel, not in eroding bedrock on the bed of the channel.

Dam operations have decreased the frequency and magnitude of debris-fan reworking at the mouths of tributary canyons. Graf (1980), in an analysis of debris fans on the Green River in northern Utah, concluded that 62 percent of the rapids were stable before construction of Flaming Gorge Dam, but that 93 percent of the rapids were stable after the dam began operation. Kieffer's (1985) study of Crystal Rapid suggests the 1966 debris fan could only be removed by a flood larger than the largest historical discharge in the Colorado River (6,200 m<sup>3</sup>/s). At Lava Falls, two debris fans that formed after closure of Glen Canyon Dam were completely removed by flows that were less than the pre-dam 2-year flood. Although previous studies suggest otherwise, historical reworking of Lava Falls Rapid indicates that modest dam releases—in the case of Glen Canyon Dam, above the powerplant capacity of 890 m<sup>3</sup>/s—could significantly rework aggraded debris fans. Some aggraded debris fans, such as the one at Crystal Rapid, would be unaffected, but others may be totally removed depending upon the size of particles and local channel conditions.

A comparison of the response of Crystal and Lava Falls rapids illustrates why it is difficult to make generalizations about the stability of rapids. Debris flows constricted both rapids after closure of Glen Canyon Dam, but the interaction of the river with the



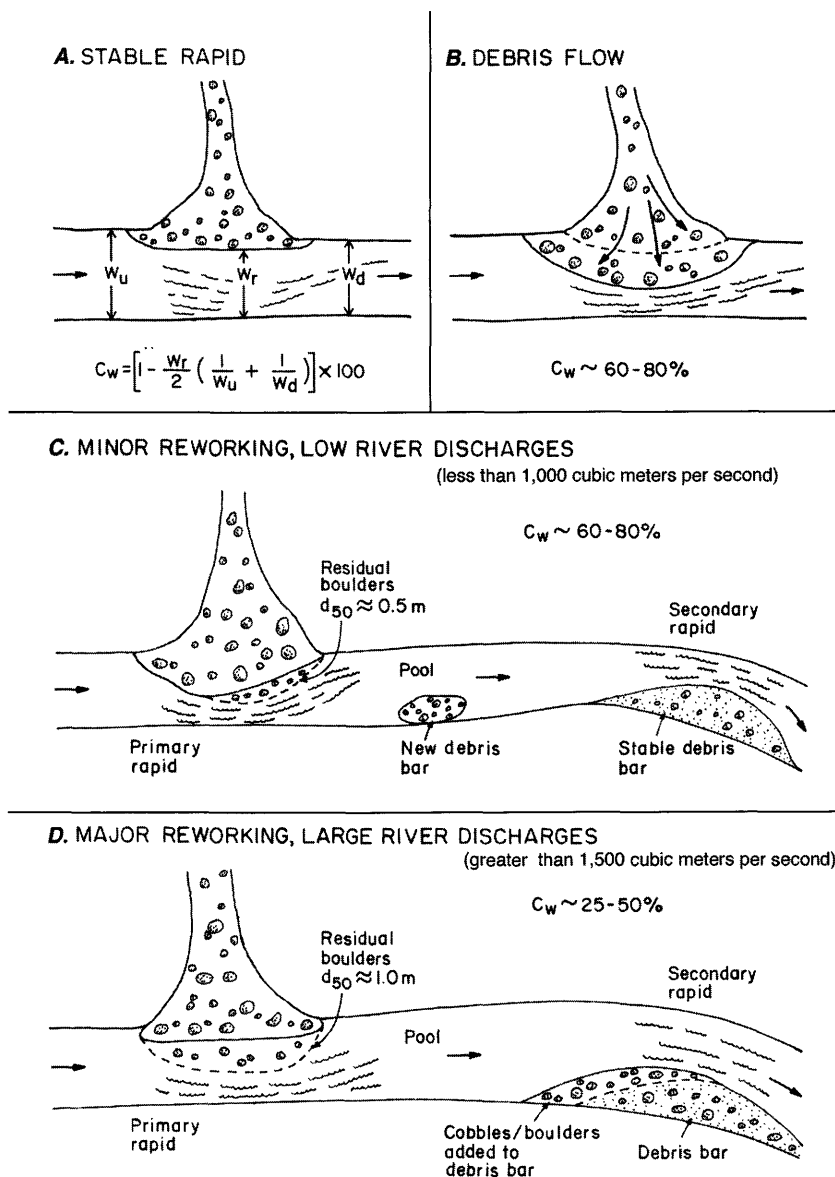


**Figure 42.** Schematic diagram showing a conceptual model of aggradation and reworking of a typical debris fan by the Colorado River in Grand Canyon. A typical fan-rapid system consists of a debris fan, a reach of whitewater, a downstream pool, and alternating bars farther downstream. This model is modified from Kieffer (1990). *A*, At stable, previously reworked rapids, the channel usually is constricted by 50 percent (Kieffer, 1985). In the case of Lava Falls Rapid, the constriction from 1872–1939 was about 3 percent. *B*, Debris flows seldom dam the Colorado River. Instead, deposition generally constricts the river by 60–80 percent. The elevation of the bed rises, partly because boulders reworked from the debris fan are deposited in the main channel or near the opposite bank. *C*, Low discharges (less than 1,500 m<sup>3</sup>/s)—whether small pre-dam floods, typical dam releases, or the 1996 controlled flood—may erode the distal margins of newly aggraded debris fans and widen the constriction. The degree of widening is dependent on local topographic conditions of the fan and mainstem channel, particularly the stage-discharge relation and water-surface fall, as well as the particle-size distribution of the debris-flow deposit. Debris eroded from the debris fan is deposited in the downstream pool. *D*, High discharges (greater than 2,000 m<sup>3</sup>/s)—large pre-dam floods or unusual dam releases such as in June 1983—typically remove most of the new deposit, leaving a residual lag of boulders on the debris fan and in the widened rapid. At low discharges, the widened rapid may be more constricted than before the debris flow owing to the arrangement of immobile boulders and deposition on the downstream edge of the debris fan. Smaller boulders and cobbles are transported through the pool to the secondary rapid and deposited on the downstream debris bar.

aggraded debris fans is different at each rapid. The difference is explained largely by the size of boulders that composed the aggraded debris fans; whereas the 1963 Prospect Canyon debris flow was relatively fine-grained ( $D_{50} = 64$  mm) and contained relatively small boulders, the 1966 debris flow at Crystal Rapid had larger particles ( $D_{50} = 256$  mm; Kieffer, 1987) and very large boulders. If a debris flow similar to that of 1939 event had occurred at Lava Falls in 1963, the debris fan might have had a history similar to that of the Crystal Rapid debris fan because dam release floods after 1963 would not have been large enough to remove the volume and size of sediment deposited by the 1939 Prospect Canyon debris flow.

The 1963 debris flow at Lava Falls Rapid was largely removed by dam releases of  $1,640 \text{ m}^3/\text{s}$  in 1965 because only small releases had occurred in the intervening 2 yrs (figs. 23B, 24). Partial reworking by typical powerplant releases tends to armor the distal fan margin with boulders and cobbles that may become interlocked or sutured. This armoring and suturing greatly increases the tractive stress necessary for subsequent entrainment. The 1965 releases cut laterally into the 1963 deposit and entrained unconsolidated boulders up to 1 m in diameter. The debris fan at Crystal Rapid, enlarged by a 1966 debris flow, was partially reworked by about  $1,080 \text{ m}^3/\text{s}$  in 1973. Consequently, major changes occurred only when dam releases exceeded  $1,410 \text{ m}^3/\text{s}$  and peaked at  $2,720 \text{ m}^3/\text{s}$  in 1983. Although much of the Crystal Creek debris fan was removed in 1983, its distal edge is armored and should withstand most future dam releases. As shown in figure 28C, the distal margin of the 1995 Prospect Canyon debris-flow deposit, reworked by powerplant releases less than  $560 \text{ m}^3/\text{s}$  between March 1995 and March 1996, is also armored.

Historical reworking of debris fans at Lava Falls Rapid has implications for dam operations, if periodic aggradation of debris fans is a consideration in the management of release schedules from Glen Canyon Dam. Because releases from the dam are limited by the size of its powerplant, spillways, and jet tubes, the frequency of large releases that could significantly rework debris fans is low. Discharges sufficient to rework debris fans could be created by a combination of powerplant releases and unregulated floods on the Paria and Little Colorado Rivers. Because the Little Colorado River has a flood of record of  $3,390 \text{ m}^3/\text{s}$  and has a larger drainage area, the Little Colorado River is more likely to generate a debris-fan reworking flood

than the Paria River, which has a flood of record of  $455 \text{ m}^3/\text{s}$  (Garrett and Gellenbeck, 1991). The magnitude of regulated flows designed to alter the river corridor, whether they are timed to augment natural floods from the tributaries or created entirely from reservoir releases, need to be large enough to remove most recently aggraded debris fans without significantly armoring their distal margins. If significant armoring develops, or boulders become sutured together, future dam releases will be ineffective in removing aggraded debris fans.

## REFERENCES CITED

- Aldridge, B.N., and Eychaner, J.H., 1984, Floods of October 1977 in southern Arizona and March 1978 in central Arizona: U.S. Geological Survey Water-Supply Paper 2223, 143 p.
- Apmann, R.P., 1973, Estimating discharge from superelevation in bends: Journal of the Hydraulics Division, Proceedings of the American Society of Civil Engineers, HY1, p. 65–79.
- Baker, V.R., Pickup, G., and Polach, H.A., 1985, Radio-carbon dating of flood events, Katherine Gorge, Northern Territory, Australia: Geology, v. 13, p. 344–347.
- Beatty, C.B., 1989, Great boulders I have known: Geology, v. 17, p. 349–352.
- Benda, L., 1990, The influence of debris flows on channels and valley floors in the Oregon Coast Range, USA: Earth Surface Processes and Landforms, v. 15, p. 457–466.
- Benda, L., and Dunne, T., 1987, Sediment routing by debris flow, in Erosion and Sedimentation in the Pacific Rim: Proceedings of the Corvallis Symposium, International Association of Hydrologic Sciences Publication No.165, p. 213–223.
- Benda, L.E., and Cundy, T.W., 1990, Predicting deposition of debris flows in mountain channels: Canadian Geotechnical Journal, v. 27, p. 409–417.
- Beverage, J.P., and Culbertson, J.K., 1964, Hyperconcentrations of suspended sediment: American Society of Civil Engineers, Journal of the Hydraulics Division, v. 90, p. 117–126.
- Bierman, P.R., 1994, Using *in-situ* produced cosmogenic nuclides to estimate rates of landscape evolution—a review from the geomorphic perspective: Journal of Geophysical Research, v. 99, p. 13,885–13,896.
- Bierman, P.R., Gillespie, A.R., and Caffee, M.W., 1995, Cosmogenic ages for earthquake recurrence intervals

- and debris flow fan deposition, Owens Valley, California: Science, v. 270, p. 447–450.
- Billingsley, G.H., Jr., and Huntoon, P.W., 1983, Geologic map of Vulcans Throne and vicinity, western Grand Canyon, Arizona: Grand Canyon, Arizona, Grand Canyon Natural History Association Map, scale 1:62,500, 1 sheet.
- Birdseye, C.H., 1924, Plan and profile of the Colorado River from Lees Ferry, Arizona, to Black Canyon, Arizona-Nevada, and the Virgin River, Nevada: U.S. Geological Survey map publication, 21 sheets (A–U) scale 1:36,680.
- Birkeland, P.W., 1984, Soils and geomorphology: New York, Oxford University Press, 372 p.
- Blackwelder, E., 1928, Mudflow as a geologic agent in semiarid mountains: Geological Society of America Bulletin, v. 39, p. 465–494.
- Bowers, J.E., Webb, R.H., and Pierson, E.A., 1997, Primary succession of desert plants on debris-flow terraces, Grand Canyon, Arizona, U.S.A.: Journal of Arid Environments, v. 36, p. 67–86.
- Brian, N., 1992, River to rim: Flagstaff, Earthquest Press, 176 p.
- Brook, E.J., and Kurz, M.D., 1993, Surface exposure chronology using *in situ* cosmogenic  $^3\text{He}$  in Antarctic quartz sandstone boulders: Quaternary Research, v. 39, p. 1–10.
- Brown, E.T., Edmond, J.M., Raisbeck, G.M., Yiou, F., Kurz, M.D., and Brook, E.J., 1991, Examination of surface exposure ages of Antarctic moraines using *in situ*  $^{10}\text{Be}$  and  $^{26}\text{Al}$ : Geochimica et Cosmochimica Acta, v. 55, p. 2269–2283.
- Brown, E.T., Brook, E.J., Raisbeck, G.M., Yiou, F., and Kurz, M.D., 1992, Effective attenuation lengths of cosmic rays producing  $^{10}\text{Be}$  and  $^{26}\text{Al}$  in quartz: Implications for exposure age dating: Geophysical Research Letters, v. 19, p. 369–372.
- Burbank, D.W., Leland, J., Fielding, E., Anderson, R.S., Brozovic, N., Reid, M.R., and Duncan, C., 1996, Bedrock incision, rock uplift and threshold hillslopes in the northwestern Himalayas: Nature, v. 379, p. 505–510.
- Butler, E., and Mundorff, J.C., 1970, Floods of December 1966 in southwestern Utah: U.S. Geological Survey Water-Supply Paper 1870–A, 40 p.
- Cannon, S.H., 1989, An evaluation of the travel-distance potential of debris flows: Utah Geological and Mineral Survey, Miscellaneous Publication 89–2, 35 p.
- Carmony, N.B., and Brown, D.E., 1987, The log of the Pantho: Boulder, Colorado, Pruett Publishing, 109 p.
- Cenderelli, D.A., and Kite, J.S., 1994, Erosion and deposition by debris flows in mountainous channels on North Fork Mountain, eastern West Virginia, in Cotroneo, G.V., and Rumer, R.R. (eds.), Hydraulic Engineering '94, v. 2: New York, American Society of Civil Engineers, p. 772–776.
- Cerling, T.E., 1990, Dating geomorphic surfaces using cosmogenic  $^3\text{He}$ : Quaternary Research, v. 33, p. 148–153.
- Cerling, T.E., and Craig, H., 1994a, Geomorphology and *in-situ* cosmogenic isotopes: Annual Reviews in Earth and Planetary Sciences, v. 22, p. 273–317.
- 1994b, Cosmogenic  $^3\text{He}$  production rates from  $39^\circ\text{N}$  to  $46^\circ\text{N}$  latitude, western USA and France: Geochimica et Cosmochimica Acta, v. 58, p. 249–255.
- Cerling, T.E., Poreda, R.J., and Rathburn, S.L., 1994c, Cosmogenic  $^3\text{He}$  and  $^{21}\text{Ne}$  age of the Big Lost River flood, Snake River Plain, Idaho: Geology, v. 22, p. 227–230.
- Cerling, T.E., Webb, R.H., Poreda, R.J., Rigby, A.D., and Melis, T.S., In press, Cosmogenic  $^3\text{He}$  ages and frequency of late Holocene debris flows from Prospect Canyon, Grand Canyon, Arizona: Geomorphology.
- Clark, G.W., and Newcomb, Duane, 1977, Georgie Clark, Thirty years of river running: San Francisco, Chronicle Books, 165 p.
- Collier, M.P., Webb, R.H., and Andrews, E.D., 1997, Experimental flooding in Grand Canyon: Scientific American, v. 276, p. 82–89.
- Cook, W., 1987, The Wen, the Botany, and the Mexican Hat: Orangevale, California, Callisto Books, 151 p.
- Cooke, R., Warren, A., and Goudie, A., 1993, Desert geomorphology: London, University College London Press, 526 p.
- Cooley, J., 1988, The great unknown: Flagstaff, Arizona, Northland Publishing, 207 p.
- Cooley, M.E., Aldridge, B.N., and Euler, R.C., 1977, Effects of the catastrophic flood of December, 1966, North Rim area, eastern Grand Canyon, Arizona: U.S. Geological Survey Professional Paper 980, 43 p.
- Costa, J.E., 1984, Physical geomorphology of debris flows, in Costa, J.E., and Fleisher, P.J., (eds.), Developments and applications of geomorphology: Berlin, Springer-Verlag Publishing, p. 268–317.
- Costa, J.E., and O'Connor, J.E., 1995, Geomorphically effective floods, in Natural and anthropogenic influences in fluvial geomorphology: American Geophysical Union, Geophysical Monograph 89, p. 45–56.
- Craig, H., and Poreda, R.J., 1986, Cosmogenic  $^3\text{He}$  in terrestrial rocks: The summit lavas of Maui: Proceedings of the National Academy of Science, v. 83, p. 1970–1974.
- Damon, P.E., Laughlin, A.W., and Percious, J.K., 1967, The problem of excess argon-40 in volcanic rocks, in

- Proceedings of the Symposium on Radioactive Dating and Methods of Low-Level Counting, Monaco, 2–10 March, 1967: International Atomic Energy Agency, 24 p.
- Dolan, R., Howard, A., and Trimble, D., 1978, Structural control of the rapids and pools of the Colorado River in the Grand Canyon: *Science*, v. 202, p. 629–631.
- Eddy, C., 1929, *Down the world's most dangerous river*: New York, Frederick A. Stokes Company, 293 p.
- Ely, L.L., Webb, R.H., and Enzel, Yehouda, 1992, Accuracy of post-bomb  $^{137}\text{Cs}$  and  $^{14}\text{C}$  in dating fluvial deposits: *Quaternary Research*, v. 38, p. 196–204.
- Enzel, Y., 1992, Flood frequency of the Mojave River and the formation of late Holocene playa lakes, southern California, USA: *The Holocene*, v. 2, p. 11–18.
- Enzel, Y., Cayan, D.R., Anderson, R.Y., and Wells, S.G., 1989, Atmospheric circulation during Holocene lake stands in the Mojave Desert—evidence of regional climate change: *Nature*, v. 341, p. 44–47.
- Ferguson, C.W., 1971, Tree-ring dating of Colorado River driftwood in the Grand Canyon: Proceedings of the 1971 meetings of the Arizona Section, American Water Resources Association, and the Hydrology Section, Arizona Academy of Science, v. 1, p. 351–366.
- Folk, R.L., 1974, *Petrology of sedimentary rocks*: Austin, Texas, Hemphill Publishing, 182 p.
- Fowler, D.D. (ed.), 1972, “Photographed all the best scenery,” Jack Hillers's diary of the Powell Expeditions, 1871–1875: Salt Lake City, University of Utah Press, 225 p.
- Fradkin, P.L., 1984, *A river no more*: Tucson, University of Arizona Press, 360 p.
- Freeman, L.R., 1924, Surveying the Grand Canyon of the Colorado: *National Geographic Magazine*, v. 45, p. 471–531, 547–548.
- Friedman, G.M., and Sanders, J.E., 1978, *Principles of sedimentology*: New York, John Wiley and Sons, 792 p.
- Gallino, G.L., and Pierson, T.C., 1985, Polallie Creek debris flow and subsequent dam-break flood of 1980, East Fork Hood River basin, Oregon: U.S. Geological Survey Water-Supply Paper 2273, 22 p.
- Garrett, J.M., and Gellenbeck, D.J., 1991, Basin characteristics and streamflow statistics in Arizona as of 1989: U.S. Geological Survey Water-Resources Investigations Report 91–4041, 612 p.
- Ghiglieri, M.P., 1992, *Canyon*: Tucson, Arizona, University of Arizona Press, 311 p.
- Gibbons, A.B., Megeath, J.E., and Pierce, K.L., 1984, Probability of moraine survival in a succession of glacial advances: *Geology*, v. 12, p. 327–330.
- Glancy, P.A., 1969, A mudflow in the Second Creek drainage, Lake Tahoe Basin, Nevada, and its relation to sedimentation and urbanization: U.S. Geological Survey Professional Paper 650C, p. C195–C200.
- Goldwater, B.M., 1940, *A journey down the Green and Colorado Rivers*: Phoenix, Arizona, privately published by H. Walker Publishing, 106 p.
- Gosse, J.C., Evenson, E.B., Klein, J., Lawn, B., and Middleton, R., 1995a, Precise cosmogenic  $^{10}\text{Be}$  measurements in Western North America—support for a global younger Dryas cooling event: *Geology*, v. 23, p. 877–880.
- Gosse, J.C., Klein, J., Evenson, E.B., Lawn, B., and Middleton, R., 1995b,  $^{10}\text{Be}$  dating of the duration and retreat of the last Pinedale glacial sequence: *Science*, v. 268, p. 1329–1333.
- Graf, W.L., 1979, Rapids in canyon rivers: *Journal of Geology*, v. 87, p. 533–551.
- 1980, The effect of dam closure on downstream rapids: *Water Resources Research*, v. 16, p. 129–136.
- Granger, B.H., 1960, *Grand Canyon place names*: Tucson, University of Arizona Press, 26 p.
- Griffiths, P.G., 1995, *Initiation and frequency of debris flows in Grand Canyon, Arizona*: Tucson, University of Arizona, M.S. thesis, 52 p.
- Griffiths, P.G., Webb, R.H., and Melis, T.S., 1996, *Initiation and frequency of debris flows in Grand Canyon, Arizona*: U.S. Geological Survey Open-File Report 96–491, 35 p.
- 1997, Initiation of debris flows in bedrock canyons of the Colorado River, USA, in Chen, Cheng-lung (ed.), *Debris-flow hazards mitigation: Mechanics, prediction, and assessment*: New York, American Society of Civil Engineers, p. 12–20.
- Hamblin, W.K., 1990, Late Cenozoic lava dams in the western Grand Canyon, in Beus, S.S., and Morales, M. (eds.), *Grand Canyon geology*: New York, Oxford University Press, p. 385–433.
- 1994a, Rates of erosion by the Colorado River in the Grand Canyon, Arizona: Proceedings of the 29th International Geology Congress, Part B, p. 211–218.
- 1994b, Late Cenozoic lava dams in the western Grand Canyon: *Geological Society of America Memoir* 183, 139 p.
- Hamblin, W.K., and Rigby, J.K., 1968, *Guidebook to the Colorado River, Part 1, Lee's Ferry to Phantom Ranch in Grand Canyon National Park*: Provo, Utah, Brigham Young University, Geology Studies, v. 15, part 5, 84 p.
- Hammack, L.A., 1994, *Debris-fan formation and rapid modification at Warm Springs Rapid, Yampa River, Colorado*: Fort Collins, Colorado State University, M.S. thesis, 125 p.
- Hammack, L., and Wohl, E., 1996, *Debris-fan formation and rapid modification at Warm Springs Rapid, Yampa*



- River, Colorado: *Journal of Geology*, v. 104, p. 729–740.
- Hampton, M.A., 1975, Competence of fine-grained debris flows: *Journal of Sedimentary Petrology*, v. 45, p. 834–844.
- Hansen, E.M., and Shwarz, F.K., 1981, Meteorology of important rainstorms in the Colorado River and Great Basin drainages: National Oceanic and Atmospheric Administration, Hydrometeorological Report 50, 167 p.
- Heald, W., 1948, The eighteenth expedition, in Peattie, R. (ed.), *The inverted mountains*: New York, Vanguard Press, p. 195.
- Hereford, R., 1996, Map showing surficial geology and geomorphology of the Palisades Creek area, Grand Canyon National Park, Arizona: U.S. Geological Survey Miscellaneous Investigations Series Map I-2449, scale 1:2,000.
- Hereford, R., and Webb, R.H., 1992, Historic variation in warm-season rainfall on the Colorado Plateau, U.S.A.: *Climatic Change*, v. 22, p. 239–256.
- Hereford, R., Fairley, H.C., Thompson, K.S., and Balsom, J.R., 1993, Surficial geology, geomorphology, and erosion of archaeologic sites along the Colorado River, eastern Grand Canyon, Grand Canyon National Park, Arizona: U.S. Geological Survey Open-File Report 93–517, 46 p.
- Hereford, R., Thompson, K.S., Burke, K.J., and Fairley, H.C., 1996, Tributary debris fans and the late Holocene alluvial chronology of the Colorado River, eastern Grand Canyon, Arizona: *Geological Society of America Bulletin*, v. 108, p. 3–19.
- Hereford, R., Thompson, K.S., and Burke, K.J., 1997, Dating prehistoric tributary debris fans, Colorado River, Grand Canyon National Park, Arizona, with implications for channel evolution and river navigability: U.S. Geological Survey Open-File Report 97–167, 17 p.
- Hereford, R., Burke, K.J., and Thompson, K.S., 1997, Map showing Quaternary geology and geomorphology of the Nankoweap Rapids area, Marble Canyon, Arizona: U.S. Geological Survey Miscellaneous Investigations Map I-2608, 1 sheet, scale 1:2,000 (with discussion).
- Hirschboeck, K.K., 1985, Hydroclimatology of flow events in the Gila River Basin, central and southern Arizona [Ph.D dissertation]: Tucson, University of Arizona, 335 p.
- Howard, A.D., and Dolan, R., 1979, Changes in the fluvial deposits of the Colorado River in the Grand Canyon caused by Glen Canyon Dam, in Linn, R.M. (ed.), *Proceedings of the First Conference on Scientific Research in the National Parks*, Volume II, p. 845–851.
- 1981, Geomorphology of the Colorado River in Grand Canyon: *Journal of Geology*, v. 89, p. 269–297.
- Iverson, R.M., 1997, The physics of debris flows: *Reviews of Geophysics*, v. 35, p. 245–296.
- Iverson, R.M., Reid, M.E., and LaHusen, R.G., 1997, Debris-flow mobilization from landslides: *Annual Review of Earth and Planetary Sciences*, v. 25, p. 85–138.
- Jackson, G.W., 1990a, The Toroweap Fault—One of the most active faults in Arizona: *Arizona Geology*, v. 20, p. 7–10.
- 1990b, Tectonic geomorphology of the Toroweap Fault, western Grand Canyon, Arizona: Implications for transgression of faulting on the Colorado Plateau: Tucson, Arizona Geological Survey Open-File Report 90–4, 67 p.
- Jackson, L.E., Jr., 1977, Dating and recurrence frequency of prehistoric mudflows near Big Sur, Monterey County, California: *Journal of Research of the U.S. Geological Survey*, v. 5, p. 17–32.
- Johnson, A.M., and Rodine, J.R., 1984, Debris flow, in Brunsden, D., and Prior, D.B. (eds.), *Slope instability*: New York, John Wiley and Sons, p. 257–361.
- Kaliser, B.N., and Slosson, J.E., 1988, Geologic consequences of the 1983 wet year in Utah: Utah Geological and Mineral Survey, Miscellaneous Publication 88–3, 109 p.
- Kieffer, S.W., 1985, The 1983 hydraulic jump in Crystal Rapid: Implications for river-running and geomorphic evolution in the Grand Canyon: *Journal of Geology*, v. 93, p. 385–406.
- 1987, The rapids and waves of the Colorado River, Grand Canyon, Arizona: U.S. Geological Survey Open-File Report 87–096, 69 p.
- 1988, Hydraulic map of Lava Falls Rapid, Grand Canyon, Arizona: U.S. Geological Survey Miscellaneous Investigations Series, Map I-1897-J, scale 1:1,000, 1 sheet.
- 1990, Hydraulics and geomorphology of the Colorado River in the Grand Canyon, in Beus, S.S., and Morales, M. (eds.), *Grand Canyon geology*: New York, Oxford University Press, p. 333–383.
- Kite, G.W., 1988, Frequency and risk analyses in hydrology: Littleton, Colorado, Water Resources Publications, 257 p.
- Klein, J., Giegengack, R., Middleton, R., Sharma, P., Underwood, J.R., and Weeks, R.A., 1986, Revealing histories of exposure using *in situ* produced  $^{26}\text{Al}$  and  $^{10}\text{Be}$  in Libyan desert glass: *Radiocarbon* v. 28, p. 547–555.

- Kochel, R.C., 1987, Holocene debris flows in central Virginia: Reviews in Engineering Geology, v. 7, p. 139–155.
- Kolb, E.L., 1914, Through the Grand Canyon from Wyoming to Mexico: New York, MacMillan Company, 344 p.
- Kurz, M.D., 1986, Cosmogenic helium in a terrestrial igneous rock: Nature, v. 320, p. 435–439.
- Lal, D., 1987, Cosmogenic nuclides produced *in situ* in terrestrial solids: Nuclear Instruments Methods and Physics Research, v. B29, p. 238–245.
- 1988, *In situ* produced cosmogenic isotopes in terrestrial rocks: Annual Review of Earth and Planetary Sciences, v. 16, p. 355–388.
- 1991, Cosmic ray labeling of erosion surfaces—*in situ* nuclide production rates and erosion models: Earth and Planetary Sciences Letters, v. 104, p. 424–439.
- Lal, D., Nishiizumi, K., and Arnold, J.R., 1987, *In situ* cosmogenic  $^3\text{H}$ ,  $^{14}\text{C}$ , and  $^{10}\text{Be}$  for determining the net accumulation and ablation rates of ice sheets: Journal of Geophysical Research, v. 92, p. 4947–4952.
- Laughlin, A.W., Poths, J., Healey, H.A., Reneau, S., and WoldeGabriel, Giday, 1994, Dating of Quaternary basalts using the cosmogenic  $^3\text{He}$  and  $^{14}\text{C}$  methods with implications for excess  $^{40}\text{Ar}$ : Geology, v. 22, p. 135–138.
- Lavender, D., 1985, River runners of the Grand Canyon: Grand Canyon, Arizona, Grand Canyon Natural History Association, 147 p.
- Leopold, L.B., 1969, The rapids and the pools—Grand Canyon, *in* The Colorado River region and John Wesley Powell: U.S. Geological Survey Professional Paper 669, p. 131–145.
- Lindemann, L.L., and Lindemann, D.K., 1995, Colorado River briefs for a trip through the Grand Canyon: Tucson, Arizona, Lundquist Press, 152 p.
- Lips, E.W., and Wiczorek, G.F., 1990, Recurrence of debris flows on an alluvial fan in central Utah, *in* Hydraulics/Hydrology of Arid lands: Proceedings of the International Symposium, Hydraulics and Irrigation Divisions, American Society of Civil Engineers, p. 555–560.
- Machette, M.N., 1985, Calcic soils of the southwestern United States: Geological Society of America Special Paper 203, p. 1–21.
- Major, J.J., 1993, Rheometry of natural sediment slurries, *in* Shen, H.W., Su, S.T., and Wen, F., (eds.), Hydraulic Engineering '93: New York, American Society of Civil Engineers, Proceedings of the ASCE Conference, San Francisco, California, p. 1415–1421.
- 1997, Depositional processes in large-scale debris-flow experiments: Journal of Geology, v. 105, p. 345–366.
- Major, J.J., and Pierson, T.C., 1990, Rheological analysis of fine-grained natural debris-flow material, *in* Hydraulics/Hydrology of Arid lands: Proceedings of the International Symposium, Hydraulics and Irrigation Divisions, American Society of Civil Engineers, p. 225–231.
- 1992, Debris flow rheology: Experimental analysis of fine-grained slurries: Water Resources Research, v. 28, p. 841–857.
- Marron, D.C., and Laudon, J.A., 1986, Susceptibility to mudflows in the vicinity of Lassen Peak, California, *in* Subitzky, S. (ed.), Selected papers in the hydrologic sciences, 1986: U.S. Geological Survey Water-Supply Paper 2310, p. 97–106.
- Marston, O.D., 1976, Separation marks, notes on “the Worst Rapid” in the Grand Canyon: Journal of Arizona History, v. 17, p. 1–20.
- Masarik, J., and Reedy, R.C., 1995, Terrestrial cosmogenic nuclide production systematics calculated from numerical simulations: Earth and Planetary Sciences Letters, v. 136, p. 381–395.
- McFadden, L.D., and Tinsley, J.C., 1985, Rate and depth of pedogenic-carbonate accumulation in soils—Formulation and testing of a compartment model: Geological Society of America Special Paper 203, p. 23–41.
- Melis, T.S., 1997, Geomorphology of debris flows and alluvial fans in Grand Canyon National Park and their influences on the Colorado River below Glen Canyon Dam, Arizona, Ph.D Dissertation, Tucson, University of Arizona, 495 p.
- Melis, T.S., and Webb, R.H., 1993, Debris flows in Grand Canyon National Park, Arizona: Magnitude, frequency and effects on the Colorado River, *in* Shen, H.W., Su, S.T., and Wen, F., (eds.), Hydraulic Engineering '93: New York, American Society of Civil Engineers, Proceedings of the ASCE Conference, San Francisco, California, p. 1290–1295.
- Melis, T.S., Webb, R.H., Griffiths, P.G., and Wise, T.J., 1994, Magnitude and frequency data for historic debris flows in Grand Canyon National Park and vicinity, Arizona: U.S. Geological Survey Water Resources Investigations Report 94–4214, 285 p.
- Melis, T.S., Webb, R.H., and Griffiths, P.G., 1997, Debris flows in Grand Canyon National Park: Peak discharges, flow transformations, and hydrographs, *in* Chen, Cheng-lung (ed.), Debris-flow hazards mitigation: Mechanics, prediction, and assessment: New York, American Society of Civil Engineers, p. 727–736.
- Meyer, G.A., Wells, S.G., and Jull, A.J.T., 1995, Fire and alluvial chronology in Yellowstone National Park—Climatic and intrinsic controls on Holocene geomorphic processes: Geological Society of America Bulletin, v. 107, p. 1211–1230.
- Miller, A.J., 1994, Debris-fan constrictions and flood hydraulics in river canyons—Some implications from

- two-dimensional flow modelling: *Earth Surface Processes and Landforms*, v. 19, p. 681–697.
- Nash, R.F., 1989, The big drops, ten legendary rapids of the American west: Boulder, Colorado, Johnson Books, 216 p.
- Nishiizumi, K., Lal, D., Klein, J., Middleton, R., Arnold, J.R., 1989, Cosmic ray production rates of  $^{10}\text{Be}$  and  $^{26}\text{Al}$  in quartz from glacially polished rocks: *Journal of Geophysical Research*, v. 94, p. 17907–17915.
- Nishiizumi, K., Kohl, C. P., Arnold, J. R., Klein, J., Fink, D., and Middleton, R., 1991, Cosmic ray produced  $^{10}\text{Be}$  and  $^{26}\text{Al}$  in Antarctic rocks—exposure and erosion history: *Earth and Planetary Sciences Letters*, v. 104, p. 440–454.
- O'Connor, J.E., Ely, L.L., Wohl, E.E., Stevens, L.E., Melis, T.S., Kale, V.S., and Baker, V.R., 1994, A 4500-year record of large floods on the Colorado River in the Grand Canyon, Arizona: *Journal of Geology*, v. 102, p. 1–9.
- Osterkamp, W.R., Hupp, C.R., and Blodgett, J.C., 1986, Magnitude and frequency of debris flows, and areas of hazard on Mount Shasta, Northern California: U.S. Geological Survey Professional Paper 1396–C, 21 p.
- Osterkamp, W.R., and Hupp, C.R., 1987, Dating and interpretation of debris flows by geologic and botanical methods at Whitney Creek gorge, Mount Shasta, California: *Reviews in Engineering Geology*, v. 7, p. 157–163.
- Péwé, T.L., 1968, Colorado River guidebook, Lees Ferry to Phantom Ranch: Tempe, Arizona, privately published, 78 p.
- Phillips, B.G., Phillips, A.M., III, and Bernzott, M.A.S., 1987, Annotated checklist of vascular plants of Grand Canyon National Park: Grand Canyon Natural History Association Monograph Number 7, 79 p.
- Phillips, F.M., Leavy, B.D., Jannik, N.O., Elmore, D., and Kubik, P.W., 1986, The accumulation of cosmogenic chlorine-36 in rock—a method for surface exposure dating: *Science*, v. 231, p. 41–43.
- Phillips, F.M., Zreda, M.G., Smith, S.M., Elmore, D., Kubik, P.W., Dorn, R.I., and Roddy, D.J., 1991, Age and geomorphic history of Meteor Crater, Arizona, from cosmogenic  $^{16}\text{Cl}$  and  $^{14}\text{Cl}$  in rock varnish: *Geochimica et Cosmochimica Acta*, v. 55, p. 2695–2698.
- Phillips, W.M., 1997, Applications of noble gas cosmogenic nuclides to geomorphology: Tucson, University of Arizona, unpublished Ph.D dissertation, 256 p.
- Pierson, T.C., 1985, Initiation and flow behavior of the 1980 Pine Creek and Muddy River lahars, Mount St. Helens, Washington: *Geological Society of America Bulletin*, v. 96, p. 1056–1069.
- Pierson, T.C., and Scott, K.M., 1985, Downstream dilution of a lahar: Transition from debris flow to hyperconcentrated streamflow: *Water Resources Research*, v. 21, p. 1511–1524.
- Pierson, T.C., and Costa, J.E., 1987, A rheologic classification of subaerial sediment-water flows: *Reviews in Engineering Geology*, v. 7, p. 1–12.
- Poreda, R.J., and Cerling, T.E., 1992, Cosmogenic neon in recent lavas from the western United States: *Geophysical Research Letters*, v. 19, p. 1863–1866.
- Poreda, R.J., and Farley, K. A., 1992, Rare gases in Samoan xenoliths: *Earth and Planetary Science Letters*, v. 113, p. 129–144.
- Postma, G., 1986, Classification for sediment gravity-flow deposits based on flow conditions during sedimentation: *Geology*, v. 14, p. 291–294.
- Powell, J.W., 1875, Exploration of the Colorado River of the West and its tributaries: Washington, D.C., 43rd U.S. Congress, 1st Session, House Miscellaneous Document 300, 291 p.
- Rice, S., and Church, M., 1996, Sampling surficial fluvial gravels: The precision of size distribution percentile estimates: *Journal of Sedimentary Research*, v. 66, p. 654–665.
- Rihs, J., 1995, Analysis of the March 1995 Bright Angel Creek flood event, Grand Canyon National Park: Grand Canyon, Arizona, Division of Resource Management Report, 11 p.
- Rodine, J.D., and Johnson, A.R., 1976, The ability of debris, heavily freighted with coarse clastic materials, to flow on gentle slopes: *Sedimentology*, v. 23, p. 213–234.
- Roeske, R.H., Cooley, M.E., and Aldridge, B.N., 1978, Floods of September 1970 in Arizona, Utah, Colorado, and New Mexico: U.S. Geological Survey Water-Supply Paper 2052, 135 p.
- Roeske, R.H., Garrett, J.M., and Eychaner, J.H., 1989, Floods of October 1983 in southeastern Arizona: U.S. Geological Survey Water-Resources Investigations Report 85–4225–C, 77 p.
- Savage, S.B., and Hutter, K., 1989, The motion of a finite mass of granular material down a rough incline: *Journal of Fluid Mechanics*, v. 199, p. 177–215.
- Schmidt, J.C., 1990, Recirculating flow and sedimentation in the Colorado River in Grand Canyon, Arizona: *Journal of Geology*, v. 98, p. 709–724.
- Schmidt, J.C., and Graf, J.B., 1990, Aggradation and degradation of alluvial sand deposits, 1965–1986, Colorado River, Grand Canyon National Park, Arizona: U.S. Geological Survey Professional Paper 1493, 74 p.
- Schmidt, J.C., and Rubin, D.M., 1995, Regulated streamflow, fine-grained deposits, and effective discharge in canyons with abundant debris fans, in *Natural and Anthropogenic Influences in Fluvial Geomorphology*: Washington, D.C., American Geophysical Union, Geophysical Monograph 89, p. 177–195.

- Scott, K.M., 1988, Origins, behavior, and sedimentology of lahars and lahar-runout flows in the Toutle-Cowlitz river system: U.S. Geological Survey Professional Paper 1447-A, 74 p.
- Sharp, R.P., and Nobles, L.H., 1953, Mudflow of 1941 at Wrightwood, southern California: Geological Society of America Bulletin, v. 64, p. 547-560.
- Shlomon, R.J., Wright, R.H., and Montgomery, D.R., 1987, Anatomy of a debris flow, Pacifica, California: Reviews in Engineering Geology, v. 7, p. 181-199.
- Simmons, G.C., and Gaskill, D.L., 1969, River runner's guide to the canyons of the Green and Colorado Rivers, with emphasis on geologic features, Volume III, Marble Gorge and Grand Canyon: Flagstaff, Arizona, Northland Press, 132 p.
- Smith, D.L., and Crampton, C.G. (eds.), 1987, The Colorado River survey: Salt Lake City, Utah, Howe Brother Books, 305 p.
- Smith, W., 1986, The effects of eastern North Pacific tropical cyclones on the southwestern United States: Salt Lake City, Utah, National Oceanic and Atmospheric Administration, Technical Memorandum NWS-WR-197, 229 p.
- Stanton, R.B., 1965, Down the Colorado (edited by D.L. Smith): Norman, University of Oklahoma Press, 237 p.
- Stedinger, J.R., and Cohn, T.A., 1986, Flood frequency analysis with historical and paleoflood information: Water Resources Research, v. 22, p. 785-793.
- Stedinger, J., Surani, R., and Therivel, R., 1988, MAX users guide: Ithaca, NY, Cornell University, Department of Environmental Engineering, no page numbers.
- Stephens, H.G., and Shoemaker, E.M., 1987, In the footsteps of John Wesley Powell: Boulder, Colorado, Johnson Books, 286 p.
- Stevens, L., 1990, The Colorado River in Grand Canyon, A guide: Flagstaff, Red Lake Books, 115 p.
- Stone, J.F., 1932, Canyon country: New York, G.P. Putnam's Sons, 442 p.
- Stringfield, V.T., and Smith, R.C., 1956, Relation of drainage, floods, and landslides in the Petersburg area, West Virginia: West Virginia Geological and Economic Survey, Report of Investigations No. 13, 19 p.
- Stuiver, M., and Becker, B., 1993, High-precision calibration of the radiocarbon time scale AD 1950-6000 BC: Radiocarbon, v. 35, p. 35-65.
- Stuiver, M., and Reimer, P.J., 1993, CALIB user's guide for Macintosh computers, Rev 3.0.3A: Seattle, Washington, Quaternary Research Center publication.
- Thomas, B.E., Hjalmarson, H.W., and Waltemeyer, S.D., 1994, Methods of estimating magnitude and frequency of floods in the southwestern United States: U.S. Geological Survey Open-File Report 93-419, 211 p.
- Thomas, H.E., 1962, The meteorologic phenomenon of drought in the Southwest: U.S. Geological Survey Professional Paper 372-A, 42 p.
- U.S. Department of Commerce, 1963, Arizona, Hourly precipitation data, September 1963: U.S. Department of Commerce, Environmental Science Services Administration, v. 13, no. 9, 5 p.
- 1966, Arizona, Hourly precipitation data, December 1966: U.S. Department of Commerce, Environmental Science Services Administration, v. 16, no. 12, 5 p.
- U.S. Water Resources Council, 1981, Guidelines for determining flood flow frequency: Hydrology Subcommittee Bulletin 17B, 183 p.
- Vasek, F.C., 1980, Creosote bush, long-lived clones in the Mojave Desert: American Journal of Botany, v. 67, p. 246-255.
- Webb, R.H., 1996, Grand Canyon, a century of environmental change: Rephotography of the 1889-1890 Stanton expedition: Tucson, University of Arizona Press, 290 p.
- Webb, R.H., and Betancourt, J.L., 1992, Climatic variability and flood frequency of the Santa Cruz River, Pima County, Arizona: U.S. Geological Survey Water-Supply Paper 2379, 40 p.
- Webb, R.H., and Melis, T.S., 1995, The 1995 debris flow at Lava Falls Rapid: Nature Notes, v. 11, p. 1-4.
- Webb, R.H., Steiger, J.W., and Turner, R.M., 1987, Dynamics of Mojave Desert shrub vegetation in the Panamint Mountains: Ecology, v. 50, p. 478-490.
- Webb, R.H., Pringle, P.T., Reneau, S.L., and Rink, G.R., 1988a, Monument Creek debris flow, 1984: Implications for formation of rapids on the Colorado River in Grand Canyon National Park: Geology, v. 16, p. 50-54.
- Webb, R.H., Steiger, J.W., and Newman, E.B., 1988b, The response of vegetation to disturbance in Death Valley National Monument, California: U.S. Geological Survey Bulletin 1793, 103 p.
- Webb, R.H., Pringle, P.T., and Rink, G.R., 1989, Debris flows from tributaries of the Colorado River, Grand Canyon National Park, Arizona: U.S. Geological Survey Professional Paper 1492, 39 p.
- Webb, R.H., Melis, T.S., Wise, T.W., and Elliott, J.G., 1996, "The great cataract," Effects of late Holocene debris flows on Lava Falls Rapid, Grand Canyon National Park and Hualapai Indian Reservation, Arizona: U.S. Geological Survey Open-File Report 96-460, 96 p.
- Webb, R.H., Melis, T.S., Griffiths, P.G., and Elliott, J.G., 1997, Reworking of aggraded debris fans by the 1996 controlled flood on the Colorado River in Grand Canyon National Park, Arizona: U.S. Geological Survey Open-File Report 97-16, 36 p.

- Wells, S.G., McFadden, L.D., Poths, J., and Olinger, C.T., 1995, Cosmogenic  $^3\text{He}$  surface exposure dating of stone pavements—implications for landscape evolution in deserts: *Geology*, v. 23, p. 613–616.
- Wells, W.G., II, 1986, The influence of fire on erosion rates in California chaparral, in DeVries, J.J. (ed.), *Proceedings of the chaparral ecosystems research conference*: Davis, California Water Resources Center Report No. 62, p. 57–62.
- 1987, The effects of fire on the generation of debris flows in southern California: *Reviews in Engineering Geology*, v. 7, p. 105–114.
- Wells, W.G., II, Wohlgemuth, P.M., Campbell, A.G., and Weirich, F.H., 1987, Postfire sediment movement by debris flows in the Santa Ynez Mountains, California, in *Erosion and Sedimentation in the Pacific Rim: Proceedings of the Corvallis Symposium*, International Association of Hydrologic Sciences Publication No. 165, p. 275–276.
- Wenrich, K.J., Billingsley, G.H., and Blackerby, B.A., 1995, Spatial migration and compositional changes of Miocene-Quaternary magmatism in the western Grand Canyon: *Journal of Geophysical Research*, v. 100, p. 10,417–10,440.
- Whipple, K.X., and Dunne, T., 1992, The influence of debris-flow rheology on fan morphology, Owens Valley, California: *Geological Society of America Bulletin*, v. 104, p. 887–900.
- Wieczorek, G.F., Lips, E.W., and Ellen, S.D., 1989, Debris flows and hyperconcentrated floods along the Wasatch Front, Utah, 1983 and 1984: *Bulletin of the Association of Engineering Geologists*, v. 236, p. 191–208.
- Wieczorek, G.F., Morgan, B.A., Campbell, R.H., Orndorff, R.C., Burton, W.C., Southworth, C.S., and Smith, J.A., 1996, Preliminary inventory of debris-flow and flooding effects of the June 27, 1995, storm in Madison County, Virginia showing time sequence of positions of storm-cell center: U.S. Geological Survey Open-File Report 96–13, 8 p.
- Williams, G.P., and Guy, H.P., 1971, Debris avalanches—a geomorphic hazard, in Coates, D. (ed.), *Environmental geomorphology*: Binghamton, State University of New York, p. 25–46.
- Wright, T.L., and Pierson, T.C., 1992, Living with volcanoes: U.S. Geological Survey Circular 1073, 57 p.
- Wohl, E.E., and Pearthree, P.P., 1991, Debris flows as geomorphic agents in the Huachuca Mountains of southeastern Arizona: *Geomorphology*, v. 4, p. 273–292.
- Wolman, M.G., 1954, A method for sampling coarse river-bed material: *American Geophysical Union Transactions*, v. 35, p. 951–956.
- Zreda, M.G., Phillips, F.M., Elmore, D., Kubik, P.W., Sharma, P., and Dorn, R.I., 1991, Cosmogenic chlorine-36 production rates in terrestrial rocks: *Earth and Planetary Sciences Letters*, v. 105, p. 94–109.